The Institute of Paper Chemistry

Appleton, Wisconsin

Doctor's Dissertation

The Effect of Stress Applied During Drying on Some of the Properties of Individual Pulp Fibers

Carl A. Jentzen

June, 1964

THE EFFECT OF STRESS APPLIED DURING DRYING ON SOME OF THE PROPERTIES OF INDIVIDUAL PULP FIBERS

A thesis submitted by

Carl A. Jentzen

B.Ch.E. 1959, Rensselaer Polytechnic Institute
M.S. 1961, Lawrence College

in partial fulfillment of the requirements
of The Institute of Paper Chemistry
for the degree of Doctor of Philosophy
from Lawrence College,
Appleton, Wisconsin

June, 1964

TABLE OF CONTENTS

	Page
SUMMARY	1
INTRODUCTION AND OBJECTIVES	4
HISTORICAL REVIEW	5
Structure of Cellulose Fibers	5
Molecular Structure	5
Microscopic Structure	10
Factors Affecting the Axial Mechanical Properties of Cellulose Fibers	13
Relation Between Mechanical Behavior and Structure	17
Prerupture Response to Stress	17
Bond Stretching	17
Bond Breaking	18
Chain Straightening and Fiber Stiffening	19
Thermodynamics of Stretching Fibers	19
Effect of Moisture	21
Ultimate Strength	21
APPROACH TO THE PROBLEM	23
EXPERIMENTAL APPARATUS AND PROCEDURES	25
Preparation of Pulp	25
Drying Fibers Under Load	26
Apparatus	26
Procedure	35
Load-Elongation Measurements	39
Mass Per Unit Length Measurements	40
General Discussion	40
Anthrone Method	41

Crystallinity and Crystallite Orientation Measurements 44

Microdensitometer 44

Film Calibration 50

Film Developing Procedure 52

X-ray Camera 52

Crystallinity 54

Crystallite Orientation 61

EXPERIMENTAL DATA AND DISCUSSION OF RESULTS 66

Characterization of Pulp 66

Fiber-Drying Forces in a Sheet 67

Elongation Behavior When Fibers Are Dried Under Load 68

Crystallinity of Wet Fibers 77

Mechanical Properties of Fibers 79

Summerwood 79

Springwood 88

Crystallinity and Crystallite Orientation 93

Summerwood 93

Springwood 94

Interpretation of Results in Terms of Changes in Fiber Structure 101

Considerations on Sheet Structure in Terms of the Results Obtained with Drying Fibers Under Load 106

SUMMARY OF RESULTS 110

GENERAL DISCUSSION AND CONCLUSIONS 112

ACKNOWLEDGMENTS 114

LITERATURE CITED 115

APPENDIX I. CALCULATION OF THE AMOUNT OF THE TOTAL LOAD ON A SHEET WHICH AN INDIVIDUAL FIBER SUPPORTS 120

APPENDIX II. EQUATIONS OF A CIRCULAR HELIX 124

APPENDIX III. DETERMINATION OF THE PROPER MEAN AREA TO BE USED FOR YOUNG'S MODULUS CALCULATIONS 125

APPENDIX IV. CRYSTALLINITY AND CRYSTALLITE ORIENTATION DATA 126

SUMMARY

Recently several theories have been presented which relate the mechanical properties of paper to the mechanical properties of the component fibers. Before these theories can be applied properly, it is important to have a knowledge of the factors which significantly affect the mechanical properties of pulp fibers. By an application of Van den Akker's theory to sheets dried under a stress in one direction, the conclusion is reached that the fibers in a sheet are dried under different tensions depending on their angular orientation. Thus, the purpose of this investigation was to study the effect of applying an axial tensile force during drying on the mechanical properties of individual pulp fibers.

Previous workers have determined that drying cotton fibers under an axial tensile load increased Young's modulus, the tensile strength, the crystallite orientation, and the crystallinity and decreased the ultimate elongation. This study was concerned with the springwood and summerwood fibers of a longleaf pine holocellulose pulp.

It was shown that when drying commenced, the fiber underwent a sudden extension which was independent of the drying stress used and which was about twice as large for springwood as for summerwood. The amount of the extension is hypothesized to increase as the initial fibril orientation decreases and the percentage radial shrinkage increases. After the sudden extension, the normally reported axial shrinkage occurred in the fiber.

Drying under load increased Young's modulus, the tensile strength and work-to-rupture and decreased the ultimate elongation. The magnitude of the changes decreased in the order listed. These alterations were much larger for springwood than for summerwood fibers. It was noted that the percentage

standard deviation of the mechanical properties decreased as the fibers were dried under load, which indicates that the fibers became more uniform.

The load-elongation behavior of the fibers was linear for fibers dried without a load, and it changed to a nonlinear relationship concave to the strain axis for fibers dried under load. Loading and unloading cycles of the fibers dried under no load showed that Young's modulus increased because of the cycling. Fibers dried under load did not experience a change in Young's modulus on cycling and therefore creep caused the curved load-elongation relationship. It was hypothesized that for fibers dried under no load the increase in Young's modulus equalled the creep effects, and this quality resulted in a linear load-elongation behavior.

The Laue x-ray diffraction patterns indicated that there was a considerable increase in the crystallite orientation due to drying under load, and there was no significant change in crystallinity. The increase in orientation was much greater for the springwood fibers than the summerwood fibers; however, the latter were initially more oriented. The changes in mechanical properties caused by drying under load were, therefore, attributed to an increase in orientation and to a more uniform distribution of stress among the fibrils.

The results showed that the ratio of the Young's moduli for summerwood and springwood fibers equalled the ratio of the percentage of the S_2 layer in the two types of fibers. This indicates that only the S_2 layer is effective in determining Young's modulus. The highest value of Young's modulus calculated, assuming that only the S_2 layer is effective, approaches that theoretically calculated for perfectly oriented crystalline cellulose.

The difference between the largest values of the tensile strength for summerwood and springwood fibers cannot be accounted for totally on the basis of the percentage of S_2 layer, and therefore it is concluded that the springwood has more discontinuities and imperfections which cause stress concentrations.

One of the more practical implications of this work is the conclusion that the large difference in the directional mechanical properties of paper is attributable to the change in fiber mechanical properties caused by drying under load.

650 10-3

INTRODUCTION AND OBJECTIVES

In recent years, as our understanding of the response of paper to an applied stress has increased, several theories have been proposed which relate the stress/strain behavior of the sheet to the stress/strain behavior of the component fibers. However, relatively little is known about the mechanical properties of individual pulp fibers and about the factors which influence these mechanical properties.

The textile industry has done much work on the stress/strain behavior of cotton and other long natural and synthetic fibers and on the variables which influence this behavior. Among the important variables which influence the mechanical properties are the crystallite orientation, the relative humidity and temperature conditions during testing, and the stress and strain applied during drying. The latter two factors are also known to influence greatly the response of paper to stress. However, it is not known if the influence is due to changes in the individual fiber properties or to changes in the bonding and structure of the sheet, or to both.

The objectives of this thesis are to determine the effects of drying individual pulp fibers under an axial tensile load on the mechanical properties of the individual fibers and on the structural changes which take place in the fibers.

HISTORICAL REVIEW

Many investigators have studied the structure and mechanical properties of fibers. The bulk of these investigations have been concerned with textile fibers, and not until recently has much work been done with papermaking fibers. However, there are many similarities between the structure and mechanical properties of textile and papermaking fibers, and in many cases the same basic principles are involved.

The purpose of this review is to familiarize the reader with the structure of fibers with particular emphasis placed on the pulp fiber, to discuss the factors which influence the mechanical properties of fibers, and then to discuss the relationship between the response of a fiber to stress and the fiber structure. The work in this area has been compiled and summarized by several authors, and therefore the review will be taken largely from books by Ott and Spurlin (1), Meredith (2), and Morton and Hearle (3).

STRUCTURE OF CELLULOSE FIBERS

MOLECULAR STRUCTURE

Pulp fibers are composed of three major chemical constituents: cellulose, hemicellulose, and lignin. Cellulose consists of long, straight chains of glucose anhydride units linked together by beta-1,4 glycosidic bonds, having in the natural state an average degree of polymerization of about 3000 (4).

Pulp fibers are polycrystalline materials, due to the tendency of cellulose to crystallize. Crystallization is favored by the rigid chains, the tendency of the hydroxyl groups to form hydrogen bonds, and the geometric arrangement of the atoms within the glucose unit, which allows a closely packed structure. Those

hemicelluloses which are branched form a less dense structure than the glucose units, and therefore do not have as large a crystallization tendency.

All natural cellulosic fibers have a crystal lattice structure which has been called cellulose I. Meyer and co-workers (5) postulated the generally accepted monoclinic unit cell shown in Fig. 1 on the basis of x-ray diffraction data. The unit cell has dimensions of a = 8.35 A., b = 10.3 A., c = 7.9 A., and $\beta = 84°$. The planes of the anhydroglucose units lie in the ab plane, and the axes of the cellobiose units are parallel to the b axis.

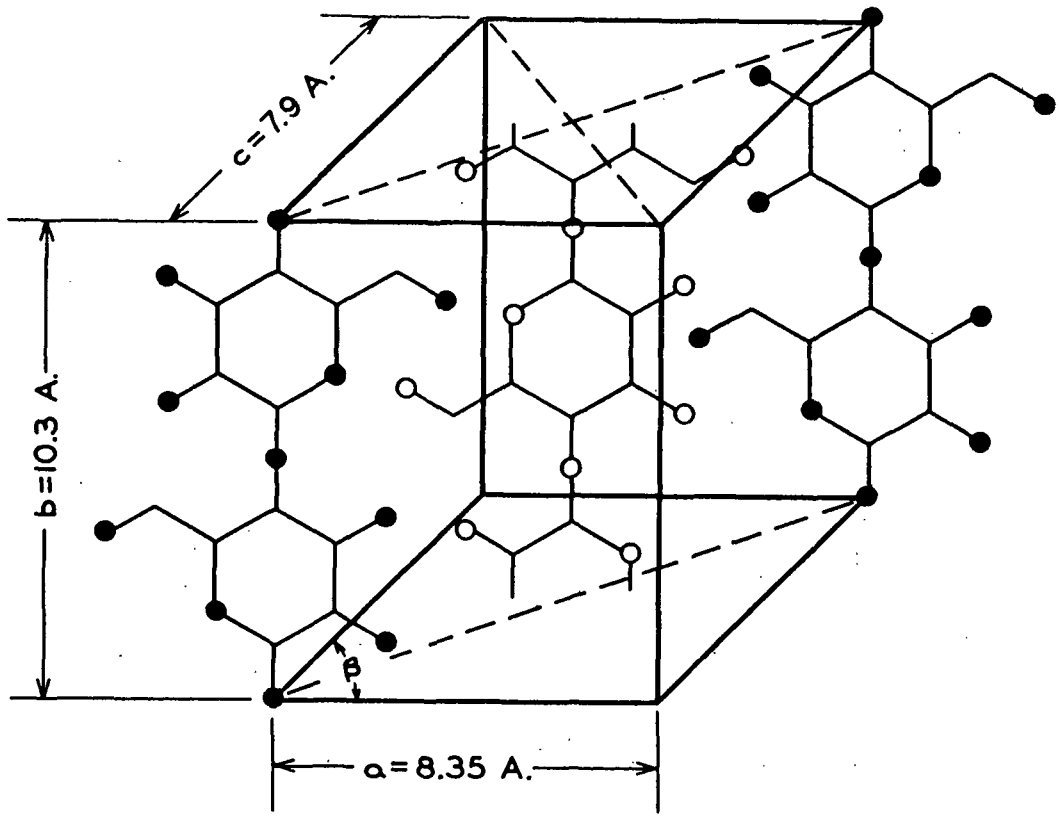

Figure 1. Unit Cell of Cellulose I
According to Meyer and Misch (5)

It is interesting to note the nature of the forces which hold the lattice together (6). Along the b axis the glucose units are held together by the 1,4-glucosidic primary valence bonds, which have a dissociation energy of about 80 kcal./mole. The formation of hydrogen bonds between oxygen atoms of adjacent molecules is suggested by the 2.5 A. separation of the glucose rings along the a axis and the types of atoms present. These hydrogen bonds have an average bond energy of about 5 kcal./mole. Along the c axis the nearest distance between atomic centers is 3.1 A., which indicates van der Waals forces are holding the lattice together; these forces are calculated to be 2 to 3 kcal./mole.

Since cellulose is polycrystalline, it is important to know the arrangement, size, and shape of the crystalline and noncrystalline regions. On the basis of chemical and physical methods for measuring crystallinity, it is generally agreed that there are not distinct crystalline and amorphous regions; but rather there are gradual transitions from crystalline to amorphous, i.e., there are various degrees of lateral order.

Several theories have been presented which fit the general criterion that cellulose has varying degrees of lateral order. The fringed micelle theory—the older theory—states (8) that the micelles or crystallites are considered as statistically distributed regions of lattice order in a mass of substance consisting of approximately parallel chain molecules. For the most part, the "crystalline" regions alternate with the less ordered "amorphous" regions, and within broad limits there is no connection between the length of the crystalline regions and the molecular chain length. There are no sharply defined crystalline limits, but rather there are gradual transitions from regions of high lateral order to regions of low lateral order. In general, the crystalline regions can have any of an indefinite number of distributions of size, shape, and degree of perfection.

Hearle (9, 10) recently proposed the fringed fibril theory of fiber structure. He suggested abandoning the assumption, implicit in the fringed micelle theory, that all molecules in a crystalline region diverge from one another at approximately the same position, giving rise to discrete crystallites. Instead, the crystalline regions are regarded as continuous "fringed fibrils," composed of molecules diverging from the fibril at different positions along its length.

X-ray diffraction data indicated the crystallites to be about 50 A. in width and thickness and 500 A. in length (8). Hearle suggested that this apparent length of the crystallites was due to imperfections in the crystalline fibril rather than to more discrete crystallites as suggested by the fringed micelle theory. The essential difference in the theories is that the fringed micelle theory has the less ordered "amorphous" regions alternating along the axis of the fibril, while the fringed fibril theory has the "amorphous" regions occurring around the circumference of the fibril. This difference is important when the response to stress is interpreted in terms of structure.

The possibility of chain folding in natural fibers has led to a third plausible theory of fiber structure. Lindenmeyer (7) has reviewed the work which has been done on chain folding, and evidence has been presented which indicates chain folding occurs when polymer molecules crystallize from the melt and from solution. Tønnesen and Ellefsen (11) discuss the possibility of chain folding in connection with the cellulose molecule. If chain folding occurs, the chains are hypothesized to form a monomolecular layer parallel to the 101 plane with a length of 500 A., and the less ordered regions would be located at 500 A. intervals along the length of the fibrils. Thus, Tønnesen's version of the folded chain theory and the fringed micelle theory would suggest that the

amorphous regions alternate along the fiber length. Chain folding probably would affect the mechanical properties of fibers; however, due to the limited knowledge on this theory it will not be given further consideration.

From the preceding discussion the term "percentage of crystalline material" is seen to be rather poorly defined. The crystalline structure can be accurately defined only by the lateral order distribution. However, the terms "percentage of crystallinity" and "crystallinity" appear frequently in the literature, and they are arbitrarily defined by the method used to measure them. The methods used to measure accessibility are usually chemical and those that measure crystallinity are usually physical.

In the chemical methods the rate of chemical reaction with the cellulose is measured in either a swelling or nonswelling medium. The accessibility is calculated by assuming that the initial fast reaction rate is caused by reactions in the amorphous regions and the subsequent slower rate is caused by reactions in the crystalline regions. In some cases the reactions in the crystalline regions are so slow that they are considered negligible.

The principal physical method used consists of separating the crystalline and amorphous scatter on an x-ray diffraction pattern. Other proposed methods consist of measuring the density of the cellulose, the amount of moisture sorption by the cellulose, the dielectric constant of the cellulose as suggested by Calkins (12) and Verseput (13). Recently Ticknor (14) has based a method on measuring the difference in the free energy of the polymer molecules in their structure and in a completely amorphous state. It should be pointed out that while none of these methods by itself can determine the lateral order distribution, they rank different celluloses in the same order and are useful for comparison purposes.

MICROSCOPIC STRUCTURE

Morphologically, the fiber consists of a layered structure as shown in Fig. 2. In most fibers there are five distinct layers: (1) the intercellular substance or middle lamella, (2) the primary wall or P layer, (3) the outer layer of the secondary wall or S_1 layer, (4) the central layer of the secondary wall or S_2 layer, and (5) the inner layer of the secondary wall or tertiary wall, referred to as the S_3 layer. Except for the middle lamella, each of these layers is composed of a fibrillar structure which in turn can be broken down into finer fibrils., Frey-Wyssling (15) presented the results shown in Table I of the cross-sectional dimensions of the fibrillar elements of cotton. The fibrils are generally considered to be of indefinite length.

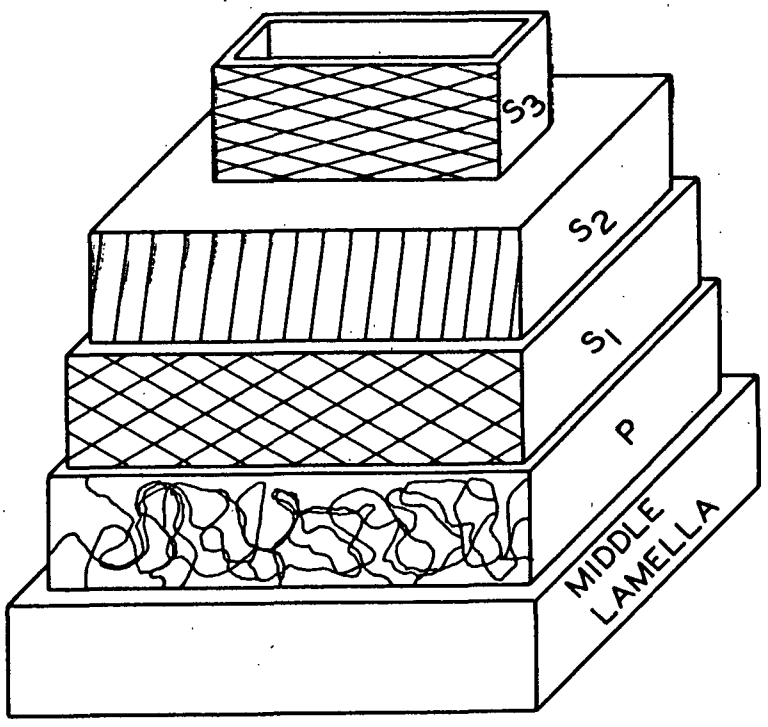

Figure 2. Layer Structure of Fiber

TABLE I

CROSS-SECTIONAL DIMENSIONS OF FIBRILLAR ELEMENTS

	Area of Cross Section	Number of Cellulose Chains in Cross Section
Cotton hair	$\pi(10\ \mu)^2 = 314\ \mu^2$	1,000,000,000
Macrofibril	$(0.4\ \mu)^2 = 0.16\ \mu^2$	500,000
Microfibril	$(250\ A.)^2 = 62{,}500\ A.^2$	2,000
Elementary fibril	$50\ A. \times 60\ A. = 3{,}000\ A.^2$	100
Cellulose molecule	$4\ A. \times 8\ A. = 32\ A.^2$	1

It should be pointed out that the numbers given are for cotton, and these will vary for different types of fibers and for the different layers within the fibers; however, the order of magnitude presumably will not change.

Frey-Wyssling (16) proposed that the elementary fibrils or micellar strands consist of a crystalline core flattened parallel to the 101 plane and that this core is embedded in a cortex of paracrystalline cellulose. The x-ray data on crystallite size corresponds to the size of the crystalline core of the elementary fibrils. The paracrystalline cellulose is responsible for the aggregation of the elementary fibrils to form microfibrils. When the fiber sorbs water and swells, the water is sorbed in the paracrystalline cellulose as well as in the more coarse submicroscopic capillaries located between the microfibrils. This capillary system is consistent with that presented by Wardrop (17).

The fibrillar structure of all layers except the primary wall are wound helically around the fiber axis. The fibrils of the primary wall are randomly oriented in a loosely woven texture, except at the corners where they are longitudinal (17). The S_1 layer has at least two counterrotating and symmetrical

helices, which have a helix angle of 55 to 75° for softwood tracheids (18). The fibrils of the S_2 layer wind around the fiber axis in a single direction and have a small helix angle (17). The S_3 layer has a crossed helical structure (17), and for most softwood tracheids the helix angle is between 65 and 90° (19).

Although springwood and summerwood have the same layered structure, they differ in the cell wall thickness, the size of the lumen, and the diameter of the fiber (20). The springwood fibers have a thinner wall but a larger lumen and diameter. The difference in the cell wall thickness is mainly in the amounts of the S_2 layer. For a spruce springwood tracheid (21) the P layer comprises about 10% of the total wall, S_1 about 8%, S_2 about 78%, and S_3 about 4%. The S_2 layer accounts for the largest percentage of the cell wall material, but the S_1 layer restricts the swelling due to its large helix angle.

Chemically, there is a big difference between the layers (22), but there is only a small difference between springwood and summerwood fibers (23). Lignin, which is removed to a large extent during pulping, is located mainly in the middle lamella. Wardrop (17) estimated that 70% of the total lignin was external to the S_2 layer. Sachs, Clark, and Pew (24) found the lignin in the S_1 to be fairly compact, but it diminished in density adjacent to the S_2 layer. The lignin in the S_2 was dispersed in a random network, and the lignin in the S_3 layer was as dense and compact as the lignin in the middle lamella.

Meier (22) found that about 60 to 65% of the carbohydrate material in the S_2 layer was cellulose; 50 to 60% in the S_1 layer was cellulose, and 35 to 40% in the P layer was cellulose. The hemicelluloses were in the reverse order. The location of the hemicelluloses most likely has an important bearing on the fiber properties. The hemicelluloses are generally agreed to be located around

the outside of the microfibrils (25, 26), although there is speculation that some may be located within the microfibrils (26, 27).

A final important point to be considered in a discussion of morphology of wood fibers is the subject of discontinuities in the structure. Bucher (19) treated this subject and pointed out that the pits are the best known discontinuity, and the fibrils around the pits have a circumferential orientation. Dislocations and slip planes in the fibrils represent transverse discontinuities. The lamellae within layers and the different layers themselves can also be considered as discontinuities.

FACTORS AFFECTING THE AXIAL MECHANICAL PROPERTIES OF CELLULOSE FIBERS

Cellulose fibers, being viscoelastic materials, exhibit both instantaneous elastic deformation and delayed, time-dependent deformation when subjected to an externally applied stress. Creep, which is the delayed, time-dependent deformation, can be divided into two components: primary creep, which is recoverable; and secondary creep, which is nonrecoverable. For a thorough treatment of the creep behavior of fibers, the reader is referred to Leaderman (28).

A fast method for obtaining some knowledge of the recovery properties of a fiber is by a series of loading and unloading cycles. This method suffers from the shortcoming of not allowing sufficient time for complete recovery to take place. One test of this sort is alternately to load and unload the fiber, each time increasing the maximum load by a predetermined amount. The elastic recovery can then be defined as the ratio of the elongation which was recovered on unloading the fiber to the total elongation which took place on loading the fiber. Meredith (2) stated that for cellulosic fibers the elastic recovery decreases as

the maximum load increases, i.e., secondary creep increases as the applied stress increases. Other characteristics of this type of loading cycle are that the curves show hysteresis, the slope of the curve is steeper at the start of unloading than at the commencement of loading; and the slopes of the curves become steeper for each successive loading cycle for natural fibers, but the slopes remain the same for regenerated fibers.

The rate of extension has an effect on the load-elongation curve due to the creep exhibited by the cellulosic fibers. Meredith (2) studied this effect over a millionfold range of loading and found the strength and modulus to increase about 50% for this increase in rate of extension, but the ultimate elongation remained about the same.

The load-elongation curves of hygroscopic fibers are sensitive to changes in relative humidity. The elongation increases and the elastic modulus decreases with increasing relative humidity for both natural and regenerated fibers. Tensile strength displays the anomalous behavior of increasing with relative humidity for natural fibers but decreasing for regenerated fibers. Hartler, Kull, and Stockman (29) found pulp fiber strength to increase as relative humidity increased.

Peirce (30) and many other workers have shown that the tensile strength of cotton increases as the span decreases. This has been attributed to weak spots in the fiber. Hartler, Kull, and Stockman (31) observed a similar effect for pulp fibers.

Wakeham (32) discussed the effect of the degree of polymerization on the tensile strength of fibers. In most of the work with natural fibers the D.P. has been changed by chemical degradation, and the strength remained constant

until the D.P. fell below 800. Regenerated fibers behaved in a similar manner. Hessler, Simpson, and Berkley (33) found that for different varieties of cotton a significant correlation existed between strength and D.P. for D.P. values between 8000 and 10,000. It should be pointed out that the latter workers also found a correlation between D.P. and orientation. The basic problem with studying the effect of D.P. is that it is impossible to change D.P. and keep all other variables constant.

The effect of crystallinity on the mechanical properties of fibers has not been thoroughly studied because in most cases it is difficult to separate the effects of crystallinity from those of orientation. Howsmon and Sisson (8) stated that a few investigations have shown that an increase in crystallinity will increase tensile strength and Young's modulus but decrease the ultimate elongation. Segal, et al. (34), Orr, et al. (35), and Ward (36) have performed work with amine decrystallization treatments. They have found that the ultimate elongation increases, but the strength may increase or decrease by a small amount due to decrystallization.

Many workers have studied the effect of orientation on the mechanical properties of fibers. The orientation may be measured by either x-ray diffraction techniques or optical birefringence methods. Sisson (37) was the first to study quantitatively the increase in strength with increasing orientation. Several reviews (38, 39) have summarized the work on the effect of orientation, and it has been shown that increases in strength and Young's modulus and decreases in ultimate elongation are a strong function of increases in orientation. Wardrop (40) studied the breaking load of tangential sections of wood stressed in the longitudinal direction and found the strength correlated with the orientation.

The orientation was a function of the growth ring from the pith and became constant after the fifteenth growth ring.

The effect of drying fibers under an axial tensile stress or strain has been investigated mainly in connection with mercerization. However, Negishi (41-43) dried both cotton and ramie yarns under tension and measured the changes in the x-ray patterns and in the load-elongation curves at 30% relative humidity, at 65% relative humidity, and in water. He made several interesting observations for cotton fibers: (1) The stretching increased the strength 75% at 30% R.H., 30% at 65% R.H., and 10% when wet. (2) With no straining the wet strength was 30% greater than the dry strength at 30% R.H., but, after drying under strain, the dry strength was 20% greater than the wet strength. (3) The ultimate elongation remained constant with straining at 30% R.H., decreased 30% at 65% R.H., and decreased 35% when tested wet. (4) Young's modulus increased 130% at 30% R.H., 185% at 65% R.H., and 100% when tested wet. The x-ray patterns of the fibers dried under tension were indicative of more crystallization and a better molecular arrangement than were the patterns of the fibers which were not dried under tension.

Several workers have dried individual fibers under stress and strain. Berkley and Kerr (44) stretched never-dried cotton fibers and found that the tensile strength could be increased by 50% and the orientation angle halved. Balashov, Preston, Ripley, and Spark (45) dried sisal leaf fibers under various strains and then x-rayed the fibers to measure differences in orientation. The changes in orientation agreed well with those predicted from the elongation using a spiral spring model. Rebenfeld (46) found that by drying individual cotton fibers under a 420-milligram load the tensile strength was increased 29%,

the elastic modulus increased 270%, and the elongation decreased 35%. Here again orientation changes accompanied drying under load.

Several workers, (27, 31, 47, 48) have observed that summerwood and springwood have different mechanical properties. The summerwood fibers have a higher tensile strength and Young's modulus but a lower elongation than springwood fibers. The magnitude of the difference depends on the species tested. Leopold and McIntosh (27) have attributed this difference to the increased percentage of the S_2 layer in the summerwood fibers.

RELATION BETWEEN MECHANICAL BEHAVIOR AND STRUCTURE

PRERUPTURE RESPONSE TO STRESS

Bond Stretching

Two main molecular processes are involved when a fiber stretches, bond stretching and chain straightening. The cellulose fiber has three types of bonds present—van der Waals forces, hydrogen bonds, and primary valence bonds—all of which have different energies. The van der Waals forces and hydrogen bonds form intermolecular and interfibril bonds, while the primary valence bonds form intramolecular bonds. When a stress is applied, both types of bonds will deform to some extent.

The extension of the van der Waals and hydrogen types of secondary bonds has been estimated to be 10 to 20%. The stretching or extension of these types of bonds implies movement of the molecules and fibrils relative to one another.

Meyer and Lotmar (49) have calculated the value of Young's modulus for the cellulose molecule to be 90×10^{10} dynes/sq. cm. by taking into account bond distance elongations and valence angle distortions and by assuming the

cross-sectional area of the molecule to equal the space it occupies in the cellulose I unit cell. In order to compare the theoretical modulus with the measured modulus, it is necessary to eliminate creep effects. This is usually done by dynamic tests, and Meredith (2) reported a dynamic Young's modulus for ramie wetted and dried under tension of 90×10^{10} dynes/sq. cm. This suggests that for highly oriented, highly crystalline fibers the elastic deformation is mainly due to stretching the cellulose molecules. For less oriented fibers, secondary and primary bonds are deformed, and this undoubtedly accounts for their lower modulus. The secondary bonds are deformed by the component of the applied force which is related to the sine of the fibril orientation angle, and the primary bonds are deformed by the component of the applied force which is related to the cosine of the fibril orientation angle.

Bond Breaking

In order for a secondary bond to be most effective in resisting deformation, it must be oriented parallel to the applied stress. In a fiber the secondary bonds have a distribution of orientations which is dependent on the average orientation of the molecules within the fiber. Due to the orientations of the bonds, it is conceivable that the bonds are brought into play successively; thus, when one bond breaks the stress may be supported by one or several others. These broken bonds then have the possibilities of either forming new bonds with other broken bonds or remaining broken.

The formation of new bonds can lead to an irreversible extension, i.e., secondary creep, when the load is released. There may not be enough energy present to break them and return them to their original positions. Some of the bonds which remain broken will be reformed when the load is removed, but others will remain broken due to restraint from other newly formed bonds. The breaking

and reforming is an equilibrium process; and this explains the existence of creep or time effects, since all systems require a finite time to attain equilibrium. The rate of creep recovery depends on how far the initial bond breakage has proceeded, how many new bonds have been formed, and how stable these are in relation to the residual strength of the unbroken bonds.

Chain Straightening and Fiber Stiffening

When the fiber is stressed, the secondary bonds break, and the molecules and/or fibrils will move relative to one another. This can lead to a straightening of the molecules and fibrils and a more uniform redistribution of stress among the molecules and fibrils. This redistribution of stress will lead to a stiffening of the fiber. Stressing the fiber also causes creep to take place, and the shape of the load-elongation curve will then be dependent on which of these factors is predominant.

Dynamic modulus measurements which minimize creep effects are useful in examining the stiffening of a fiber. Meredith (2) reported that various investigators have studied the effect of strain on dynamic modulus. Cotton fibers showed a large increase in modulus with straining; and it is interesting to note that, while the static modulus and dynamic modulus are about the same at zero strain, the dynamic modulus becomes six or seven times the static modulus at large strains. Ramie and other highly oriented fibers show a smaller increase. All changes in dynamic modulus cannot be attributed to a redistribution of stress, but some may be due to changes in orientation brought about by elongation.

Thermodynamics of Stretching Fibers

It is interesting to treat the stretching of fibers thermodynamically so that more information about intermolecular rearrangements and bond stretching

can be obtained. Wakeham (32) treated this subject, and it is reviewed here. The thermodynamic equation relating to reversible changes of state in this situation is

$$FdL = dU - TdS + PdV,$$

where F is the tensile force, L is the length, U is the internal energy of the system, T is the absolute temperature, S is the entropy, P is the pressure, and V is the volume. At constant temperature and pressure and considering $P(\partial V/\partial L)_{TP}$ as negligible,

$$F = (\partial U/\partial L)_{TP} - T(\partial S/\partial L)_{TP}.$$

For small reversible changes in length the force on the fiber is the result of energy and entropy changes within the fiber.

The term $(\partial U/\partial L)_{TP}$ relates to changes in the internal potential energy of molecules and the energy changes are due to distortions of bond angles and bond distances. The term $(\partial S/\partial L)_{TP}$ relates to entropy changes within the fiber, i.e., it is related to the change in order within the fiber. A decrease in entropy with stretching indicates a change from a less ordered to a more ordered state.

It is rather difficult to measure the entropy changes with extension; however, it can be shown mathematically that

$$(\partial S/\partial L)_{TP} = -(\partial F/\partial T)_{LP}.$$

Work done with dry regenerated fibers showed that the entropy increased with stretching, and as a result the fiber went from a more ordered to a less ordered state. For oriented fibers the internal energy term is much greater than the entropy term, and therefore there is more bond stretching taking place than changes in the order.

Effect of Moisture

It is generally accepted that water does not enter the crystalline region of fibers but rather breaks hydrogen bonds in the less ordered regions. The sorption of water, therefore, reduces the number of secondary bonds between the carbohydrate molecules and, in particular, breaks bonds in the less ordered regions between the fibrils. This bond breakage, therefore, leads to less resistance to deformation, a lower Young's modulus, and to greater extensions. Water and the accompanying bond breakage also allow the stress to be more evenly distributed, and this explains the higher wet tensile strength of natural cellulosic fibers.

ULTIMATE STRENGTH

The ultimate strength of a material is not related to the average structure of a material, but it is dependent on imperfections and flaws in the structure which cause stress concentrations. It is difficult to assess how failure is initiated, whether through slippage caused by breaking of secondary bonds or through breakage of the primary valence bonds. Therefore, the breaking strength is not as easily related to structure as is Young's modulus which depends on the fiber as a whole.

It is interesting to compare the actual strength of fibers with the strength calculated theoretically for various breaking mechanisms. Wakeham (32) presented the results shown in Table II.

The tensile strengths based on cellulose chain scission are much higher than those reported for natural fibers. Highly oriented natural fibers have strengths from 7 to 9 x 10^9 dynes/sq. cm., and cotton has strengths in the range of 3 to 6 x 10^9 dynes/sq. cm. Considering the discontinuities of fibers, it is probably reasonable to obtain order of magnitude agreement.

TABLE II

CALCULATED STRENGTH BASED ON VARIOUS BREAKING MECHANISMS

	Estimated Tensile Strength, dynes/sq. cm.
Cellulose chain scission	
Based on -C-O- bond energy	72×10^9
Based on potential energy function	150×10^9
Cellulose chain separation	
No overlapping (van der Waals forces)	2.7×10^9
Slippage with breaking of secondary (hydrogen) bonds	11.7×10^9

APPROACH TO THE PROBLEM

The literature review revealed that large changes in the mechanical properties of natural fibers can be brought about by drying under various sequences of stress and strain. These changes were accompanied by changes in both the crystallinity and the crystallite orientation of the fibers, and there was speculation that the distribution of stress within the fiber may also be changed.

When investigating the effect of stress or strain applied during drying, it is desirable to study the changes in stress if the fiber is dried at constant strain, or the changes in strain if the fiber is dried at constant stress or load. The fibers in this investigation were dried at constant load, and the changes in strain were recorded. This sequence was chosen for two reasons: the fibers in a sheet probably are dried nearer to a condition of constant load than constant strain, and also it seemed experimentally easier to dry fibers under constant load and measure the changes in strain than to dry fibers under constant strain and measure the changes in load.

The mechanical properties studied as a function of drying under load were the load-elongation characteristics of the fibers. A limited number of loading and unloading cycles were run to obtain additional information on the effect of drying under load. A complete study of the mechanical properties also would involve creep tests.

To gain information on the structural changes accompanying drying under load, Laue x-ray diffraction patterns were run on the individual fibers. Analysis of these patterns determined changes in crystallinity and crystallite orientation. Unfortunately, no experimental method was available, nor could a method be conceived, for determining changes in the distribution of stress.

Both springwood and summerwood fibers were tested separately, since other investigators have shown that they have quite different mechanical properties. The majority of the work was done with summerwood fibers. Also, both never-dried and once-dried fibers were used, since it is well recognized that paper made from once-dried pulp fibers has mechanical properties different from those of paper made from never-dried fibers. Fibers which are initially dried under no load, and then rewet will hereafter be referred to as once-dried fibers.

The purpose of this investigation was to determine the order of magnitude of changes in the mechanical properties of wood fibers which could be brought about by drying under load. It should be pointed out that the objective was not to determine the effect of drying under load on a typical papermaking pulp. Prime consideration was given to selecting a wood species and pulping process which would give a uniform fiber sample, so that accurate results could be obtained by testing a reasonable number of fibers.

EXPERIMENTAL APPARATUS AND PROCEDURES

PREPARATION OF PULP

Longleaf pine (Pinus palustris) was selected as the wood species to be used in this thesis for several reasons: (1) It has a long average fiber length. (2) It has large growth rings. (3) It has relatively large amounts of springwood and summerwood in each growth ring. A 25-cm. diameter, 9-cm. thick disk of a freshly cut Georgia-grown longleaf pine was obtained from Union Bag-Camp Paper Corporation, Savannah, Georgia. The disk obtained was cut into 2-cm. thick disks with the two outer disks being discarded. The thinner disks were then cut into eight pie-shaped pieces.

The wood was pulped by a room temperature holocellulose procedure developed by Thompson and Kaustinen (50). This pulping procedure was selected because a uniformly pulped sample was desired. The pie-shaped pieces of wood were placed in a 1:1 mixture of methanol:benzene, and vacuum was applied periodically to remove air trapped in the wood. Fresh solvent was used after 24 hours, and the wood was extracted for a total period of ten days with vacuum being applied periodically. The wood was then placed in each of the following solvents for 24 hours with vacuum being applied for about the first hour: 100% methanol, 50% methanol, 25% methanol, and distilled water. At this time, two previously weighed pieces were removed to determine the amount of water and extractives.

The wood pieces were then placed in a freshly prepared solution containing 20 grams per liter of sodium chlorite and 0.25% by volume of glacial acetic acid. Vacuum was applied until the entrapped air was removed at a slow rate. Fresh sodium chlorite and acetic acid solution was added each week, and the wood was

pulped for eight months.* The pulping was judged complete when the wood could be completely defibered by 50,000 revolutions in a British disintegrator. Two previously weighed pieces of wood were removed to determine the yield.

To insure as homogeneous a fiber sample as possible, only the fibers from one growth ring of one pie-shaped piece of wood were used. The fibers were separated into springwood and summerwood with a razor blade, and the portion of the growth ring between summerwood and springwood was discarded. The 23rd growth ring of the tree, which was 31 years old, was used, because there was a large amount of springwood and summerwood in this ring, and because this ring was well beyond the juvenile wood portion of the tree. The pulp was defibered by placing 500 ml. of a 0.1% consistency slurry in a one-liter plastic bottle containing ten hard rubber balls of about 16-mm. diameter and having a total weight of 51 grams. The bottle was then rotated at a speed of six revolutions per minute for 24 hours. This method was selected to give a minimum amount of mechanical damage to the fibers. The never-dried fibers were stored in a slurry at 5°C. with about 1% formaldehyde being added as a preservative.

DRYING FIBERS UNDER LOAD

APPARATUS

In order to dry never-dried fibers under load a special piece of equipment had to be designed and built. The requirements of this apparatus were: (1) a set of clamps which would grip the fiber securely so that there was no slippage but which at the same time would not damage the fiber excessively; (2) a device

*The time required for this pulping process now has been decreased through modifications of the pulping conditions by Thompson and Kaustinen (50).

to measure the elongation of the wet fiber when the load was applied, to measure the shrinkage when the fiber was dried, and to measure the contraction when the load was released; and (3) a means of applying a constant load which would not change appreciably with the elongation, shrinkage, and contraction of the fiber and also would not change when the water was removed. The apparatus which was used and which meets these requirements is shown in Fig. 3, and a schematic diagram is shown in Fig. 4.

The fiber was gripped between the movable clamp suspended from the chains and the fixed clamp attached to the water tank. A more detailed view of a clamp is shown in Fig. 5. The clamps, which were made of chromium-plated precision-ground steel, have been surface ground on all the surfaces which come in contact with other surfaces. The fiber was clamped between the ground faces of the base plate (A) and the clamping beam (B). The loading beam (C) was used to apply the load directly on the clamping surface, so that there was no curvature in the clamping beam. The principle used is the same as that employed in the zero-span jaws (51).

The clamping pressure was applied by means of the spring (D), which was compressed with the adjustable nut (E) attached to the loading rod (F). The loading rod fits through the slightly oversized holes in the base plate, clamping beam, and loading beam. A stainless steel pin (G) through the top of the loading rod applied load to the loading beam. The pin arrangement was chosen to facilitate disassembly of the clamp. The guide plate (H) screwed to the side of the base plate kept the clamping and loading beams aligned while the fiber was being gripped.

As shown in Fig. 3, the fixed clamp (I) was fastened securely to the brass end plate of the water tank (J), and the movable clamp (K) was suspended by

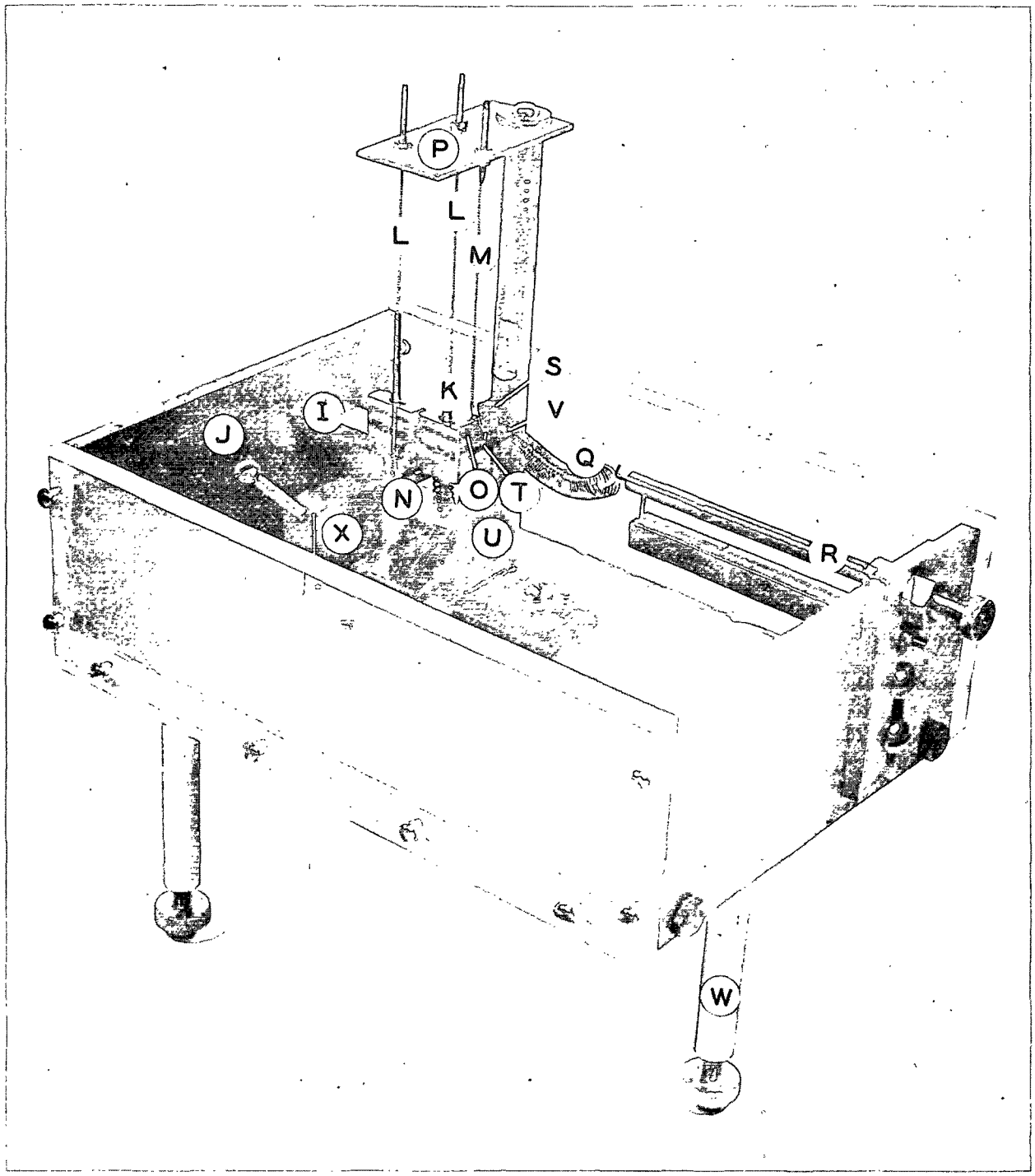

Figure 3. Apparatus to Dry Fibers Under Load

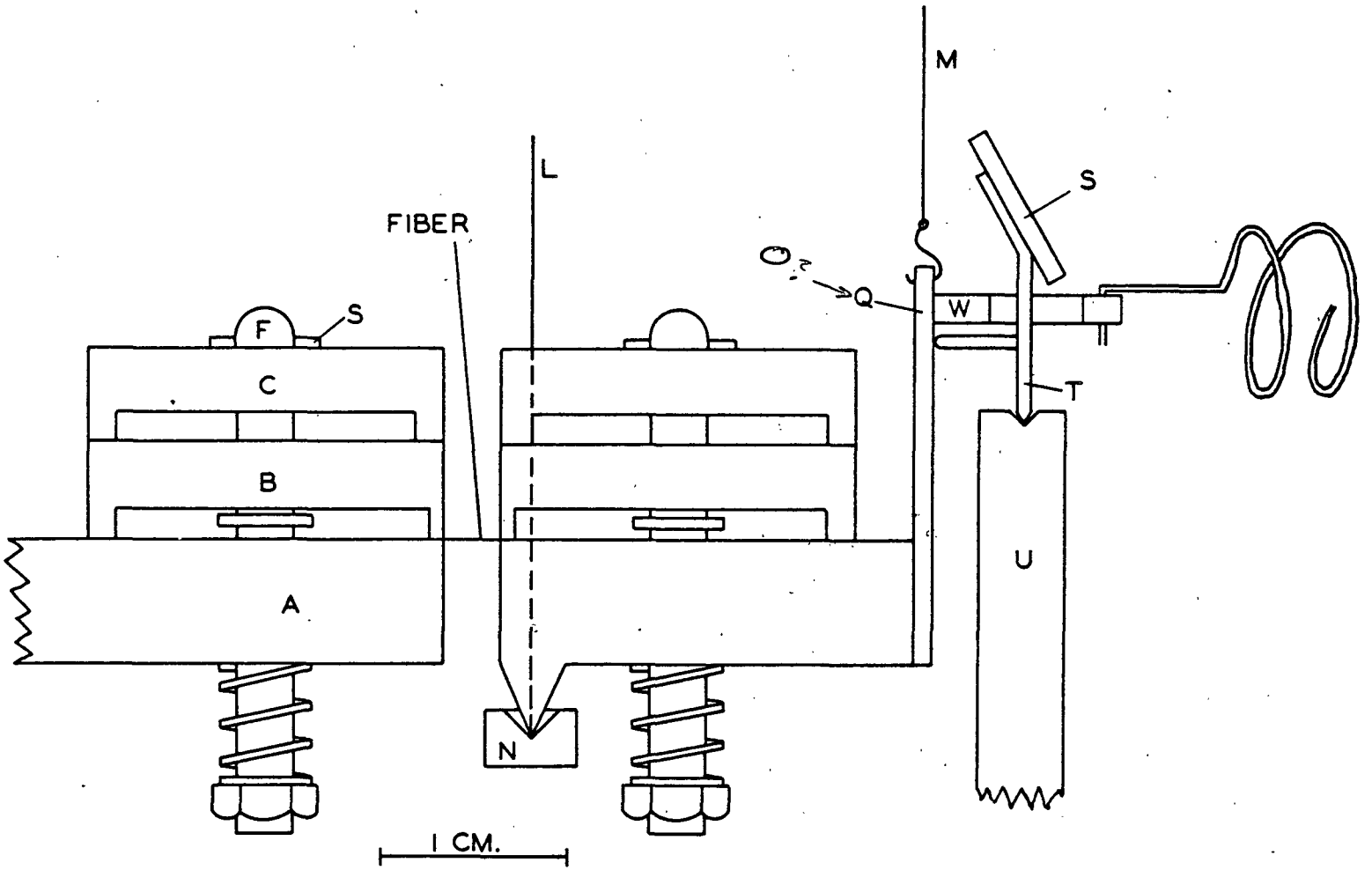

Figure 4. Schematic Diagram of Apparatus to Dry Fibers Under Load

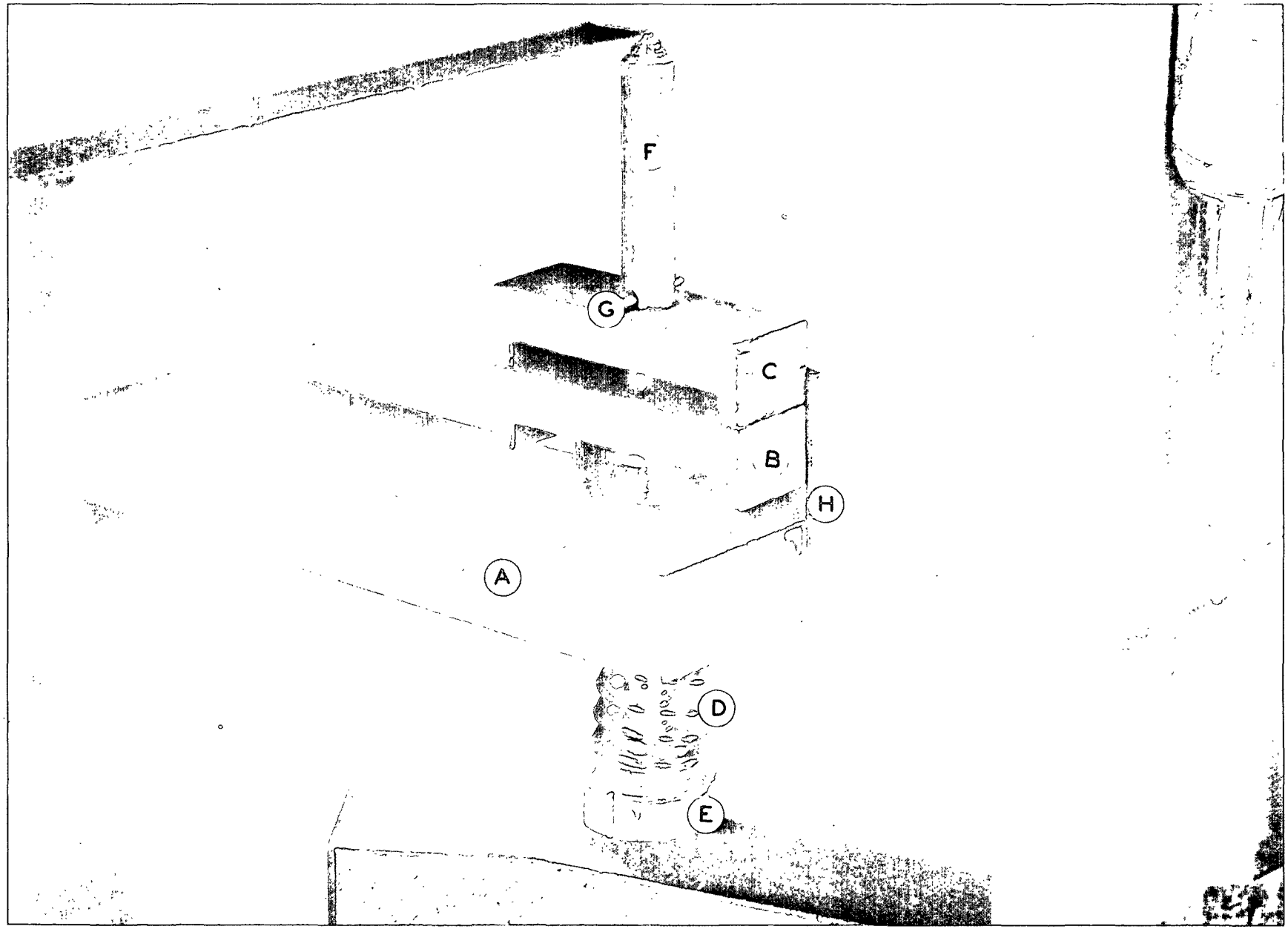

Figure 5. Detailed View of Clamp

three fine jeweler's chains (L, M). The two chains (L) closest to the fixed clamp were attached to the agate plate holder (N) on which the knife edge of the clamp rests. The back chain (M) was attached by a fine hook to the optical lever plate (O). Adjustment of the movable clamp in all directions was provided by the chain holder (P). The movable clamp was designed to be held in this manner so that it could be removed easily. The fixed clamp was opened by sliding the tapered brass bar (X) under the loading rod of the fixed clamp.

The load was applied to the fiber by the spring (Q) attached to the spring support (V). The spring support was attached to the upper part of the optical lever plate so that the spring was out of the water at all times. The extension of the spring which determined the load was controlled by the micrometer screw arrangement (R) attached to the spring. The spring characteristics were chosen so that the elongation of the fiber at a given load was less than 1% of the extension of the spring necessary to produce the load. This insured that the load remained essentially constant while the fiber elongated, shrank, and contracted.

To measure the elongation, shrinkage, and contraction, an optical lever was used. A mirror (S) was glued to the T-shaped mirror support (T). The bottom of the support had been ground to a knife edge, and this fitted in the V-shaped groove of the mirror support holder (U). A stainless steel pin was attached to the mirror support, and this rested against the optical lever plate of the movable clamp. The image of a hairline was focused on a distant scale following reflection of the beam by the mirror. When the fiber changed length the movable clamp moved the corresponding amount, which caused the mirror support to rotate on its knife edge. Thus, the position of the hairline image changed on a distant scale.

The ends and bottom of the water tank were made of brass plate, while the sides were constructed of Plexiglas as an aid to viewing the clamps. A drain was located in the bottom of the tank so that the water could be removed when the fiber was to be dried. The water tank was supported on three adjustable legs (W) for leveling the tank.

Before this apparatus could be used, it was necessary to calibrate both the spring used for applying the load and the optical lever. The apparatus shown in Fig. 6 was built to determine the spring constant. A piece of graph paper on which 45° lines were drawn was taped to the board. A rod was mounted along the top of the board in such a manner that a washer could be slid freely along it. One end of the spring was securely fastened to the board, and the other was attached by a nylon thread to the washer.

The spring was calibrated by placing the nylon filament at a 45° angle and measuring the length of the spring. A force analysis showed the effective load to be half the weight of the spring. Weights were then hung from the free end of the spring, and each time the nylon thread was adjusted to a 45° angle, the extension was measured. Again a force analysis showed the force extending the spring to be equal to the weight suspended from the end of the spring plus half the weight of the spring. The calibration curve of the spring is shown in Fig. 7, and it has a constant of 0.674 gram per centimeter.

The calibration of the optical lever was done with a micrometer screw arrangement. The fixed clamp was removed, and it was replaced with a steel rod, one end of which was tapped with a micrometer thread. The circumference of the rod was divided into 25 divisions, each corresponding to 0.001 inch. A bolt was made with a micrometer thread on one end and it was rounded on the

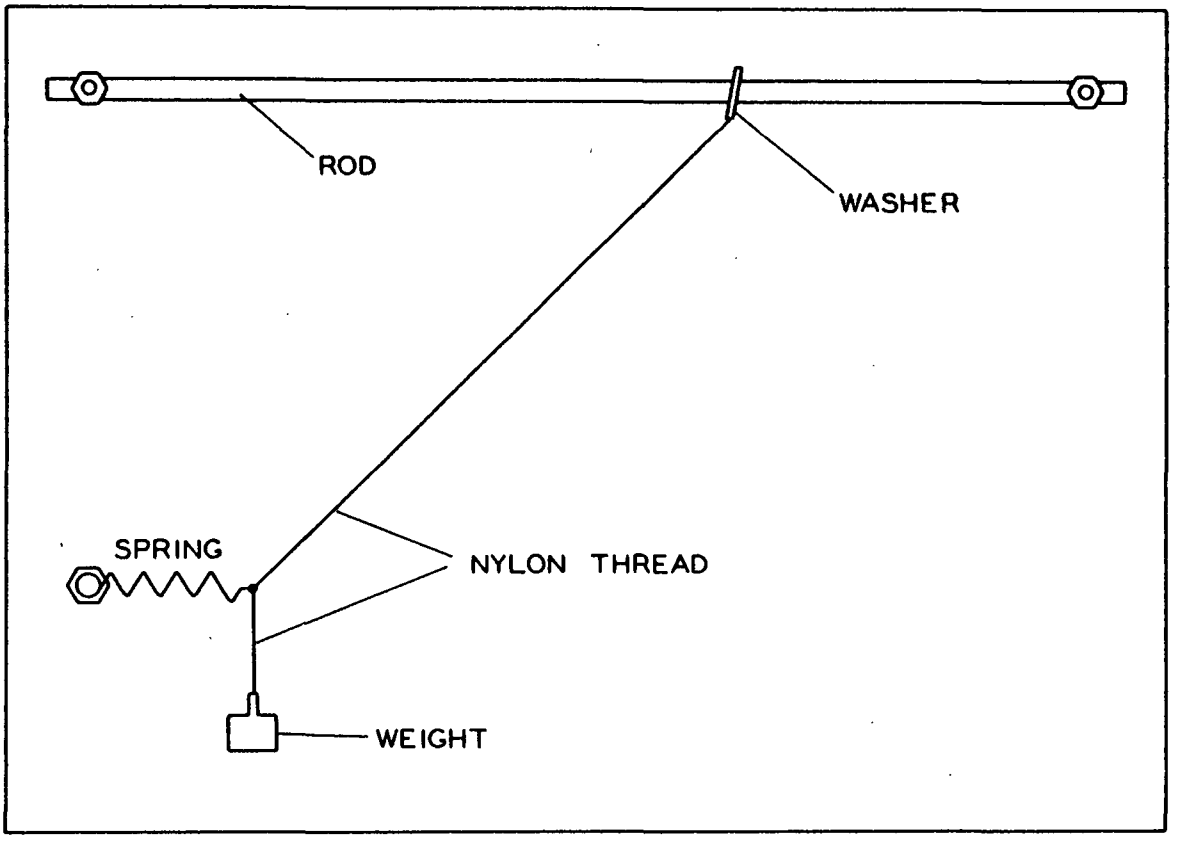

Figure 6. Spring Calibration Apparatus

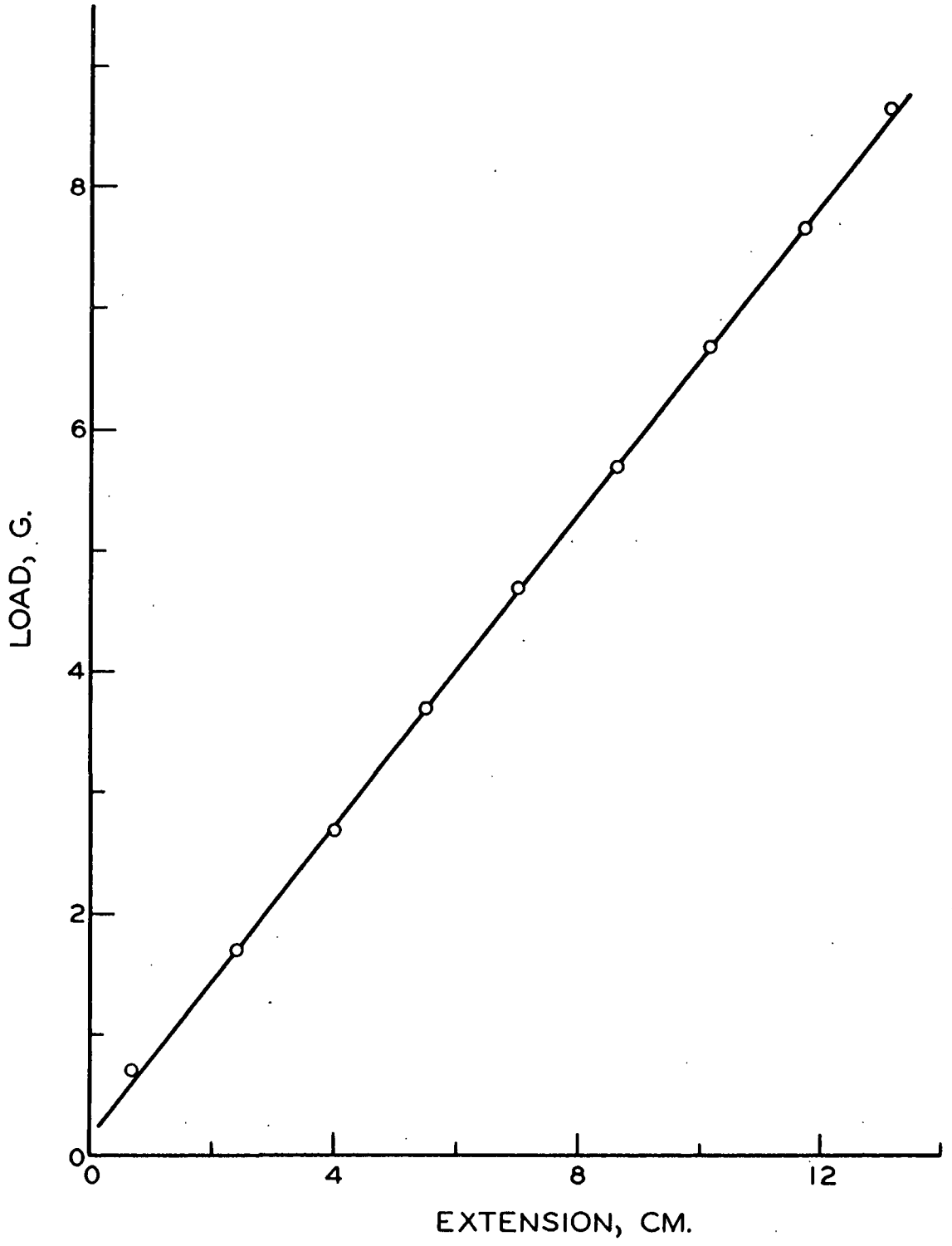

Figure 7. Spring Calibration Curve

other end. The bolt was screwed into the rod, and the movable clamp was put in place. The bolt was unscrewed until the point touched the face of the movable clamp. The scale readings were taken as the bolt was unscrewed at 0.001-inch increments, and the results are shown in Fig. 8.

If the shape of the curve in Fig. 8 is examined, a slight curvature is noticed. The curvature comes from two sources: first, the scale is not curved, and therefore greater magnification occurs at the higher scale readings, and second, the relation between the angular rotation of the mirror support and the movement of the movable clamp is not linear. The theoretical relationship based on the dimensions of the system is

$$S = 248 \tan \left[94°30.6' - 2 \cos^{-1}\left(\frac{.184 + h}{.257}\right)\right] - 17$$

where S is the scale reading and h is the movement of the movable clamp in inches If the scale readings from Fig. 8 are taken, the theoretical movement of the movable clamp h can be calculated. In Fig. 9 the actual movement is plotted against the calculated theoretical movement; a straight line is obtained with a slope equaling unity, which indicates that the theoretical equation is valid.

PROCEDURE

The procedure used to mount the fibers was developed with the main purpose of facilitating handling of the fibers. The movable clamp was placed in a jig filled with water and the jaws were opened. The fiber to be dried, which must be at least 4.5 mm. long, was removed from a dilute slurry by gripping one end with a tweezer, and it was transferred to the jig holding the movable clamp. Care was taken to insure that the fiber was kept in water at all times. The fiber was centered in the clamp and gripped; the drying apparatus was filled

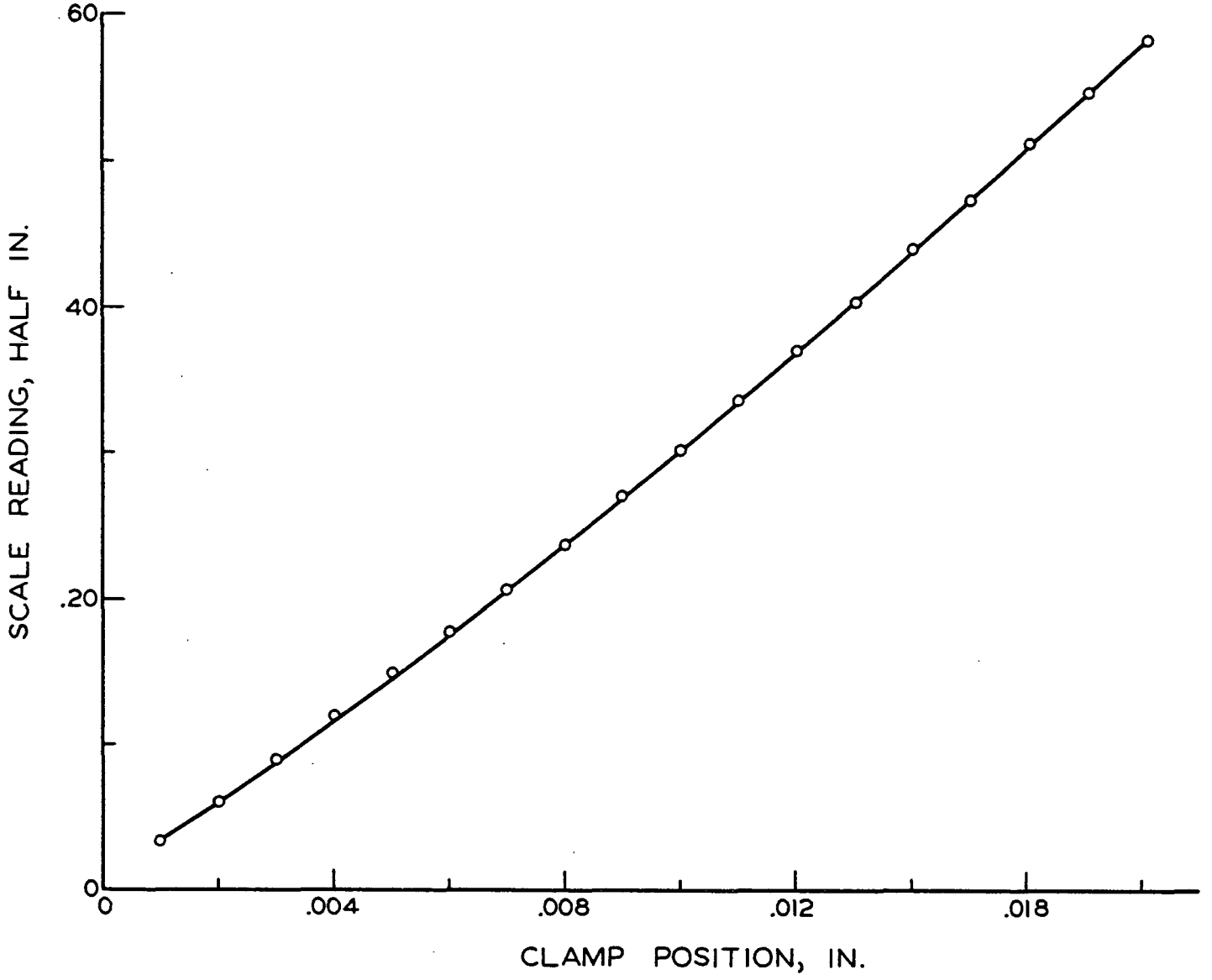

Figure 8. Optical Lever Calibration

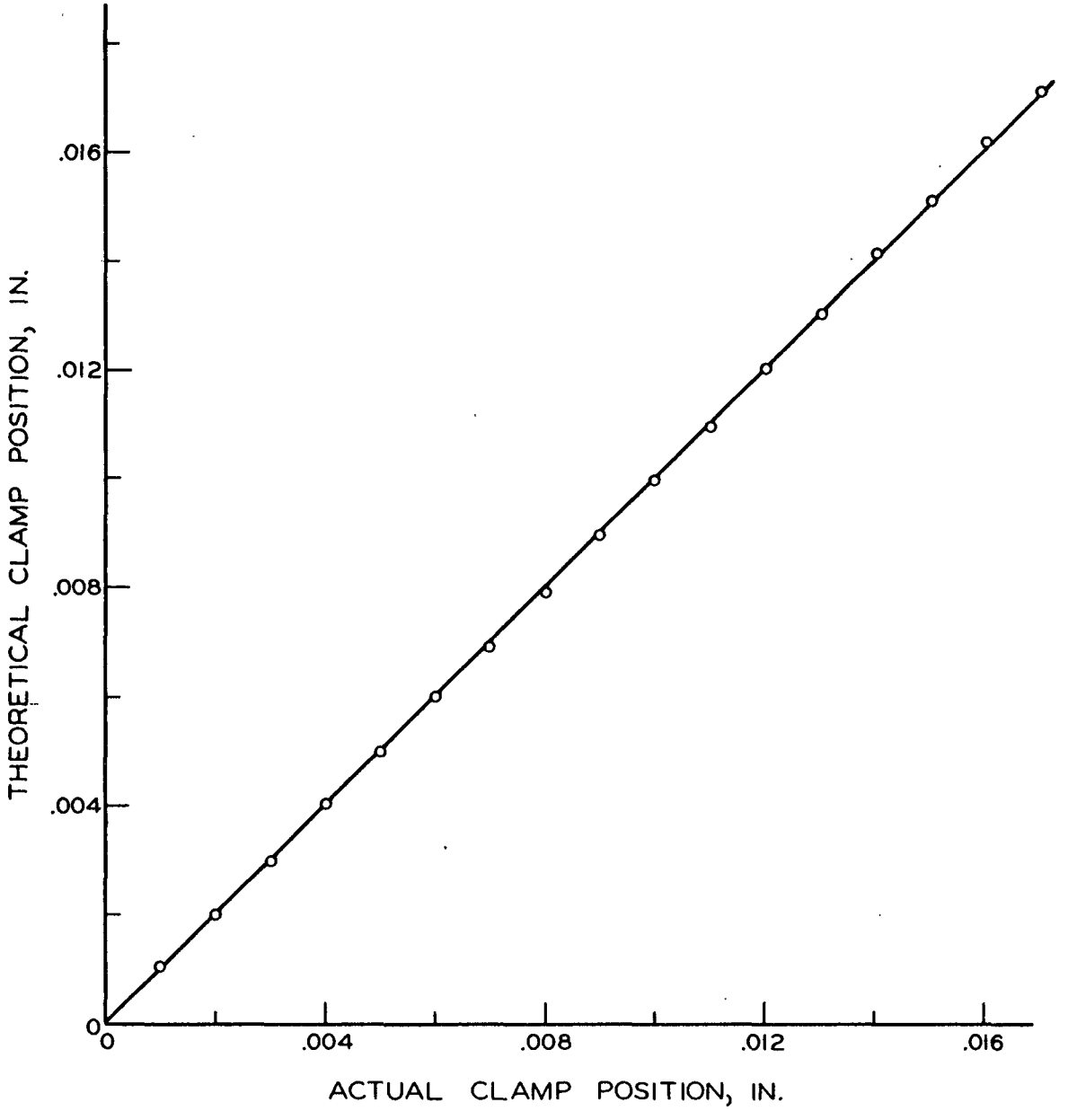

Figure 9. Comparison of Actual and Theoretical Optical Lever Calibration

with distilled water, and the jig containing the movable clamp was placed in the water. The jaws of the fixed clamp were opened, and the movable clamp holding the fiber was removed from the jig and suspended from the three chains. The free end of the fiber was guided between the jaws, and with the aid of a mirror under the clamps the fiber was aligned and gripped. The spring for applying the load was positioned, and a 1-gram load was applied. A minimum load of 1 gram was needed to straighten the fiber and to steady the movable clamp from the vibrations in the room. The optical lever mirror was positioned; it was important to have the pin of the mirror support aligned on the centerline of the fiber and spring. The fiber was then in position for initiation of the test. The fibers were dried under load at a 3-mm. span.

The following procedure was used to dry the fibers under load. A reference reading was taken at the 1-gram load, and the desired load was applied gradually during one and one-half minutes, at which time another reading was taken. Elongation readings were then taken three, nine, and fifteen minutes after the desired load was applied. The drain was opened, and drying commenced. Readings were taken one, two, three, six, nine, and fifteen minutes after the drain was opened. After this drying period, the load was reduced gradually to the initial 1 gram in one and one-half minutes, and a reading was taken then and after an additional three minutes. The whole drying procedure, which took a total of 36 minutes, was performed in a room controlled at 73°F. and 50% R.H.

Several steps were taken to remove excess water from the apparatus after the water had been drained. The water remaining in the bottom of the tank was removed with vacuum. The water between the base plate and clamping beam of the fixed clamp was removed with thin strips of blotter paper. The space between the base plate and clamping beam of the movable clamp was filled with paraffin wax to

prevent water from collecting there. The blotter paper technique was not feasible for use with the movable clamp, because it was impossible to position and remove the blotter paper without disturbing the movable clamp.

LOAD-ELONGATION MEASUREMENTS

All load-elongation measurements on the individual fibers were made on the IPC Fiber Load-Elongation Recorder (52) at 73°F. and 50% R.H. The fibers were glued to the pins by first tacking them to the pins with ethylhydroxyethyl cellulose. Care was taken to be sure the ethylhydroxyethyl cellulose was not near the ends of the pins where the epoxy resin would later go. Epon 907* was used to glue the fiber; the glue was prepared by weighing 10 parts of component A and 8 parts of component B and then mixing thoroughly. The glue was used only within 15 minutes after it had been mixed. About 25 fibers could be glued in the 15-minute period. Preliminary work showed that if the glue was allowed to set beyond 15 minutes, an appreciable number of fibers pulled out from the glue, indicating that they were not well bonded.

Any end effects which were caused by mechanically gripping the fibers in the drying apparatus were eliminated by measuring the load-elongation properties of the fibers at a nominal span of 2 mm. as compared to the 3-mm. span used to dry fibers under load. The actual span of each fiber tested was measured with an eyepiece micrometer. A 10-r.p.m. motor was used for all testing, but different chains were used for the springwood and summerwood fibers. The difference in chains led to rates of loading of 1.40 grams per second for the springwood and 2.00 grams per second for the summerwood.

*Manufactured by Shell Chemical Company.

MASS PER UNIT LENGTH MEASUREMENTS

GENERAL DISCUSSION

Several methods have been presented in the literature to measure the cross-sectional area of individual fibers. In their earlier work, Van den Akker, et al. (53), measured the cross section by assuming it to be elliptical and measuring the major and minor axis. Leopold and McIntosh (27) measured the cross-sectional area by embedding the fiber in cellulose acetate and microtoming it. Both of these methods suffer from the shortcoming of not taking into account variations in the cell wall porosity of different fibers.

It has been common practice in the textile industry to correct all fiber mechanical properties for mass per unit length. The same practice is used in the paper industry for sheets, where all tensile strengths are corrected for basis weight to give breaking length. It was therefore reasoned that it would be better to measure the mass per unit length of the pulp fiber, rather than the cross-sectional area. A reference cross-sectional area of the cellulosic material was calculated by arbitrarily taking the density of the cellulose in the cell wall to be 1.55 grams per cubic centimeter.

The mass per unit length method might be criticized by those who would suggest that the cross section at the point of break should be used rather than an average cross section. However, the cross section of a fiber does not vary greatly except at the ends where the fiber is tapered, and the cross section at the point of break should not be much different from the average cross-sectional area. There is no doubt that the average cross-sectional area is better for properties such as Young's modulus and work-to-rupture.

ANTHRONE METHOD

The anthrone method has been used for the past 15 years to determine qualitatively and quantitatively small amounts of carbohydrate material. This method, therefore, seemed applicable to determining the amount of carbohydrate material in a fiber, or more precisely, its mass per unit length. Many papers have been published on applications and procedures for the anthrone method. Helbert and Brown (54, 55) have published some of the more recent papers in this area, and these will serve as an introduction on this method. Bonting (56) was the first to apply the method to microgram quantities, and his work was particularly useful in applying the method to individual fibers.

The anthrone method is a colorimetric method to determine the amount of carbohydrate material in a sample. The carbohydrate material is dissolved in concentrated sulfuric acid; the anthrone reagent is added; the mixture is heated to react the material, and the optical density is measured. Preliminary experiments were performed on large fiber samples to determine the optimum wavelength at which to measure the optical density and to determine the optimum heating time for the reaction. Figure 10 shows the optical density at 625 mμ as a function of heating time. The maximum occurs at about three minutes, but a four-minute heating time was selected, because any small errors in measuring heating time would have no significant effect on the measured optical density. Figure 11 shows the optical density as a function of wavelength for a four-minute heating time, and the maximum quite clearly occurs at 625 mμ which agrees with the literature values.

The following procedure was found to be the most accurate when applying the method to individual fibers. The 2-mm. portion of the fiber whose load-elongation

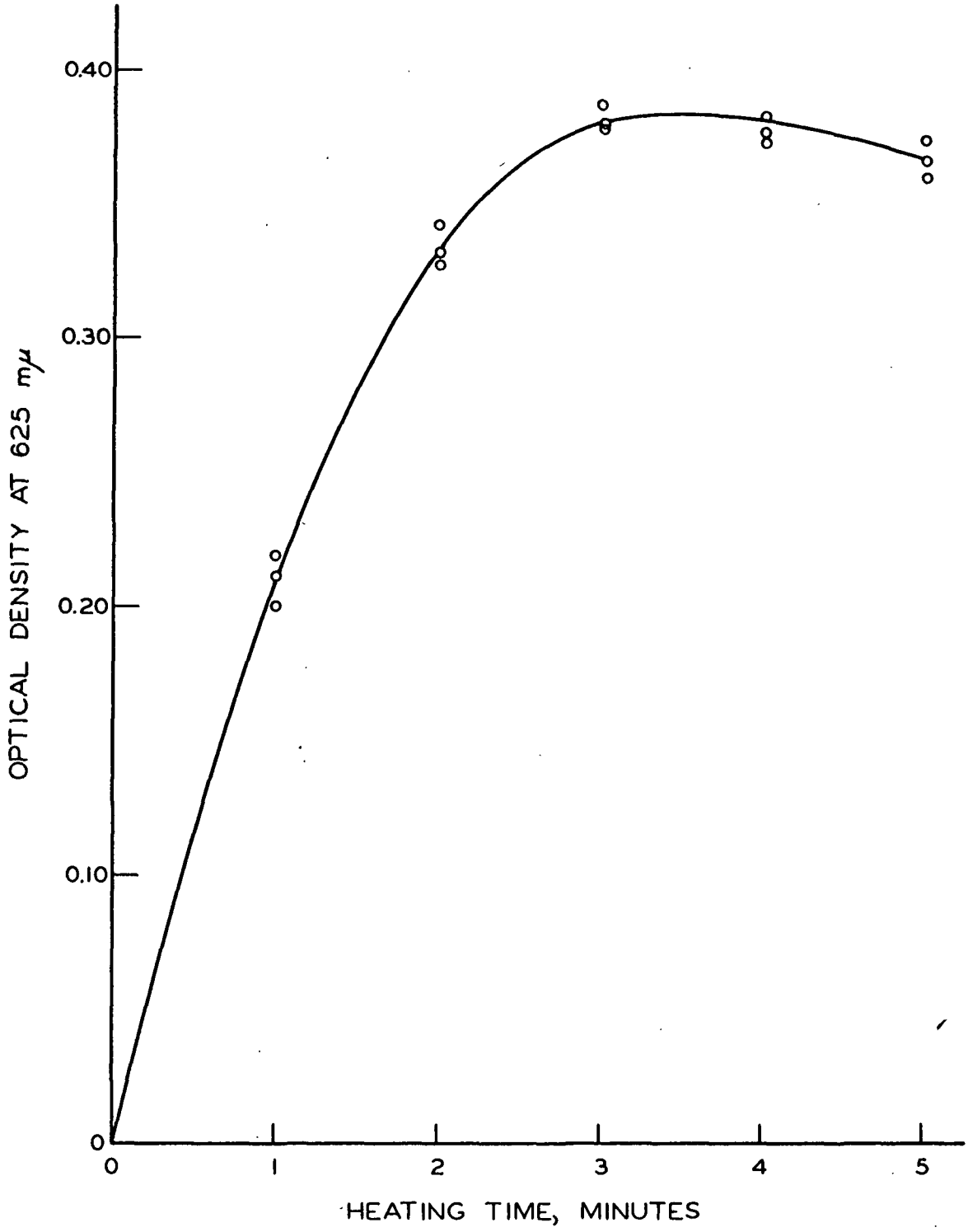

Figure 10. Relationship Between Heating Time and Optical Density for Anthrone Test

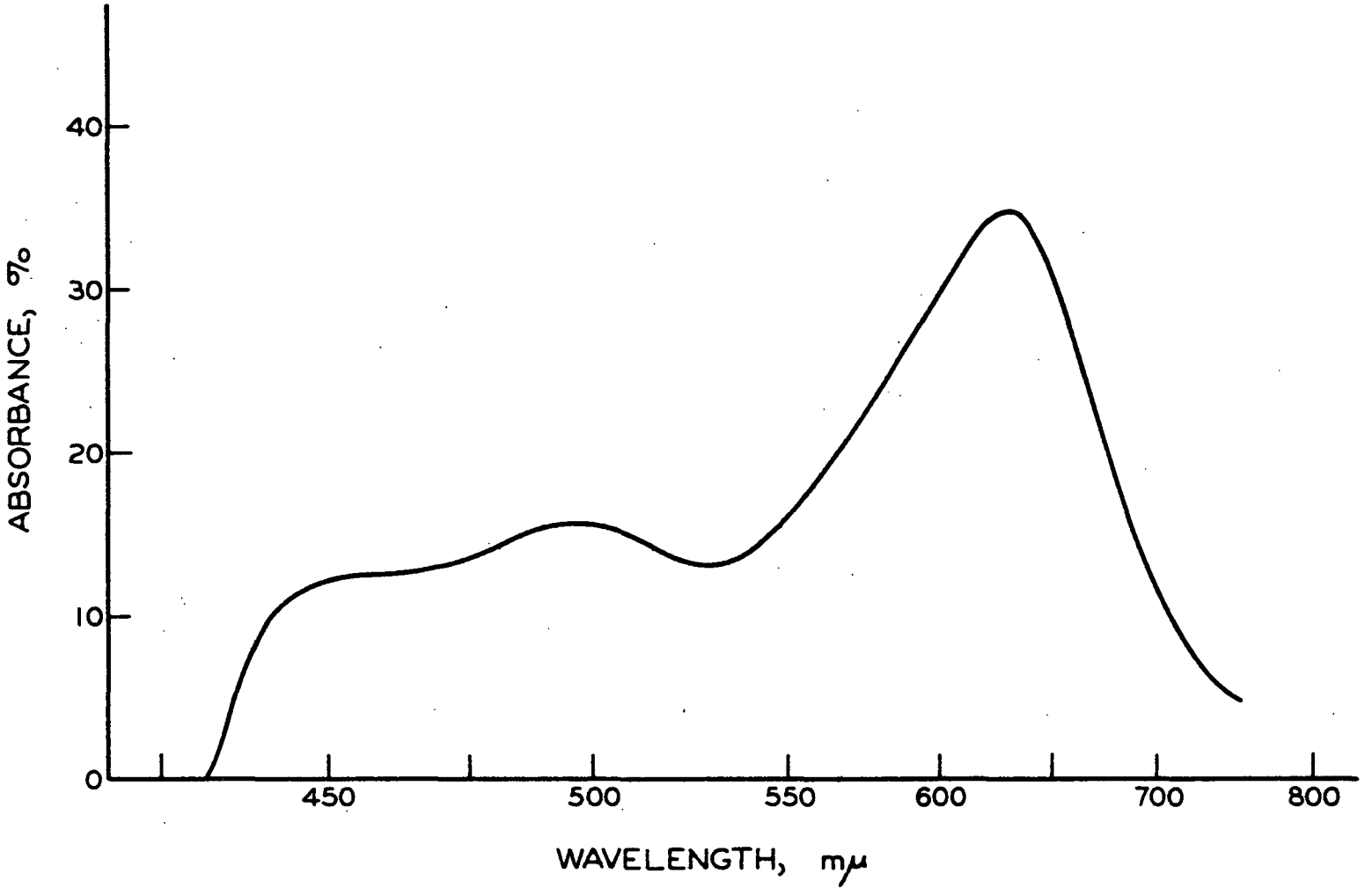

Figure 11. Relationship Between Wavelength and Absorbance for Anthrone Test

behavior was measured was cut from the pins with a razor blade and placed in a small test tube. It was hydrolyzed with 0.1 ml. of 27.5N sulfuric acid. Then 0.2 ml. of anthrone solution containing 0.0800 gram of anthrone per 50 ml. of 27.5N sulfuric acid was added. It was found that the most accurate procedure was to weigh the amounts of acid and anthrone added.

The test tubes were covered with teflon tops, heated for about four minutes in boiling water, cooled while being agitated for three minutes in ice water, and then allowed to stand about 28 hours before measuring the optical density. Because of the small volume of liquid used, special microcuvettes, as discussed by Lowry and Bessey (57) and Bonting (56), were used in the Beckman Model DU spectrophotometer to measure the optical density of the solutions at 625 mμ.

In order to apply the method to individual fibers, it was first necessary to calibrate it with amounts of bone-dried fibers which could be accurately weighed. The fibers were weighed and hydrolyzed in concentrations equivalent to those when individual fibers were used. One-tenth milliliter of fiber solution was reacted with 0.2 ml. of anthrone solution and the procedure previously described was followed. The calibration curve obtained with duplicate runs is presented in Fig. 12; it is seen to conform with Beer's Law in the region of interest. No difference could be detected between the calibration curves of springwood and summerwood fibers.

CRYSTALLINITY AND CRYSTALLITE ORIENTATION MEASUREMENTS

MICRODENSITOMETER

To obtain measurements of both crystallinity and crystallite orientation, Laue x-ray diffraction patterns were taken of the fibers. A microdensitometer

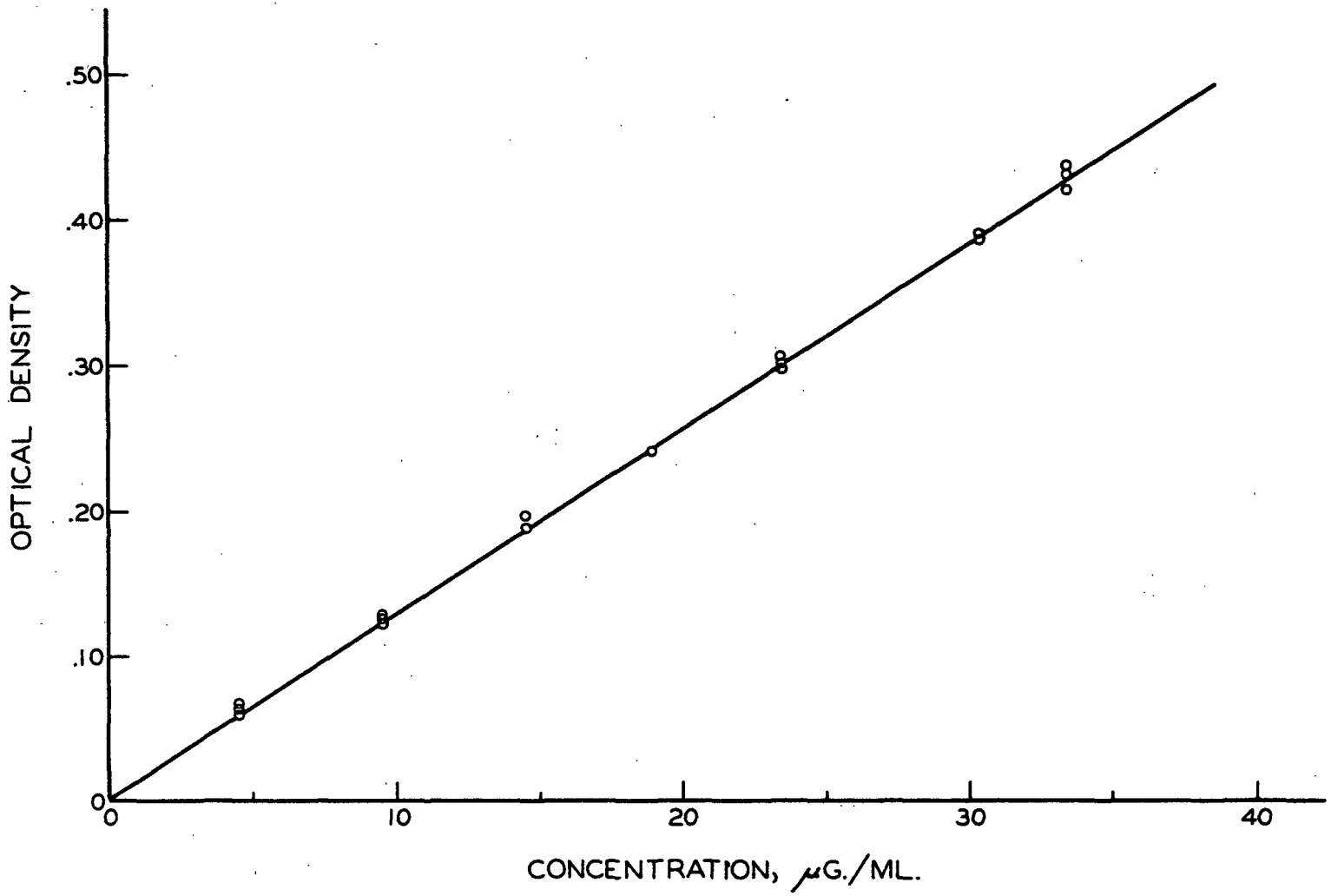

Figure 12. Calibration Curve for Anthrone Test

was built for quantitative analysis of the photographic film negative on which the diffraction patterns were obtained. A review of the literature produced many articles describing microdensitometers: Taylor (58) and Ronnebeck (59) adequately describe the main considerations involved. In general, the optical system consists of a light source followed by a slit and lens arrangement to focus the slit on the film. A second lens system is arranged on the opposite side of the film to focus the transmitted light on a photocell.

An over-all picture of the microdensitometer is shown in Fig. 13. A General Electric miniature oscillograph lamp (A) was used as the light source, which was focused on the film (B) using a microscope (C) with a 10X eyepiece and a 10X objective lens. A second microscope (D) was aligned with the first so that the illuminated portion of the film was in the middle of the field of vision. This microscope, which has the same lens system as the first, was focused on the film, and the amount of transmitted light was measured by placing the blue sensitive phototube (E), of a Densichron (F) over the eyepiece of the microscope. A pinhole placed between the eyepiece and the photocell allowed a 0.5-mm. diameter circle of the film to be viewed at any one time. The signal from the Densichron was transmitted to a Varian automatic recorder (G).

It appeared simplest to leave the optical system in a fixed position and move the film rather than the reverse. Figure 14 presents a detailed picture of the mechanism used to move the film in either a radial or circumferential direction. The mechanism consists of three parts: the upper ring (A), the lower ring (B), and the runners (C, D). The runners provide the radial or straight line movement, and the rings provide the circumferential or circular movement.

The runners on the two sides differ in their method of operation. On the left side a precision ground bar (C), which contained a row of ball bearings set

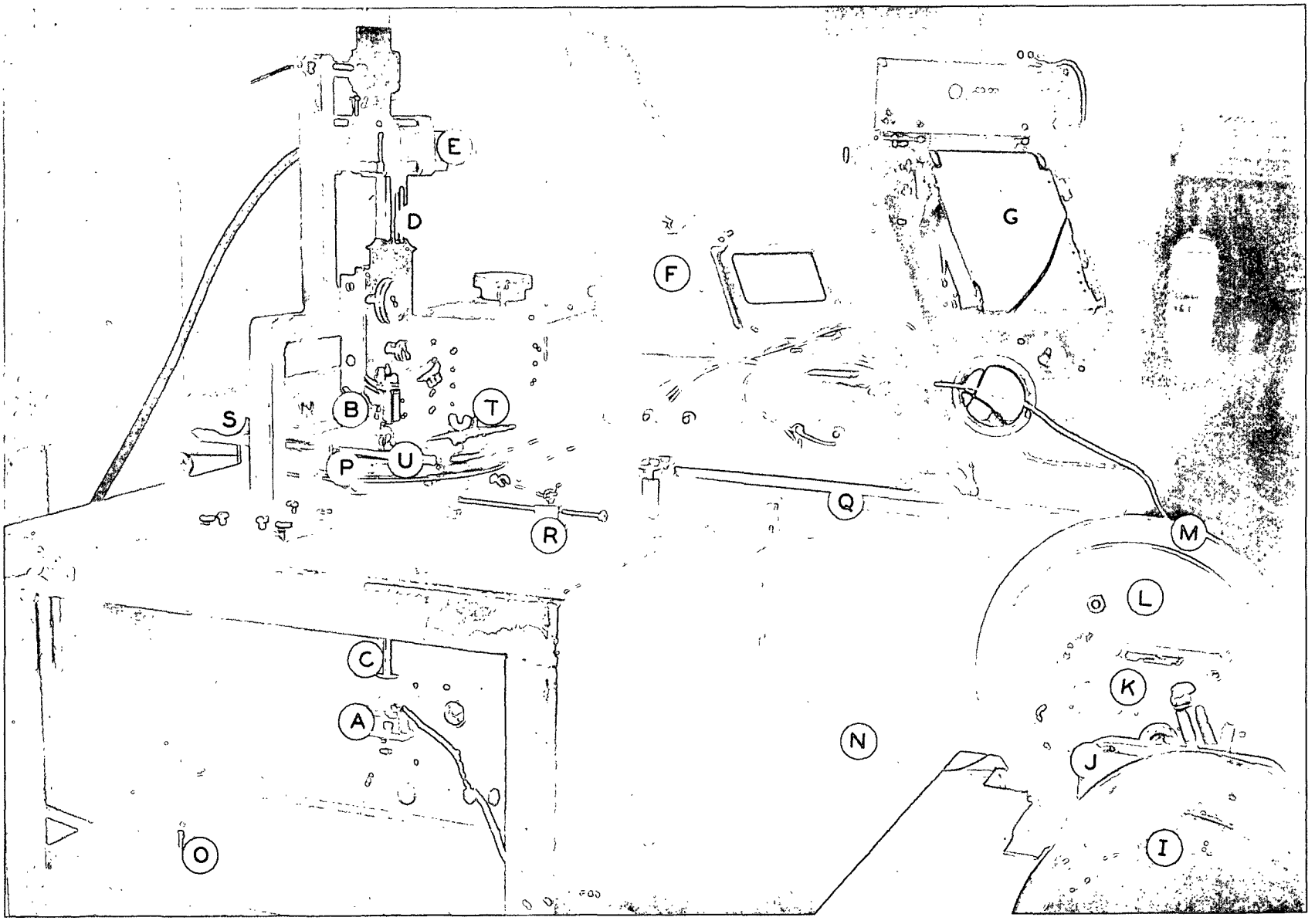

Figure 13. Microdensitometer

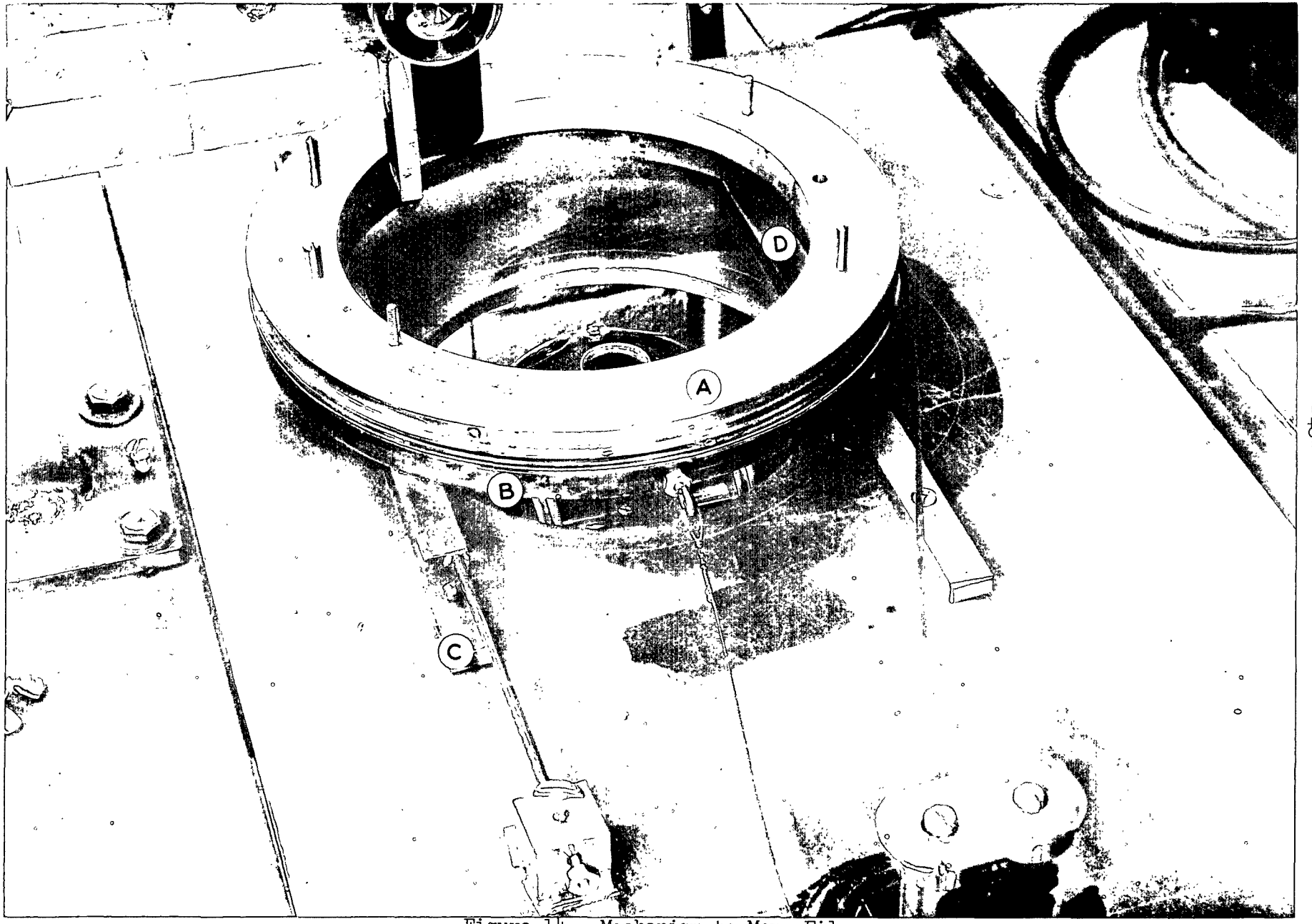

Figure 14. Mechanism to Move Film

in drilled holes, was screwed to the base plate. The ball bearings rotated in the holes and mated with a groove milled in the bar attached to the lower ring. This arrangement insured movement in a straight line. The runner arrangement on the right side consisted of a precision ground bar screwed to the base plate and a ball bearing soldered to the bar (D) attached to the lower ring. The runner on this side served just as a support, while the runner on the left side served as a support and a guide to insure straight line movement.

To provide for circular motion, identical grooves were machined into the two rings. Ball bearings, held by a retainer ring, were placed in the grooves, and this provided relatively low friction circular movement.

A constant speed drive, shown in Fig. 13, was used for both the radial and circumferential movement. A motor (I) was connected to a variable speed gear reducer (J), which in turn was connected to a second gear reducer (K). Two pulleys (L, M) were connected to a second gear reducer, one for each type of movement. For radial movement a small cable (N) was attached from the lower ring to the pulley. A counterweight (O) was attached to the back side of the lower ring to insure smooth movement, and a taper pin (P) locked the two rings together, so that there was no circumferential movement while the radial movement was taking place.

When a circumferential trace was desired, the cable was disconnected from its pulley, and the steel drive tape (Q) was attached to the second pulley. The tape was wrapped around a groove in the peripheral surface of the upper ring and anchored to the ring with a screw. To provide smooth movement, another counterweight was attached to the upper ring by a cable which occupied a second groove in the periphery of the upper ring. To prevent any radial movement while a

circumferential trace was taking place, a rod and lock screw arrangement (R) was attached to the runner on the lower ring.

The film holder (S), resting on the upper ring, was positioned by two taper pins (T), and it was held in place by two threaded studs with wing nuts (U). The film was sandwiched between two glass plates to insure that it was held flat. The film was prealigned on the film holder so that the center of the diffraction pattern was concentric with the rings, and so that the densest portion of the pattern was measured on a radial trace. To prealign the film on the film holder, a Plexiglas plate was scribed with a series of equally spaced concentric circles and radial lines. The film holder fitted over the Plexiglas plate, and the film was aligned visually with the aid of the circles and lines.

FILM CALIBRATION

The major part of the x-ray work in this thesis was done with individual fibers; to avoid extremely long exposure times it was necessary to obtain the fastest x-ray film available. In most films speed is obtained at a sacrifice of grain size, but this was unavoidable. Three types of film were calibrated: Kodak Type KK X-ray Film, Kodak Medical No-Screen X-ray Film, and Du Pont Xtra-Fast Medical X-ray Film No. 508. All calibrations took place with Cu Kα radiation, using a film-to-x-ray tube distance of 2.35 meters and operating the tube at 14 kilovolts and 8 milliamperes. Kodak Type KK was found to be the fastest, i.e., this film had the largest change in optical density for a constant amount of exposure, and its calibration curve is shown in Fig. 15. The curve is the same shape as those presented in Klug and Alexander (60) for x-ray films. All quantitative work in this thesis was done in the linear portion of this curve.

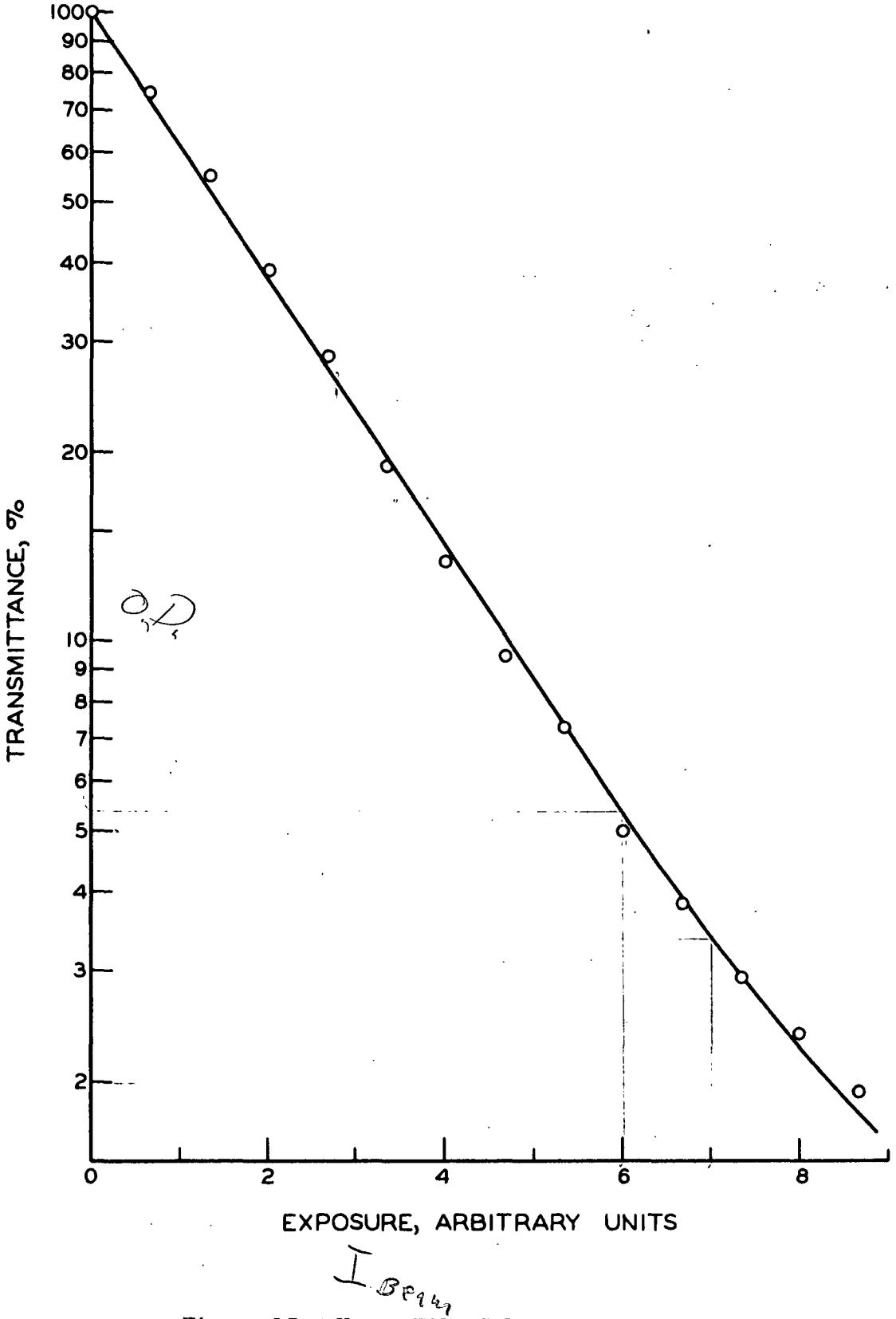

Figure 15. X-ray Film Calibration Curve

James and Higgins (61) discuss the behavior of photographic emulsions toward x-rays and the differences between x-rays and ordinary light.

FILM DEVELOPING PROCEDURE

The films used in the x-ray work were developed by the following procedure, which was chosen to give uniform reproducible development and maximum density. The developing, stop, and fixer solutions were placed in a constant temperature bath held at 20 ± 0.1°C. The film was placed in Kodak Rapid X-ray Developer for eight minutes, in a 1% by volume of glacial acetic acid stop bath for 30 seconds, in Kodak X-ray Fixer for 15 minutes, and finally in running water for 30 minutes. In all cases the film or bath was agitated to insure fresh solution on the emulsion at all times.

X-RAY CAMERA

All x-ray diffraction patterns were taken with a Norelco x-ray unit, using Cu Kα radiation obtained with the tube operating at 50 kilovolts and 20 milliamperes. In order to take Laue x-ray diffraction patterns of individual fibers, it was necessary to design and build the camera shown in Fig. 16. The x-rays emerged from the tube, passed through the nickel foil which served as a monochromator, and entered the collimator. The fiber ends were glued to a tab, and the fiber was suspended in the x-ray beam so that the x-rays were diffracted by the fiber. The undiffracted x-rays were caught by the beam catcher, and the diffracted x-rays exposed the photographic film. It was essential for the beam catcher to be aligned with the collimator, and adjustment was provided by oversized holes in the back plate. The fluorescent disk in the beam catcher was useful for aligning the beam catcher (lead glass protected the observer). The camera was evacuated while making a run so that scattering of the x-rays by air

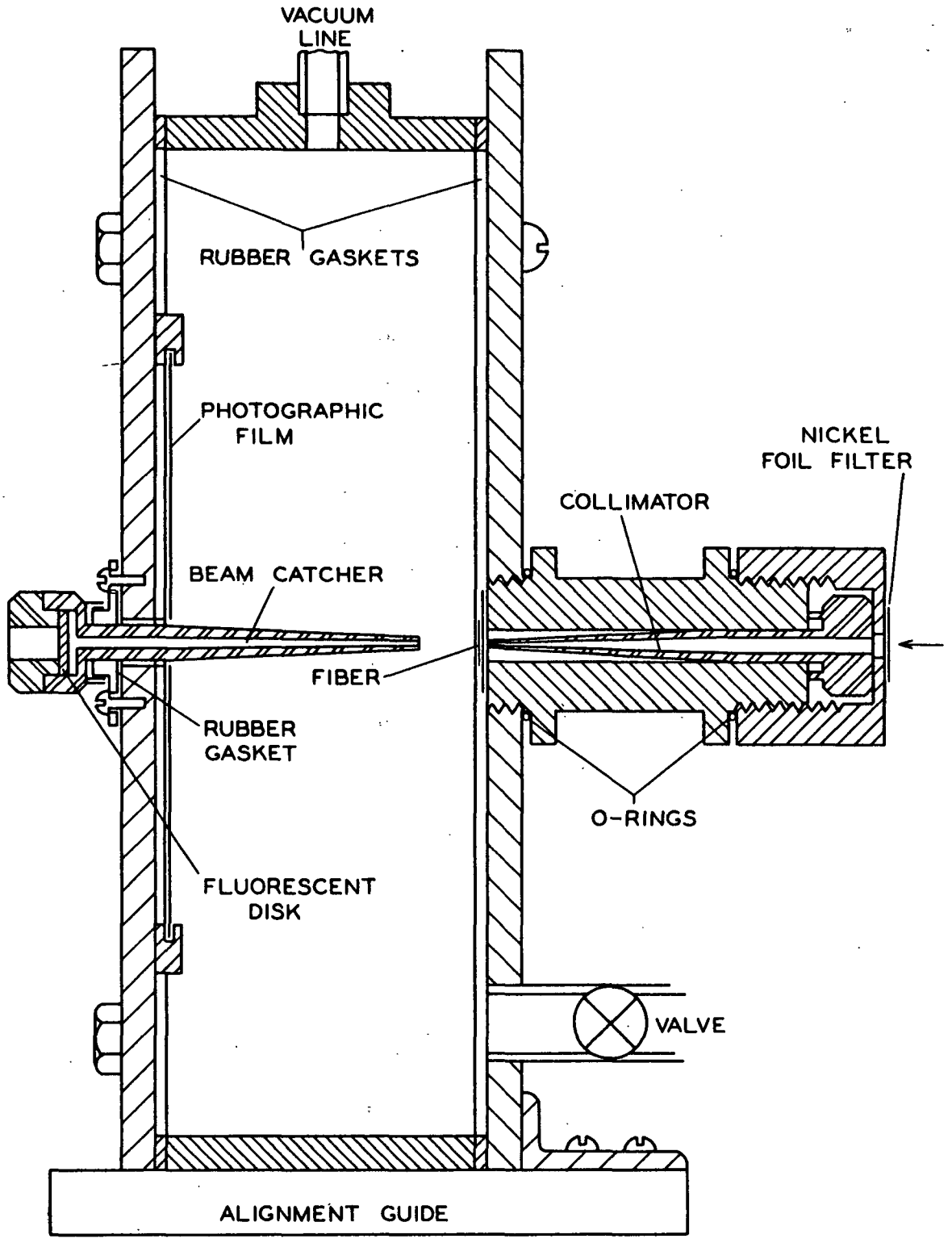

Figure 16. Single Fiber Laue X-ray Camera

was minimized. The whole camera was light-tight, and therefore no protective envelope was required around the film.

CRYSTALLINITY

A typical Laue x-ray diffraction pattern of a fiber is shown in Fig. 17. Eight spots are clearly visible on the pattern. The two spots farthest from the center of the film are caused by the 002 lattice diffraction, which is the most intense lattice diffraction for cellulose I. The other two spots along the same axis as the 002 arcs are caused by both the 101 and $10\bar{1}$ lattice diffractions. These two diffractions are not resolved due to the broadness of the peaks, which is caused by small crystal size and imperfections in the crystalline structure. The four less intense spots at a 45° angle relative to the other spots are caused by the 021 lattice diffraction.

In general, the crystallinity is related to the intensity of the arcs compared to the amorphous background. A strip at the top and bottom of the pattern is unexposed, so that the amorphous background is easily distinguishable. The crystallite orientation is related to the width of the arcs in a circumferential direction. A randomly oriented sample would have a series of concentric circles rather than a group of spots.

Many different methods have been proposed to measure the crystallinity and degree of order of cellulosic fibers. The x-ray methods are more useful in rating fibers according to their relative degree of crystallinity, rather than in calculating a percentage crystallinity. Several different methods have been proposed to estimate the relative crystallinity from diffraction patterns. One common method is the crystallinity index proposed by Segal, Creely, Martin, and

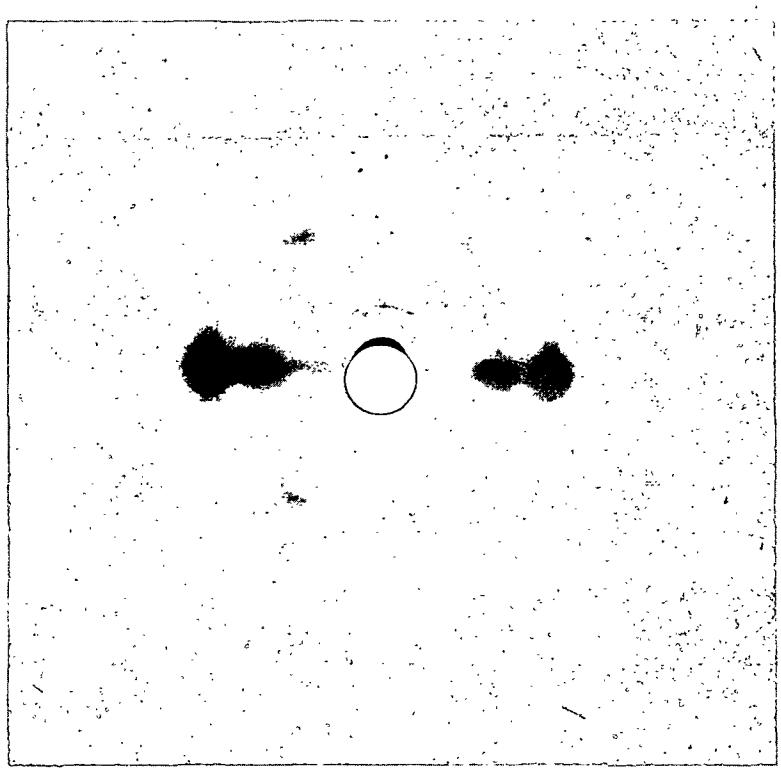

Figure 17. Laue X-ray Diffraction Pattern of a Summerwood Fiber, Which Is Typical of Those Obtained by Drying Under No Load

Conrad (62). This crystallinity index is defined as

$$CrI = (I_{002} - I_{am}) \cdot 100/I_{002},$$

where CrI is the crystallinity index, I_{002} is the maximum intensity of the 002 lattice diffraction, and I_{am} is the minimum intensity between the 002 and 101 arcs.

Gjonnes, Norman, and Viervol (63) have proposed a method of measuring crystallinity based on measuring the integral half width of the 002 lattice diffraction. They suggested that the broadening of the peak was due to small particle size and lattice distortion; and therefore, if there was a change in the crystalline structure, this would appear as a change in the integral half width.

The integral half width is calculated by fitting the 002 lattice diffraction to a Cauchy distribution, which has the form

$$I = A_0 \frac{A_1}{A_1^2 + (x - A_2)^2},$$

where I is the intensity, A_0 is a constant, $2A_1$ is the width at half height, x is the 2θ value, and A_2 is the 2θ value at the maximum I.

Hermans and Weidinger (64, 65) based a method of determining the relative crystallinity on estimating the total diffraction from the crystalline and amorphous regions. The crystalline material was estimated as the area of crystalline interferences above the background for a radial scan. The amorphous material was measured as the maximum height of the background curve corrected for scattering of the x-rays by air. This method has been further refined by Hermans and Weidinger (66), but the principle is essentially the same.

The crystallinity was calculated by both the crystallinity index and the integral half width methods. The Hermans and Weidinger method was not used because it offered no apparent advantage over the other two methods. The film was first placed in the microdensitometer, the unexposed portion of the film was adjusted to 100% transmission on the Densichron, and then a radial trace was taken. The maximum of the 002 peak was set at a 2θ angle of 22.8 degrees, and the rest of the angles were calculated with respect to this. The film calibration curve permitted the change from the percentage transmission values to the intensity values, and the latter were corrected for the film factor and the polarization factor. The crystallinity index was easily calculated, and the integral half width was calculated by a regression analysis to fit the data between the 2θ values of 20 and 25.5 degrees to the Cauchy distribution.

The film factor changed the film intensities to those which would be recorded by a goniometer at the same 2θ angle. A schematic diagram of the film and goniometer position is presented in Fig. 18. Essentially, the film factor corrects for the film not being equidistant from the fiber being x-rayed at all 2θ values. It can be shown that the film factor equals $\cos^3 2\theta$, and therefore the intensity obtained from the microdensitometer recording was divided by $\cos^3 2\theta$ at each 2θ value.

The polarization factor was discussed by Klug and Alexander (67) and equals $(1 + \cos^2 2\theta)/2$. Therefore, the intensity of the recording must also be divided by this factor. The fiber absorption factor was calculated and found to be negligible. Figure 19 shows the effect of correcting for both the film and polarization factors.

Most of the work done in this thesis was on never-dried fibers; however, some work was done to see if there was any difference between the mechanical properties of once-dried and never-dried fibers dried under an axial tensile load. In conjunction with this, it was desirable to see if there were any large differences between the crystallinity of never-dried and once-dried fibers. Therefore, it was necessary to develop a technique to x-ray fibers in the wet state.

The technique decided upon was to mount the wet fiber between two 0.00025-inch caliper films of mylar. Between the films there was also a thin layer of water which kept the fiber saturated. These patterns could not be run under vacuum, because the water vapor would diffuse through the mylar and allow the fiber to dry. Instead, helium was bubbled through a packed water column to obtain a nearly saturated gas. The saturated helium entered the top of the camera, and the valve at the bottom permitted the gas to escape. The scattering of x-rays by helium is only 4% of that by air. Figure 20 presents the pattern

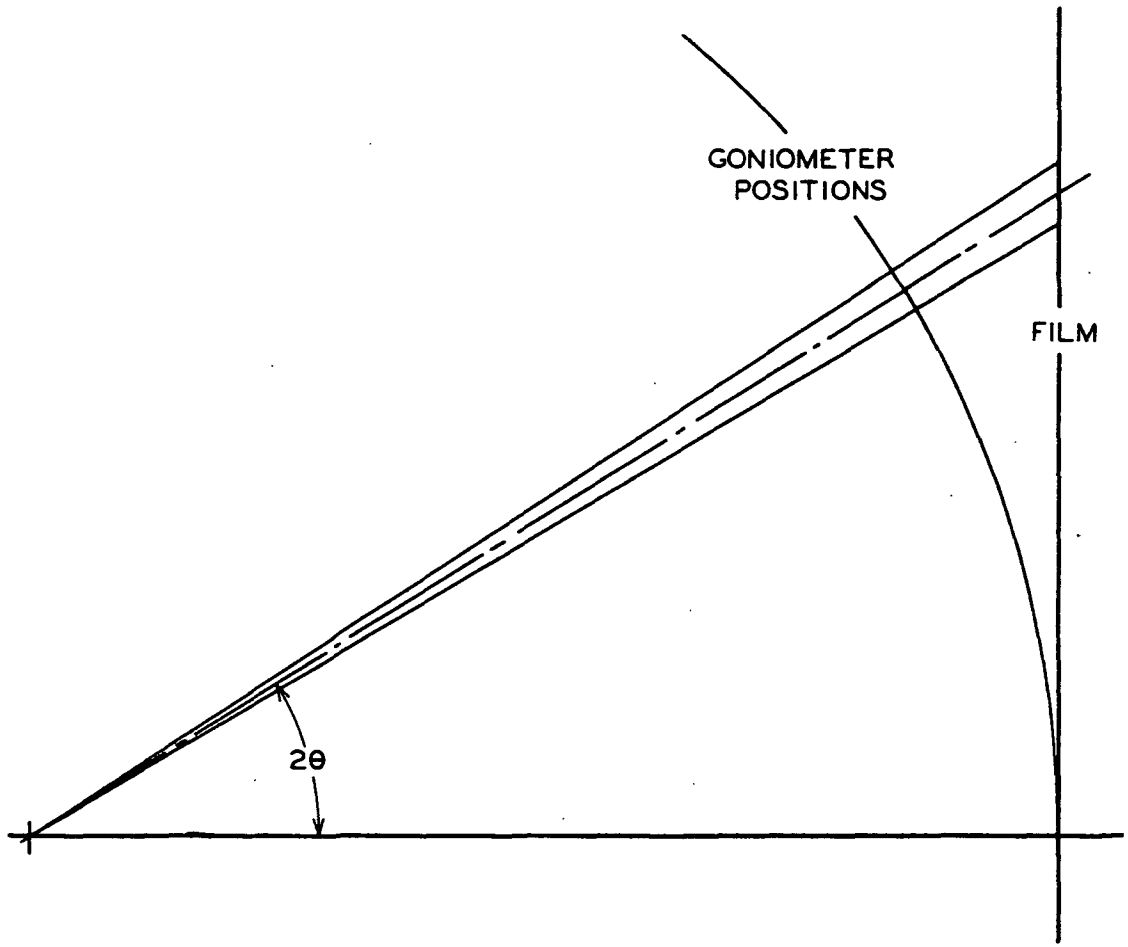

Figure 18. Schematic Diagram Showing Difference Between Film and Goniometer Positions

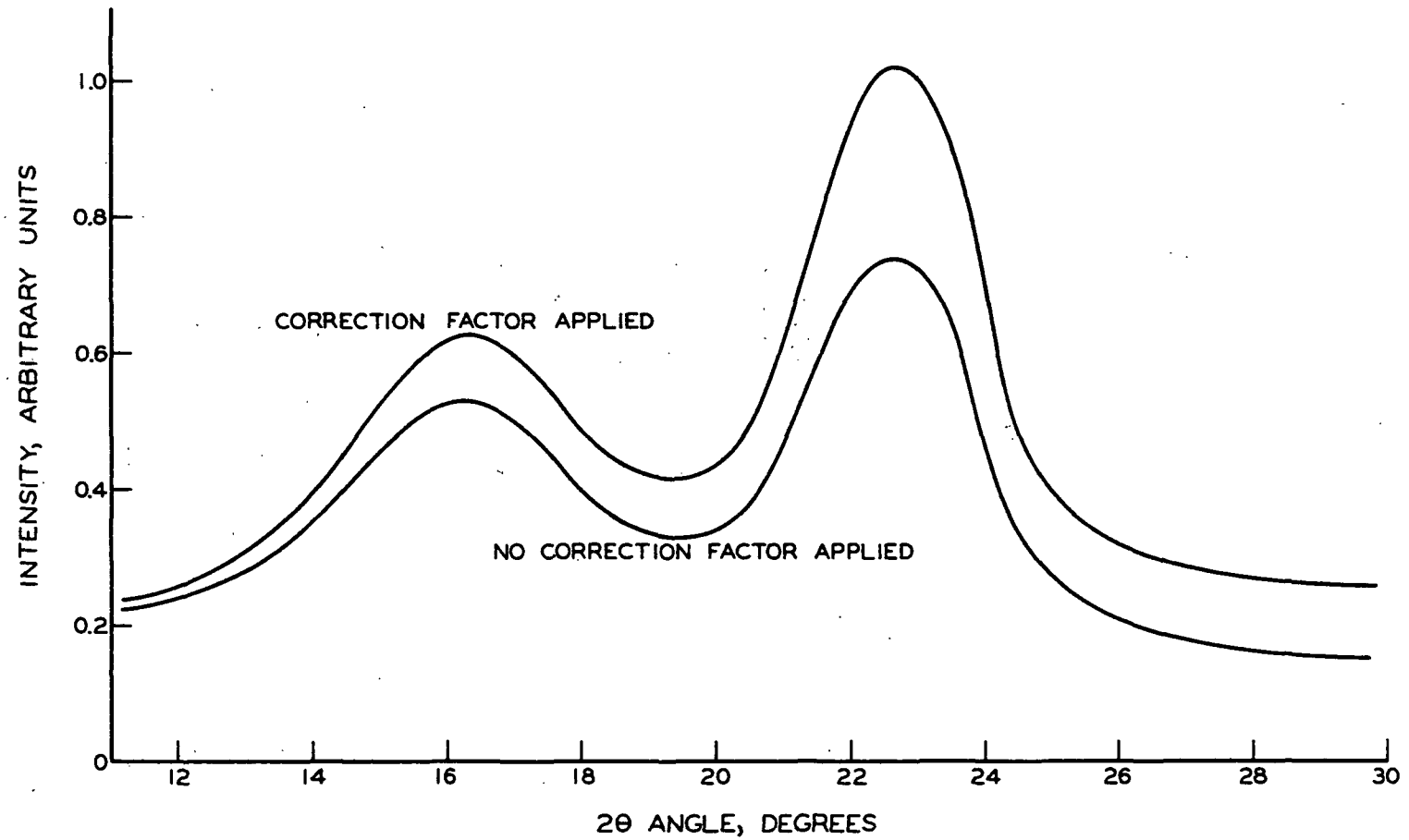

Figure 19. Effect of Correction Factors on Radial Intensity Distribution

Figure 20. Laue X-ray Diffraction Pattern of a Parallel Group of Wet Summerwood Fibers

of a parallel group of wet fibers. The patterns of water and mylar are superimposed on that of cellulose. The water is represented by the broad halo outside the 002 arcs, and the mylar by the ring through the 101 arcs. Therefore, to obtain the pattern of cellulose, the water and mylar patterns must be subtracted. Radial microdensitometer traces were taken along the cellulose pattern and at four angles which were not along the cellulose pattern. The pattern of cellulose was obtained by subtracting the intensity of the radial trace which did not contain cellulose from the intensity of the radial trace containing cellulose. Unfortunately, any random amorphous scatter from the cellulose was also subtracted, and the limitations of this procedure will be discussed in the results.

CRYSTALLITE ORIENTATION

Several methods are presented in the literature for the calculation of crystallite orientation. The most commonly used method in the textile industry was originally proposed by Sisson (37); it measures the orientation as the angle at which either 40 or 50% of the maximum intensity occurs.

Hermans (68) proposed an orientation factor based on his work with the optical birefringence and x-ray diffraction patterns of fibers. He first defined an angle by the equation

$$\sin^2\alpha_m = \int_0^{\pi/2} F(\alpha) \sin^3\alpha \, d\alpha$$

where $F(\alpha)$ is the relative intensity with the maximum intensity set equal to one. The angle α_m corresponds to the orientation angle all the molecules in a fiber would have in order to produce the same birefringence as the fiber with its orientation given by the function $F(\alpha)$. Herman's orientation factor is then calculated by the equation

$$f = 1 - 1.5 \sin^2\alpha_m$$

From Hermans. Contribution to the Physics of Cellulose Fibers. Elsevier 1946. p. 138

An analysis of the orientation factor shows that the latter will vary from 1.00 for a fiber with all molecules parallel to the fiber axis to 0.00 for a fiber with completely random orientation.

De Luca and Orr (69) have proposed a method of determining the helical angle from a circumferential scan of the 002 lattice diffraction. Their method is a quantitative treatment of an idea originally proposed by Sisson (70). The observed circumferential scan is assumed to be the sum of two normal distributions having maxima at plus and minus the spiral angle. By selecting any two

points on the observed circumferential scan, the spiral angle and standard deviation of the normal curve can be calculated. De Luca and Orr selected the points at 40 and 50% of the maximum intensity. Their results indicated that the calculated spiral angle was approximately one half the 50% intensity angle proposed by Sisson (37).

The method used in this investigation was to fit the whole circumferential scan to a normal distribution rather than dividing it up into two normal distributions as suggested by De Luca and Orr. The standard deviation of the normal curve is a measure of the width of the curve and, therefore, a measure of orientation. Actually, it is the angle at 60.6% of maximum intensity. The method consisted of first calculating the accumulative area under the circumferential intensity curve as the angle went from -90 to +90°. The accumulative area was then normalized to change it to accumulative probability. Davies (71) stated that the accumulative probability $\underline{P}(\underline{u})$ is

$$P(u) = (1/\sqrt{2\pi}) \int_{-\infty}^{U} \exp\ (-u^2/2)du.$$

The variable $\underline{u}$ equals

$$u = (x - \mu)/\sigma$$

where $\underline{x}$ is the value of an observation, μ is the universe mean of the observations, and σ is the universe standard deviation. By a trial and error solution of a series approximation, the value of $\underline{u}$ can be calculated for each value of accumulative probability. The values of $\underline{x}$ can then be plotted against the corresponding $\underline{u}$ value, and the data are fitted to a straight line by the method of least squares. The slope of the line is equal to the standard deviation of the normal curve, and the intercept is equal to the mean. Only the data with

probability values between 15 and 85% are used, since the tails of the circumferential scan do not conform to a normal distribution. Figure 21 shows the actual circumferential scan and the fitted normal distribution.

Table III gives the results for the orientation factor calculated by the different methods for a fiber which has been dried under load. This preliminary work was performed to evaluate the method which is the most reproducible and sensitive. To evaluate Herman's method properly the standard deviation of $\alpha_{\underline{m}}$ must be considered rather than the standard deviation of Herman's orientation factor itself, because for highly oriented fibers it can be seen that $\alpha_{\underline{m}}$ will change more on a percentage basis than the orientation factor itself. The large standard deviation in $\alpha_{\underline{m}}$ is due to its calculation being sensitive to the tails of the scan, where the intensity measurements are least accurate. Ellis and Warwicker (72) have recently reached a similar conclusion about Herman's method.

TABLE III

COMPARISON OF DIFFERENT METHODS OF ORIENTATION MEASUREMENT

	Average[a]	Standard Deviation	Standard Deviation, %
Angle at 50% of maximum intensity	7.68°	0.30	1.97
Angle at 40% of maximum intensity	9.06°	0.76	4.22
$\alpha_{\underline{m}}$ from Herman's orientation factor	5.88°	0.80	13.65
Herman's orientation factor	0.9842	0.0046	0.46
Standard deviation of normal curve	8.06°	0.25	3.17

[a]This represents the average of four individual determinations.

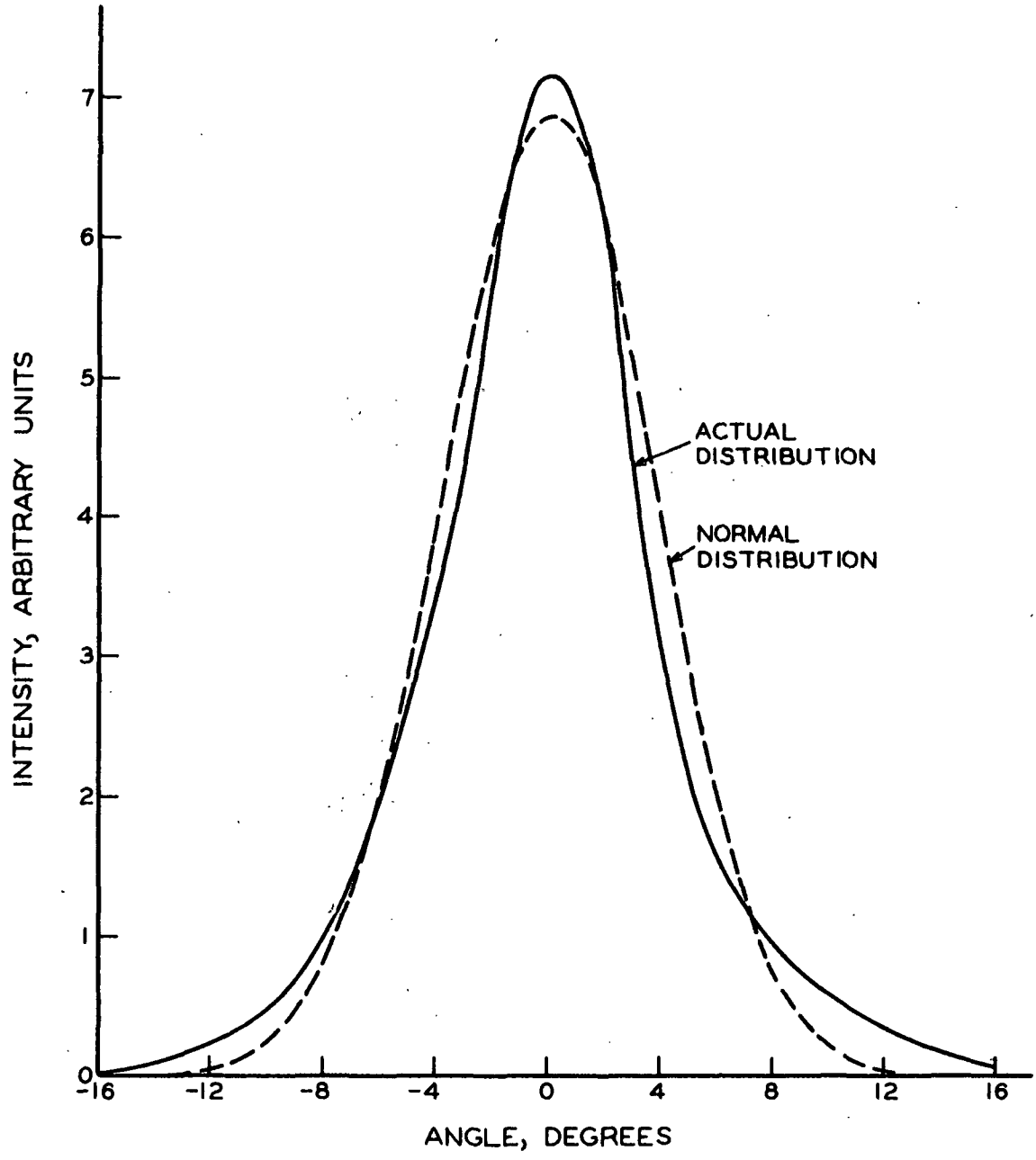

Figure 21. Comparison of Fitted Normal Curve and Actual Circumferential Scan

It is interesting to note the difference in the standard deviation of the 40 and 50% maximum intensity angles. This difference is surprising, since the points measured are close together. It should be pointed out that the measurement of each of these angles is dependent only on three points of the whole scan. Therefore, any error in measuring one of the points will produce the corresponding error in the intensity angle. The 2% standard deviation of the 50% intensity angle is quite small considering all the possible sources of error.

The method of fitting the circumferential scan to a normal distribution has the advantage of equally considering each point on the scan. The standard deviation with this method was slightly higher than the standard deviation with the 50% intensity angle method. However, this method was favored for the measurement of orientation, because it considered all the data points rather than just a preselected three, as do the intensity angle methods.

It should be noted that no results were given in Table III for the method of De Luca and Orr which evaluated the spiral angle. If the scan obtained is assumed to be the sum of two normal curves, then its shape must have several characteristics. First, the observed scan must be broader than a normal curve drawn through it in the regions of high intensity, and secondly the observed scan must be narrower than a normal curve drawn through it in the regions of low intensity. If Fig. 21 is re-examined, the observed scan has just the opposite characteristics of those required by the method of De Luca and Orr. It should be pointed out that the fibers to which De Luca and Orr applied their method were less oriented than the fibers used in this study; the smallest 50% intensity angle was about 20°.

EXPERIMENTAL DATA AND DISCUSSION OF RESULTS

CHARACTERIZATION OF PULP

The first step in this study was to characterize the pulp which was used. The data in Table IV give the yield and chemical analysis of the pulp. The results of the sugar analysis were quite similar to those reported by Leopold (23) for a loblolly pine holocellulose. It is interesting to note that the summerwood and springwood fibers are quite similar in chemical composition, and this is the reason for both types of fibers giving the same calibration curve with the anthrone test.

TABLE IV

CHEMICAL PROPERTIES OF LONGLEAF PINE HOLOCELLULOSE PULP

Extractives and moisture	46%	
Yield[a]	56%	
	Summerwood, %	Springwood, %
Klason lignin[b]	0.3	0.4
Total sugars[c]	90.6	91.6
Glucan	70.5	71.8
Xylan	5.98	6.46
Mannan	12.20	10.90
Arabanan	1.12	1.42
Galactan	0.79	1.04

[a]Based on extractive- and moisture-free wood.

[b]Institute Method 428.

[c]Method of Saeman, J. F., Moore, W. E., Mitchell, R. L., and Millett, M. A., Tappi 37:336(1954).

FIBER-DRYING FORCES IN A SHEET

Before commencing work on drying fibers under load, it was desirable to estimate the magnitude of the loads under which the fibers in a sheet are dried. By applying Van den Akker's theory (73) for the mechanical properties of a sheet, the contribution of each of the fibers to supporting the external load can be estimated by the method outlined in Appendix I. Van den Akker's theory shows that the fibers oriented in the direction of external loading will be under the largest tensile load, that the fibers oriented at 90° to the direction of external loading will be under the largest compressive load, and that those fibers oriented between the two principal directions will be under intermediate loads.

The work of Schulz (74) and Brecht and Pothmann (75) has given information on the stresses developed in a sheet when it is dried. Schulz dried sheets at a constant strain and measured the maximum stress developed when the sheet dried. He found that the maximum tension developed was 1.5 kg./sq. mm., which, using the method outlined in Appendix I, would lead to drying loads of 1.6 grams for summerwood and 1.2 grams for springwood on the fibers used in this thesis. Brecht and Pothmann dried sheets under constant stress and found that the largest stress which the sheet could support was 0.3 kg./sq. mm. This leads to drying loads of 0.32 gram for the summerwood fibers and 0.24 gram for the springwood fibers.

Many assumptions were made in the calculation of these drying loads; however, it is doubtful if the calculated loads could be in error by as much as a factor of two. It was decided to dry the summerwood fibers under loads of one, three, and five grams and to dry the springwood fibers under loads of one and three grams.

ELONGATION BEHAVIOR WHEN FIBERS ARE DRIED UNDER LOAD

When fibers are dried under load, it is interesting to follow their elongation behavior during drying. From the drying procedure previously outlined, it can be seen that all elongation measurements were relative to the elongation of the wet fiber under a 1-gram load being set equal to zero. This 1-gram load was needed to straighten the fiber and to steady the movable clamp because of vibrations in the room.

The results for the average elongation behavior of the summerwood fibers dried under various loads are presented in Table V, and the elongation of a typical fiber is illustrated in Fig. 22. The wet fiber initially extended by an amount related to the applied load, after which creep occurred. The amount of creep was related to the applied load. Creep was measured for fifteen minutes; the water was removed, and drying commenced.

During the initial stages, an unexpected sudden extension occurred. To illustrate the rapidity of this extension, the elongation data of a typical fiber are presented in Fig. 22. This sudden extension was examined more thoroughly by observing the fiber with a microscope while simultaneous elongation readings were taken. When the water was drained, several droplets clung to the fiber. As these droplets evaporated, no elongation took place; the fiber appeared to be transparent and fully water-saturated. The moment the droplets had completely evaporated, the sudden elongation commenced and the fiber became less transparent. This loss of transparency apparently was caused by drying; however, it was not possible to judge at which stage of drying the extension stopped. For any one fiber this elongation took place over a period of 30 to 60 seconds, and it occurred while the fiber apparently was shrinking in cross section. Because

TABLE V

ELONGATION DATA DURING DRYING FOR SUMMERWOOD FIBERS

Schedule of Reading	Elongation, %[a] 1-Gram Load Av.	1-Gram Load S.D., %[b]	3-Gram Load Av.	3-Gram Load S.D., %	5-Gram Load Av.	5-Gram Load S.D., %	Once-Dried 5-Gram Load Av.	Once-Dried 5-Gram Load S.D., %
1.0 gram wet	0.00	--	0.00	--	0.00	--	0.00	--
Loaded wet	0.00	--	0.56	28.7	0.94	28.9	0.94	24.5
+ 3 min.	0.01	46	0.59	28.8	1.00	28.5	0.99	24.2
+ 9 min.	0.04	45	0.63	28.9	1.04	28.3	1.02	23.8
+15 min.	0.05	40	0.64	28.6	1.05	28.0	1.04	24.1
Water removed								
+ 1 min.	0.06	37	0.65	28.9	1.06	27.8	1.06	23.4
+ 2 min.	0.12	80	0.74	36.0	1.13	28.4	1.16	24.8
+ 3 min.	0.15	80	0.79	33.4	1.21	29.2	1.18	25.4
+ 6 min.	0.13	100	0.77	34.1	1.19	30.0	1.15	26.8
+ 9 min.	0.10	128	0.75	35.2	1.17	30.9	1.13	27.1
+15 min.	0.08	168	0.73	36.6	1.14	31.6	1.12	27.4
1.0 gram dry	0.08	178	0.52	50.5	0.78	40.7	0.76	34.2
+ 3 min.	0.07	190	0.51	50.7	0.75	41.3	0.73	34.9
Number of fibers tested	39		41		109		40	

[a]All fibers were tested at a 3-mm. span.

[b]Standard deviation as defined in Davies (71).

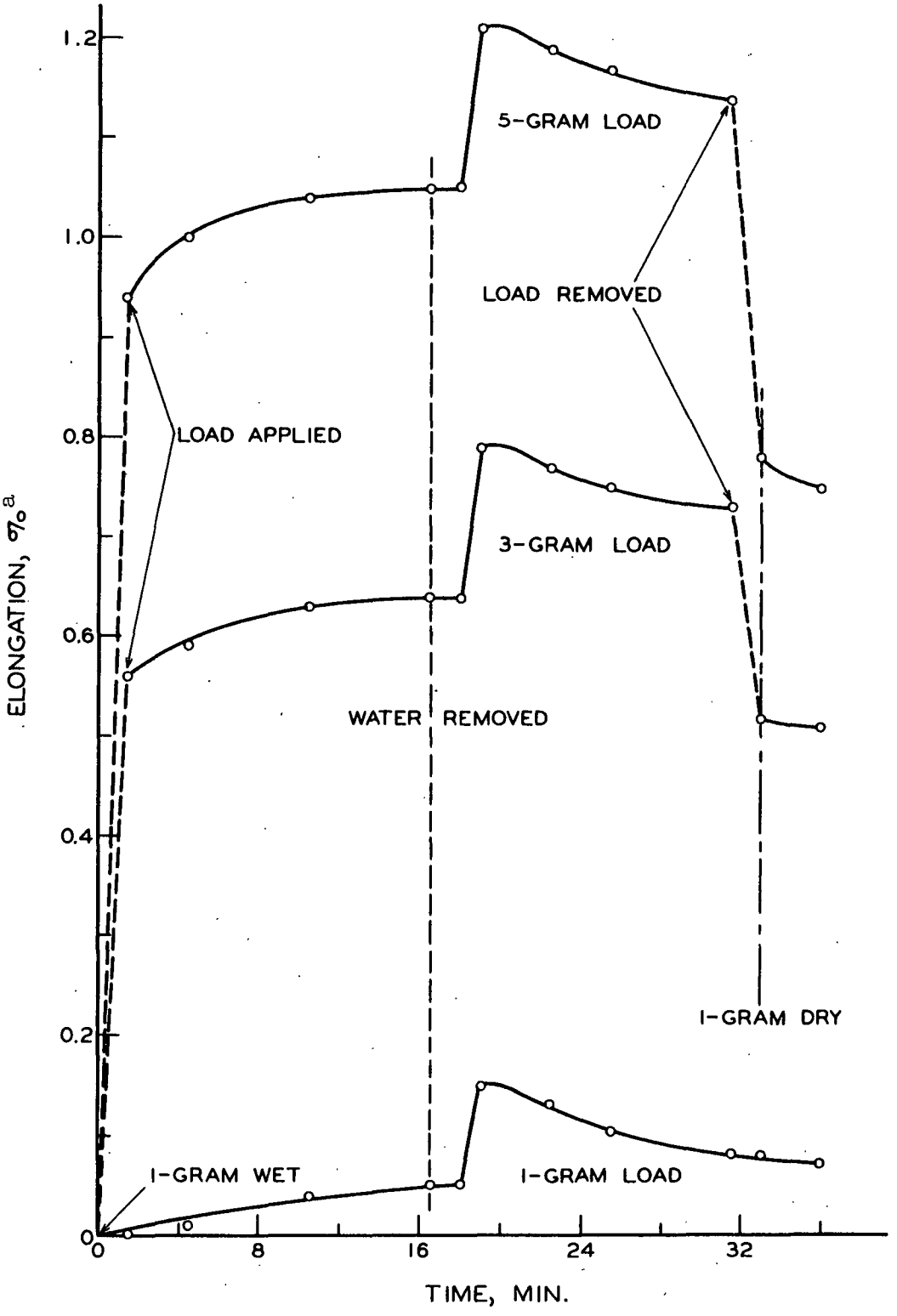

Figure 22. Elongation Behavior During Drying of Summerwood Fibers

[a]All elongation measurements are relative to the fiber length for a 1-gram load on the wet fiber.

of the variations in the time required for the droplets to evaporate from the fiber, the extension does not appear to be as sudden when the average elongation data are examined. It should be noted that the extension occurred in all fibers tested and that the extension was quick.

It was important to be certain that this extension was not due to an end effect at the point of clamping or to fiber slippage in the jaws. Therefore, fibers were dried at a one-millimeter span, and it was observed that the same percentage elongations occurred. Thus, it can be concluded that this is a real effect. It should be pointed out that this sudden extension cannot be due to surface tension effects on the apparatus, because the extension occurred a minimum of 30 seconds after the water had been completely drained.

It is interesting to note that the amount of the sudden extension observed at the beginning of drying did not vary greatly with the drying load but was the same for the 3 and 5-gram loads and was somewhat less for the 1-gram load. The implications of this and the reasons for the sudden extension will be discussed later.

After the sudden extension occurred, the commonly reported shrinkage took place. When the load was removed, the fiber contracted, and a small amount of creep recovery took place. The permanent set put in the fiber was related to the drying load that was used. The elongation data on loading the wet fiber and unloading the dry fiber indicated that the Young's modulus of the dry fiber was about 2.5 times the Young's modulus of the wet fiber.

It is interesting to compare the results given in Table V for never-dried fibers and fibers that had been once-dried without a load, rewet, and then dried

under a load. No significant difference can be seen in the results of the never-dried and once-dried fibers.

The results for the elongation behavior of the springwood fibers are shown in Table VI and Fig. 23. Simple calculations show that the springwood fibers have a much lower Young's modulus in the wet state than the summerwood fibers. Also, the sudden elongation at the commencement of drying for the springwood fibers was about twice that for the summerwood fibers, and for springwood this elongation was about the same magnitude for both the 1 and 3-gram drying loads. In general, the elongation behavior during drying was the same for both springwood and summerwood fibers, but the magnitudes of the elongations were different.

There appear to be at least two possible reasons why a fiber undergoes a sudden elongation at the commencement of drying. First, consider what happens when a swollen structure shrinks in cross section due to the evaporation of water, by assuming the fibrils to have a circular, helical shape. In Appendix II the equations of a circular helix are derived. The length of the fibril per revolution is represented by

$$s = 2\pi r/\sin \theta,$$

where s is the fibril length per revolution, r is the radius of the helix, and θ is the angle the fibril makes with the fiber axis. The length of the helix along the fiber axis is given by

$$Z = 2\pi r/\tan \theta,$$

where Z is the length along the fiber axis per revolution of the helix,

TABLE VI

ELONGATION BEHAVIOR DURING DRYING FOR SPRINGWOOD FIBERS

Schedule of Reading	Elongation, %[a] 1-Gram Load Av.	1-Gram Load S.D., %	3-Gram Load Av.	3-Gram Load S.D., %
1.0 gram wet	0.00	--	0.00	--
Loaded wet	0.01	82.7	1.87	14.3
+ 3 min.	0.04	57.2	1.93	14.0
+ 9 min.	0.07	48.6	1.97	14.0
+15 min.	0.09	69.0	1.99	13.9
Water removed				
+ 1 min.	0.10	63.0	2.00	14.2
+ 2 min.	0.29	8.21	2.12	15.1
+ 3 min.	0.51	70.4	2.29	15.4
+ 6 min.	0.53	67.8	2.31	15.2
+ 9 min.	0.52	67.3	2.29	15.6
+15 min.	0.50	70.7	2.27	15.8
1.0 gram dry	0.50	70.4	1.95	17.7
+ 3 min.	0.50	71.2	1.93	17.7
Number of fibers tested	39		39	

[a]All fibers were tested at a 3-mm. span.

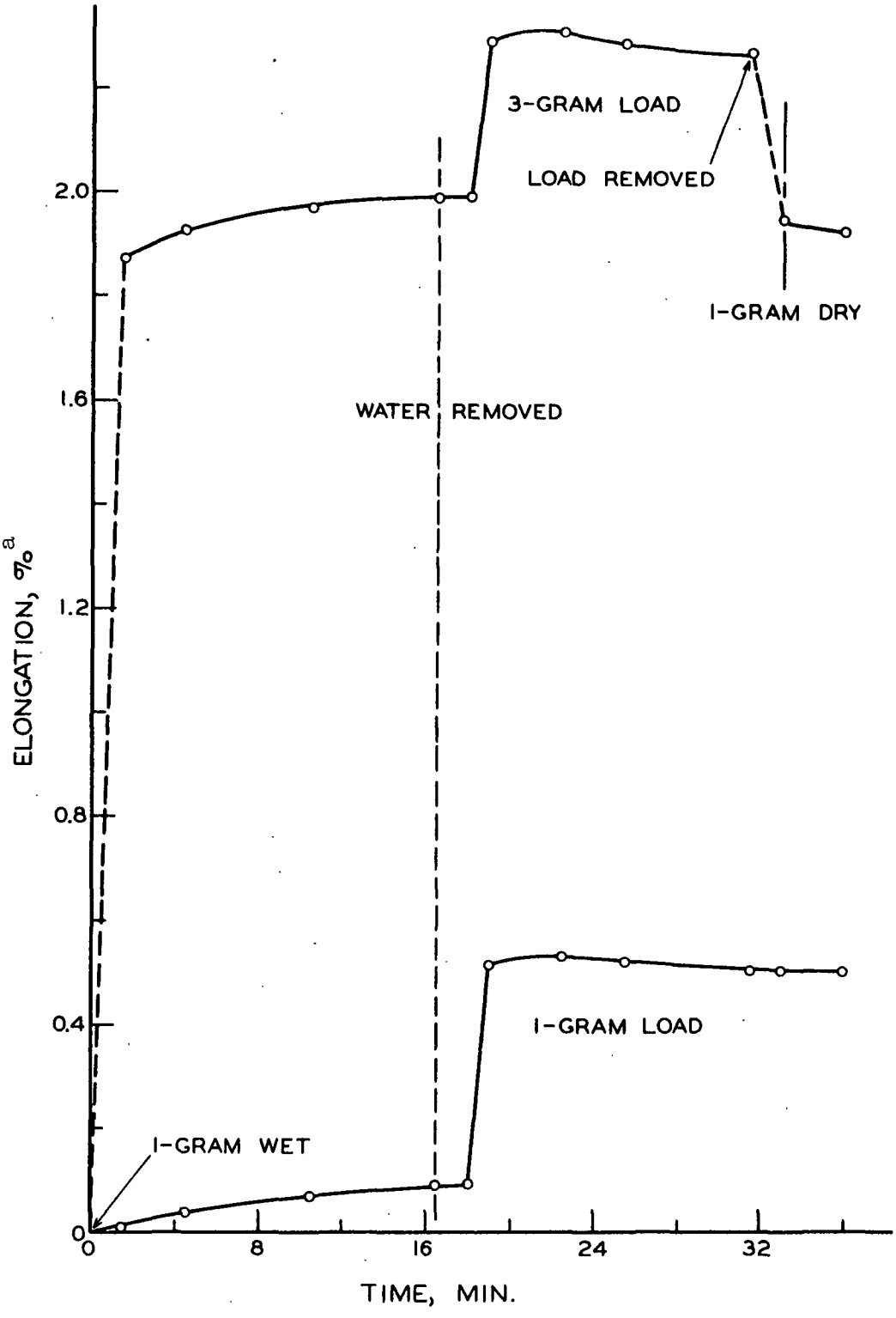

Figure 23. Elongation Behavior During Drying of Springwood Fibers

[a]All elongation measurements are relative to the fiber length for a 1-gram load on the wet fiber.

When the fiber shrinks in cross section, the radius of the helix becomes smaller. If the fibril length and the number of revolutions of the helix along the fiber are assumed to remain constant, sample calculations will show the magnitude of elongations due to this mechanism. Weidner (76) and Page and Tydeman (77) have shown the width of fibers to shrink 10 to 20% on drying from the wet state, and x-ray data on the springwood and summerwood fibers used in this thesis show orientation angles of about 14 and 8°, respectively. Sample calculations show that, assuming an initial orientation of 8° and a shrinkage in diameter of 20%, the fiber will extend 0.36%; assuming an initial orientation of 14° and a shrinkage of 20%, the fiber will extend 1.11%; and assuming an initial orientation of 14° and a shrinkage of 10%, the fiber will extend 0.59%. These extensions are of the correct order of magnitude; an extension of 0.15% was observed for summerwood fibers and 0.35% for the springwood fibers.

These calculations are based on the radial shrinkage of the fibrils at the outside of the fiber. It has not been ascertained if the fibrils toward the lumen undergo the same percentage radial shrinkage as those at the outside. However, the order of magnitude predicted is in agreement with that determined experimentally.

This extension analysis leads to two interesting conclusions. First, the amount of extension should be relatively independent of the drying load. Second, the amount of extension should be related to the initial fibril angle. The results showed that the extension was not strongly dependent on drying load but was dependent on fibril angle. Therefore, it was concluded that this is one of the mechanisms by which the sudden extension can take place.

In the mechanism previously discussed the assumption was made that the fibril did not change in length due to drying. This assumption would be valid

if the fringed fibril theory is correct for the fiber structure, i.e., if the fibrils have an essentially continuous crystalline core. However, if the fringed micelle theory is correct, there might be an additional extension of the fibril due to water evaporating from the less-ordered regions. The first diagram of Fig. 24 illustrates two crystalline regions connected by a water-swollen amorphous region. When the water evaporates, the amorphous region will become more consolidated and extend in length, as illustrated in the second diagram. It is difficult to estimate the magnitude of extension by this mechanism; however, the extension probably would be relatively independent of drying load.

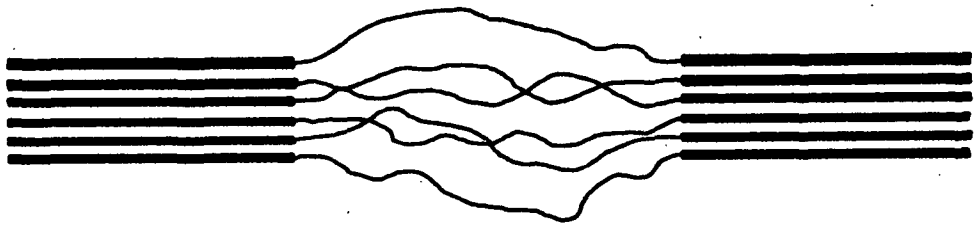

WET FIBER

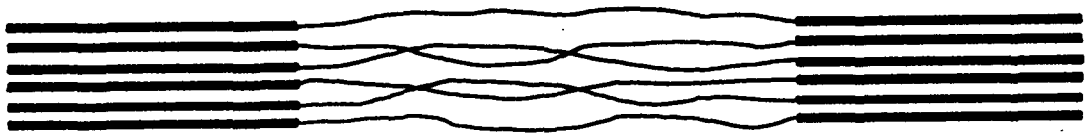

DRY FIBER

Figure 24. Schematic Diagram Showing the Possible Extension During Drying of a Water-Swollen Amorphous Region

CRYSTALLINITY OF WET FIBERS

An attempt was made to determine if any large difference could be noted between the crystallinity of never-dried fibers and that of once-dried fibers which have been rewet. Berkley and Kerr (44) reported that never-dried cotton fibers, when handled carefully, gave no evidence of a crystalline x-ray diffraction pattern. Sumi, Hale, and Rånby (78) measured the accessibility of Acetobacter microfibrils by deuterium exchange and found that the never-dried fibrils have an accessibility of 40% and the once-dried and rewet fibrils have an accessibility of 32%.

As discussed earlier, the x-ray diffraction pattern obtained from wet fibers contained the lattice diffractions of cellulose, water, and mylar. To obtain the pattern of cellulose, the intensity of the patterns of water and mylar were subtracted from the intensity of the composite pattern. Figure 25 presents the radial intensity curve for a never-dried and a once-dried and rewet fiber sliver. The two patterns are identical within experimental error, indicating that there is no large difference between the wet once-dried and never-dried fibers. The curves show very little amorphous scatter. Figure 17 shows that the majority of the amorphous scatter is not preferential in the direction of the fiber pattern, and therefore no account of this random amorphous scatter can be made by analyzing the patterns of wet fibers. The random amorphous scatter is subtracted along with the patterns of water and mylar because they cannot be separated. If there were any large differences in crystallinity, one might expect a difference in the width at half height, which is related to the size of the crystallites and imperfections in the crystal structure.

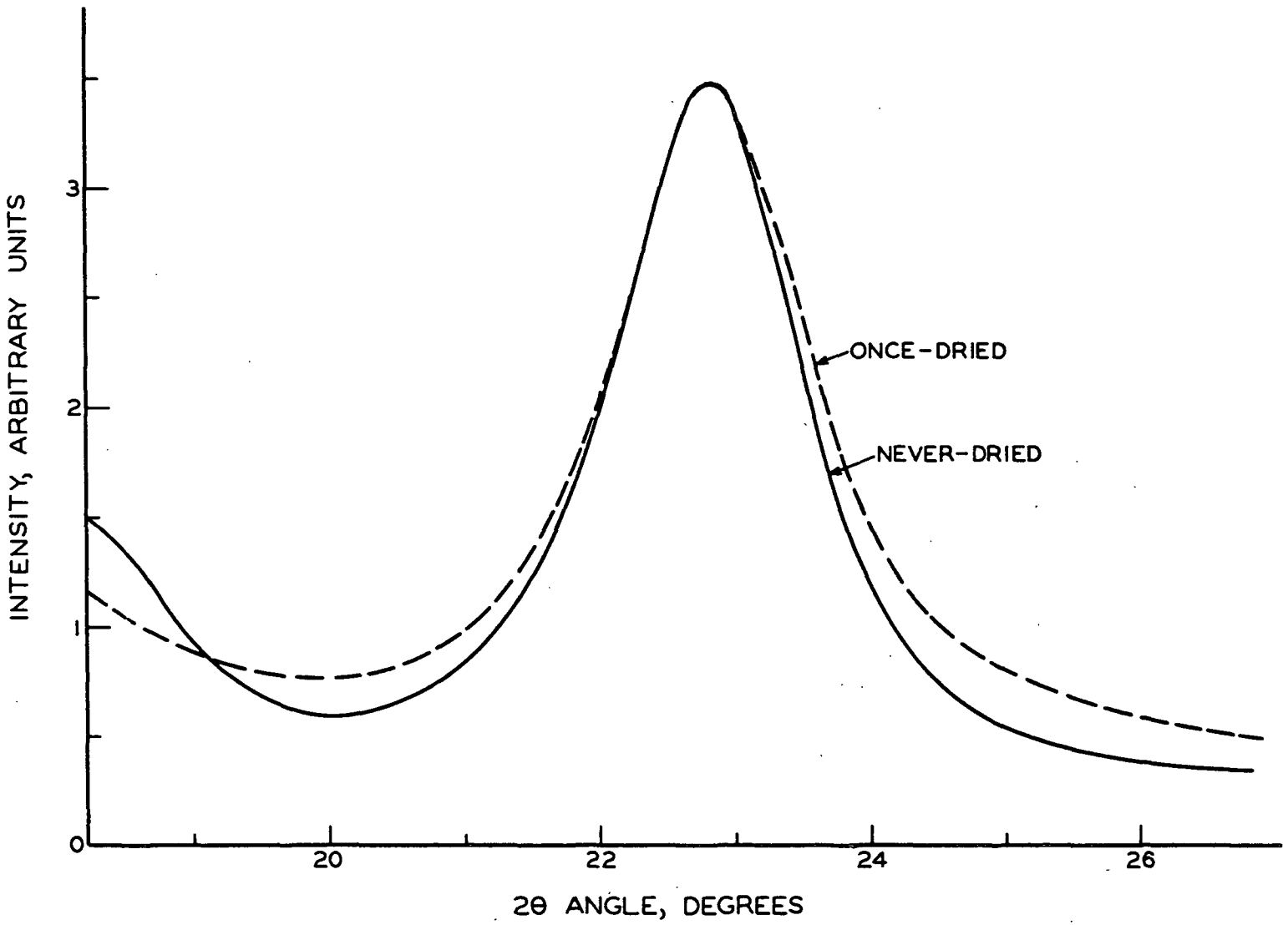

Figure 25. Radial Intensity Curve of a Never-Dried and Once-Dried Summerwood Pulp Sliver

MECHANICAL PROPERTIES OF FIBERS

SUMMERWOOD

The majority of the work on the mechanical properties was done with summerwood fibers; however, enough work was done with springwood fibers to ascertain the significant differences between the two types of fibers. The mechanical properties of the summerwood fibers are tabulated in Table VII. The fiber properties listed in the first two columns of Table VII are for fibers dried without an axial load. In the first case the fibers were dried freely, being allowed to twist and curl; and in the second, the fibers were dried in the apparatus used to dry fibers under load, which prevented them from twisting and curling, although they were still dried without an axial tensile load. The mechanical properties did not differ within 95% confidence limits except for Young's modulus. All future reference to significance will be based on the 95% confidence limits as discussed in Davies (71). This difference in Young's modulus can be attributed to preventing the fibers from twisting and curling.

In Fig. 26 the change in mechanical properties is plotted as a function of drying load.

Young's modulus and the tensile strength go through a significant maximum at a drying load of three grams, while ultimate elongation and work-to-rupture level off. Young's modulus undergoes the largest change, and this is consistent with the findings of Rebenfeld (46) and Negishi (43) for cotton fibers.

The shape of the load-elongation curve changes as the fiber is dried under load, as shown in Fig. 27. The relationship between load and elongation is quite linear for fibers dried without a load, and as the drying load is increased the

TABLE VII

MECHANICAL PROPERTIES OF SUMMERWOOD FIBERS DRIED UNDER VARIOUS LOADS

		No Load	No Load in Apparatus[a]	1-Gram Load	3-Gram Load	5-Gram Load	5-Gram Load Rewet	5-Gram Load Once Dried
Cross-sectional area, μ^2	Av.	395	410	417	396	427	425	397
	S.D., %	15.7	12.8	12.2	10.0	14.1	13.0	11.6
Breaking load, g.	Av.	42.4	47.6	54.6	58.2	58.9	46.1	57.2
	S.D., %	25.9	24.5	17.2	13.1	19.9	20.0	14.6
Tensile strength, dynes/μ^2	Av.	106.1	114.3	129.3	145.1	135.4	107.0	141.5
	S.D., %	24.4	23.3	18.4	13.2	16.2	18.2	11.6
	Change, %	0.0	+7.7	+21.8	+36.8	+27.6	+0.8	+33.3
Ultimate elongation, %	Av.	3.22	3.18	2.98	2.90	3.00	2.81	2.78
	S.D., %	23.6	22.9	15.0	14.7	17.2	19.3	12.7
	Change, %	0.0	-1.2	-7.5	-9.9	-6.8	-12.7	-13.7
Initial slope of load-strain curve, kilodynes	Av.	1360	1610	2230	2500	2400	1770	2470
	S.D., %	27.4	28.2	13.0	11.5	14.4	22.0	11.9
Young's modulus, dynes/μ^2	Av.	3470	3930	5370	6370	5630	4160	6220
	S.D., %	25.7	26.4	12.6	7.5	7.7	18.3	6.8
	Change, %	0.0	+13.3	+54.8	+82.2	+62.3	+19.9	+79.3
Area under load-strain curve, dyne-μ/μ	Av.	680	772	852	908	968	675	856
	S.D., %	34.1	33.2	28.8	23.9	33.2	34.8	24.8
Work-to-rupture, dyne-μ/cu. μ	Av.	1.74	1.90	2.06	2.32	2.27	1.60	2.16
	S.D., %	34.5	33.5	30.9	25.1	32.3	35.0	23.6
	Change, %	0.0	+9.2	+18.4	+33.4	+30.4	-8.0	+24.2
Number of fibers tested		73	40	40	36	36	30	41

[a]These fibers were dried with no load applied in the apparatus used to dry fibers under load.

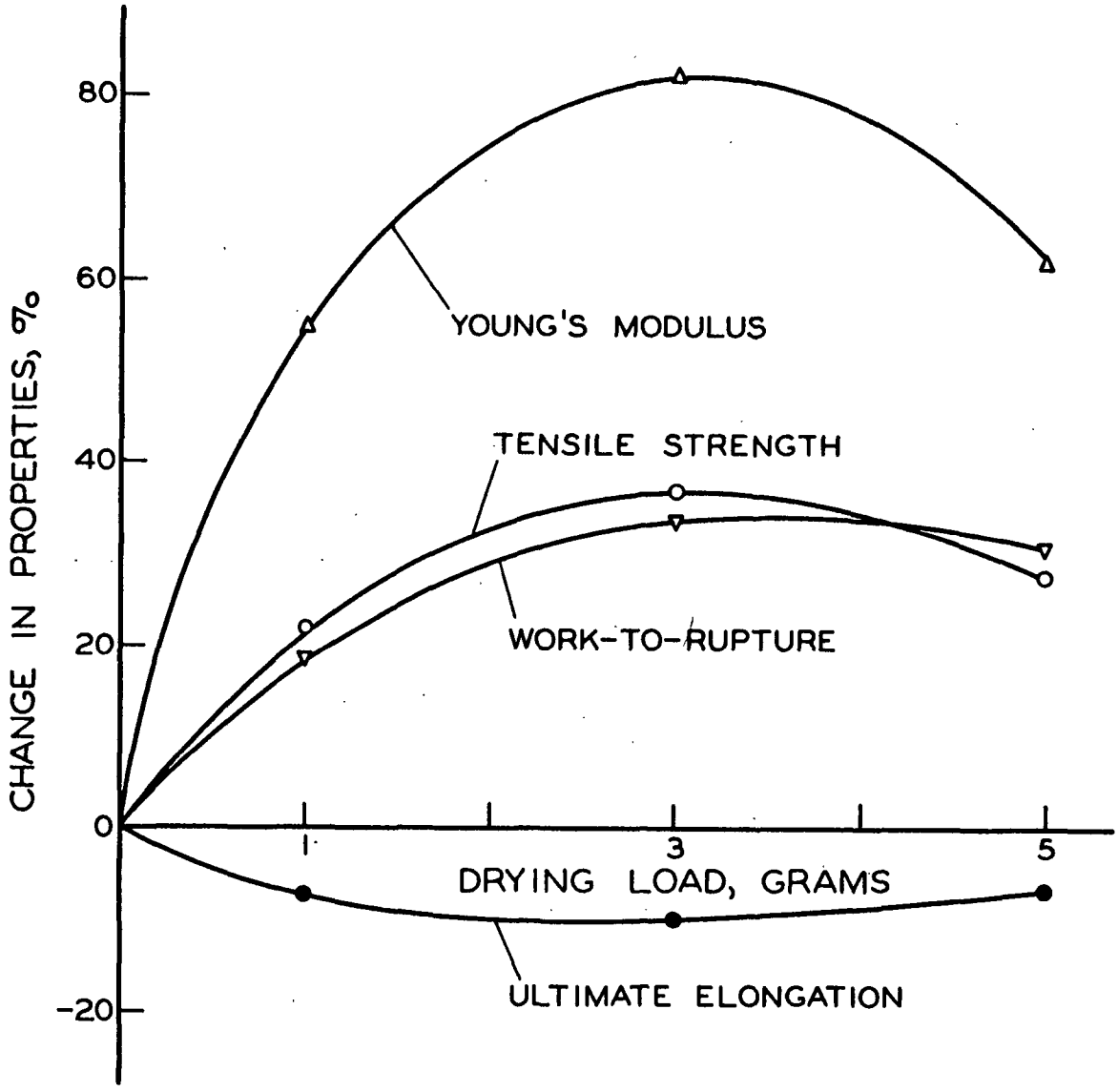

Figure 26. Change in Mechanical Properties of Summerwood Fibers Due to Drying Under a Load

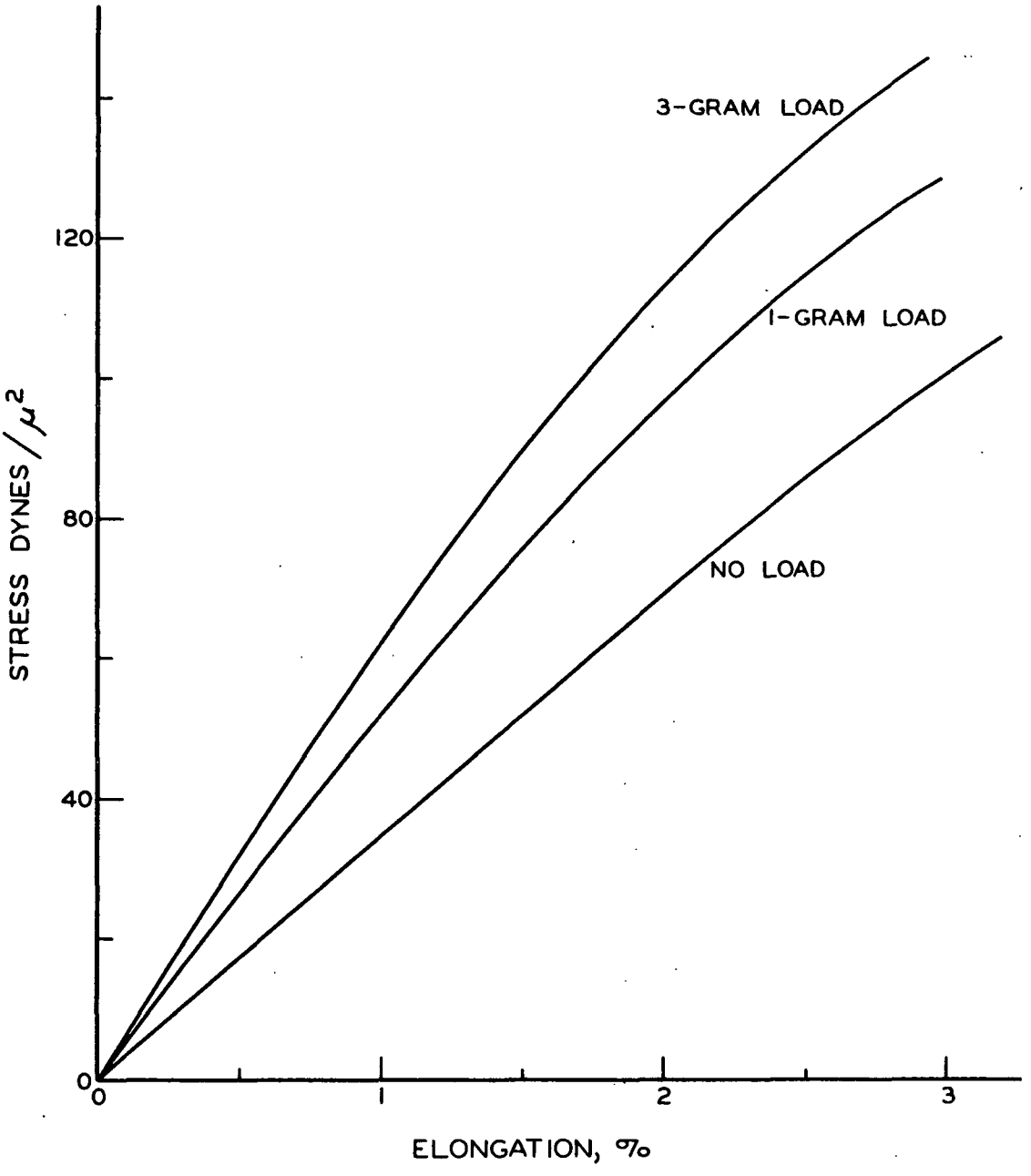

Figure 27. Average Load-Elongation Curves of Summerwood Fibers Dried Under Load

load-elongation relationship becomes more curved and concave toward the elongation axis. An analysis based strictly on the shape of the curves would lead to the conclusion that the fibers dried under load become more viscoelastic. To investigate this area more fully, loading and unloading cycles were run.

Table VIII and Fig. 28 show the results for fibers dried under no load and under a 3-gram load. The fibers which were dried under no load became stiffer as they underwent repeated loading and unloading cycles to higher strains. Young's modulus increased by 45% when the fiber was strained to 2.25% in the dry state. The fibers dried under a 3-gram load underwent a much different behavior when subjected to the loading and unloading cycles—their Young's modulus remained remarkably constant at a high value. The increase in modulus of the fibers dried under no load for each successive loading cycle was similar to the behavior Meredith (2) reported for natural cellulosic fibers; however, the behavior of the fibers dried under load was similar to that which he reported for regenerated fibers which were strained in their manufacture.

Fibers dried by the two methods also differed markedly in their nonrecoverable deformation after a loading and unloading cycle. The nonrecoverable deformation of the fibers dried under no load was about three times that for the fibers dried under a 3-gram load, and therefore it can be concluded that fibers dried under load show less secondary creep than fibers dried under no load. The elastic recovery (the ratio of the elongation recovered to the total elongation on loading) is shown to decrease as the maximum load increases for both types of fibers. This behavior has been observed for other cellulosic fibers (2) and is characteristic of viscoelastic materials in general.

The loading and unloading cycles give considerable insight into the reason that fibers dried under no load give a linear load-elongation curve and fibers

TABLE VIII

LOADING AND UNLOADING CYCLE RESULTS FOR SUMMERWOOD FIBERS DRIED WITH AND WITHOUT LOAD

	No Drying Load		3-Gram Drying Load	
	Av.	S.D., %	Av.	S.D., %
Initial elastic modulus, dynes/μ^2	3770	20.6	6180	4.6
Nonrecoverable deformation after cycling to 0.75% elong., %	0.158	39.5	0.047	24.2
Elastic modulus at start of second loading and unloading cycle, dynes/μ^2	4410	20.1	6320	4.9
Nonrecoverable deformation after cycling to 1.50% elong., %	0.433	32.2	0.151	13.9
Elastic modulus at start of third loading and unloading cycle, dynes/μ^2	4940	17.9	6300	4.7
Nonrecoverable deformation after cycling to 2.25% elong., %	0.721	31.7	0.315	11.7
Elastic modulus at start of final loading, dynes/μ^2	5290	16.3	6290	4.6
Number of fibers tested	34		33	

All these tests were run at a rate of loading and unloading of 1.4 grams per second.

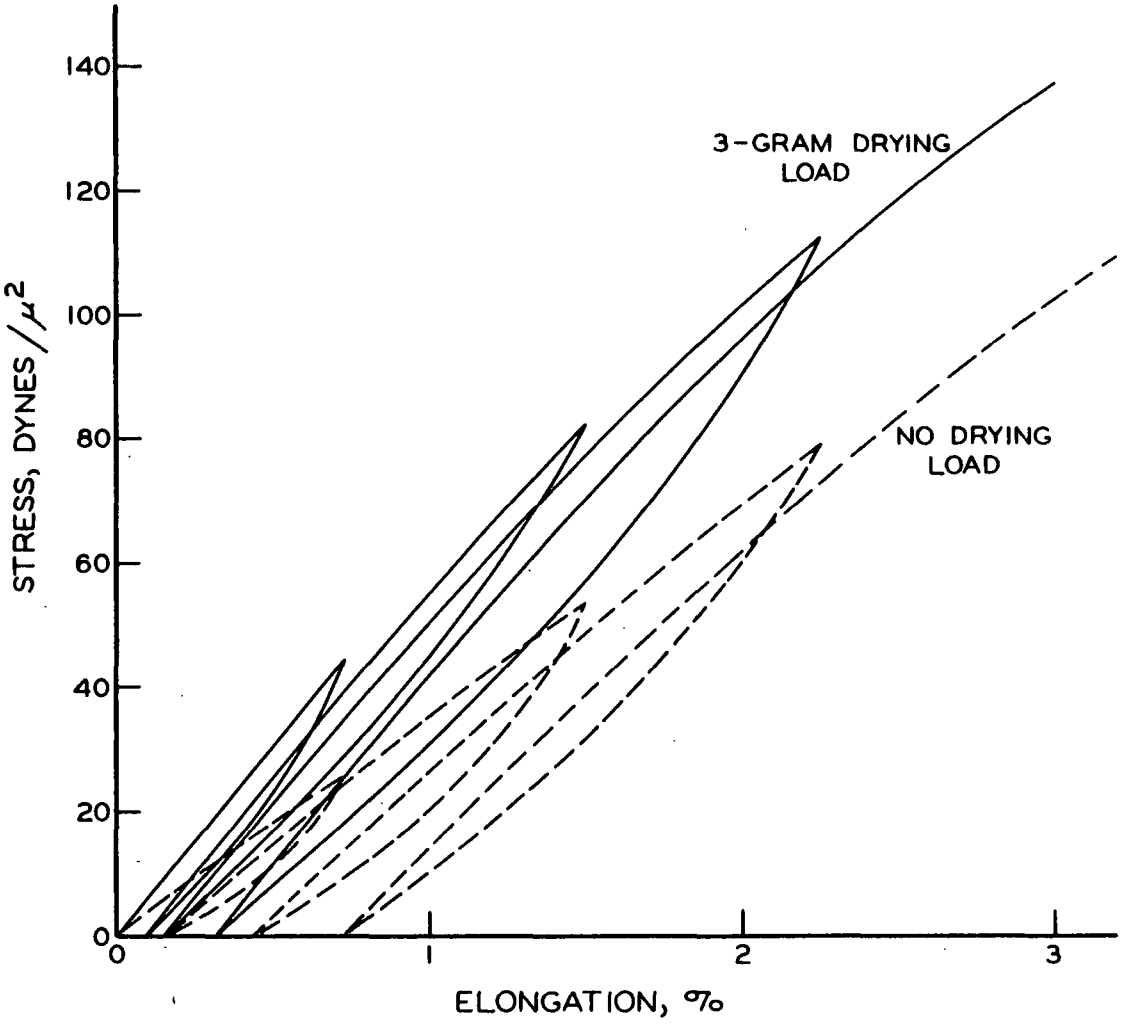

Figure 28. Loading and Unloading Cycles for Summerwood Fibers Dried With and Without Load

dried under load give a nonlinear load-elongation behavior. When a fiber which has not been dried under load is stressed, two competing mechanisms determine the shape of the load-elongation relationship. First, creep takes place, which is shown by the large amount of nonrecoverable deformation, and this tends to make the curve concave toward the elongation axis. Second, the fiber becomes stiffer as was shown by the increase in Young's modulus for successive loading cycles, and this causes the load-elongation curve to become concave toward the stress axis. This stiffening of the fiber undoubtedly is due to a redistribution of stress within the fiber.

The two mechanisms appear to be of equal magnitude for the rate of loading used, and the resulting load-elongation curve is linear except when the failure point is approached and creep appears to predominate. If a very high rate of loading were used to decrease the creep effect, one would expect the resultant curve to be concave toward the load axis. Conversely, if an extremely slow rate of testing were used to accentuate the creep effect, the resulting curve could be concave toward the strain axis. It should be pointed out that some of the individual tests were slightly concave toward the load axis, and others were slightly concave toward the elongation axis. The net effect was a linear curve. For the fibers dried under a 3-gram load, the loading and unloading cycles show that no further stiffening takes place when the fibers are stressed in the dry state. The resultant load-elongation curve is therefore concave toward the elongation axis.

The results in Table VII show that drying under load decreases the percentage standard deviation of the mechanical properties. It appears as though drying under load reduces the number of imperfections and defects in the fiber and makes them more uniform.

It is also interesting to note the effect of correcting for the differences in the fiber cross-sectional area on the percentage standard deviation of the mechanical properties. The ultimate elongation is theoretically independent of cross-sectional area and, therefore, cannot be corrected for it. The standard deviation of the tensile strength, which is dependent on structural flaws and imperfections, is only improved slightly, if at all, when corrections are made for cross-sectional area. It is highly doubtful if the standard deviation could be reduced more by a method which measures the cross-sectional area at the apparent point of break rather than the average cross-sectional area for the whole span. Microscopic examination of the fibers has revealed that there are no large local variations in the cross-sectional area.

In Appendix III it is shown that the correct average cross-sectional area to be used when calculating Young's modulus is the harmonic mean. The mass per unit length method measures the arithmetic mean; however, it can be shown that where the variations in cross-sectional area are small the two means are almost identical. When the initial slope of the load-elongation curve is divided by the cross-sectional area to obtain Young's modulus, a reduction in the percentage standard deviation is noted. This reduction is not surprising when it is realized that Young's modulus is the only mechanical property which was measured that is not dependent on the failure point. Rather, Young's modulus is dependent on the prerupture response of the whole span.

The results of two other interesting experiments are presented in Table VII. In the sixth column are results for fibers which were dried under a 5-gram load, rewet under no load, and redried under no load. The purpose of this experiment was twofold. First, an experiment of this sort can give information about the

mechanisms involved when fibers are dried under load; and second, it was desirable to ascertain if it would be feasible to study the drying load on fibers in a sheet by rewetting the sheet so that the fibers could be removed to be tested individually. The results show that most of the change caused by drying under load is lost by rewetting.

The small residual increase in Young's modulus is the only change which is significant. These results indicate that most of the structural changes due to drying under load occur in the less-ordered regions of the fiber, because these changes are removed when the fiber is rewet and allowed to dry freely.

The results of the final experiment are for never-dried fibers which were first dried without a load and then were rewet and dried under a 5-gram load. The results show that there is little difference between the mechanical properties of a once-dried and a never-dried fiber, when they are both dried under a load. Young's modulus of the once-dried fiber is much closer to the modulus of a never-dried fiber dried under a 3-gram load than to the modulus of a never-dried fiber dried under a 5-gram load. This small difference in the mechanical properties of once-dried and never-dried fibers is consistent with the results obtained for these two types of fibers in elongation behavior during drying and in crystallinity measurements.

SPRINGWOOD

The mechanical properties of the springwood fibers are presented in Table IX. There is no significant difference between the mechanical properties of the fibers dried freely under no load and those dried under no load in the drying apparatus. This is similar to the results obtained with the summerwood fibers.

TABLE IX

MECHANICAL PROPERTIES OF SPRINGWOOD FIBERS
DRIED UNDER VARIOUS LOADS

		No Load	No Load[a] in Apparatus	1-Gram Load	3-Gram Load
Cross-sectional area, μ^2	Av.	289	305	282	272
	S.D., %	19.6	13.7	15.1	16.7
	S.E.	9.44	6.52	6.83	7.10
Breaking load, g.	Av.	17.5	17.5	26.1	30.4
	S.D., %	42.8	29.6	21.5	21.6
Tensile strength, dynes/μ^2	Av.	59.4	56.5	91.0	109.8
	S.D., %	33.8	27.4	16.9	13.4
	Change, %	0.0	-4.9	+53.3	+84.9
	S.E.	3.35	2.42	2.93	2.30
Ultimate elongation, %	Av.	4.46	4.48	2.70	2.83
	S.D., %	39.4	41.7	19.5	12.0
	Change, %	0.0	+0.4	-39.5	-36.6
Initial slope of load-strain curve, kilodynes	Av.	525	502	1337	1499
	S.D., %	64.0	56.9	16.6	19.9
Young's modulus, dynes/μ^2	Av.	1770	1640	4750	5510
	S.D., %	54.8	54.9	9.5	10.9
	Change, %	0.0	-7.4	+168	+212
	S.E.	151.6	140.6	72.4	94.0
Area under load-strain curve, dyne-μ/μ	Av.	359	381	401	486
	S.D., %	39.4	39.2	34.8	26.0
Work-to-rupture, dyne-μ/cu. μ	Av.	1.29	1.26	1.43	1.79
	S.D., %	43.8	39.6	33.8	21.6
	Change, %	0.0	-2.3	+10.4	+38.8
	S.E.	.09	.08	.08	.06
Number of fibers tested		36	41	39	41

All fibers were tested at a rate of loading of 1.4 grams per second.

[a]These fibers were dried with no load applied in the apparatus used to dry fibers under load.

The percentage change in mechanical properties is plotted as a function of drying load in Fig. 29. The springwood fibers behaved quite similarly to the summerwood fibers, except that the percentage change in mechanical properties was larger for the springwood, and there appears to be no maximum as a function of drying load.

It is interesting to compare the absolute magnitudes of the springwood and summerwood mechanical properties. The summerwood fibers have an average cross-sectional area of 407 μ^2; an area of 287 μ^2 was observed for the springwood fibers. The ratio of areas is similar to those reported by Jayne (48) and Leopold (23) for southern pine fibers, although the absolute values reported by these two investigators are about 50% higher, and this may be at least partially due to the differences in the methods of measuring area.

Young's modulus and the tensile strength are plotted as a function of drying stress for both springwood and summerwood fibers in Fig. 30. Young's modulus of the springwood fibers is only 50% of that of the summerwood when the fibers are dried without a load, but it becomes 85% of the summerwood modulus when both types of fibers are dried under a stress of 7.5 dynes/μ^2. Although the modulus for both types of fibers increases as the fibers are dried under stress, the modulus for springwood increases at a faster rate, and the absolute value of the springwood modulus approaches that of the summerwood modulus.

The tensile strength of the springwood is 55% of that of the summerwood when the fibers are dried without a load. At a drying stress of 7.5 dynes/μ^2, it becomes 73% of the tensile strength of the summerwood. The tensile strength does not increase as rapidly as Young's modulus when the fibers are dried under stress. Also, the tensile strength of the springwood does not approach that of

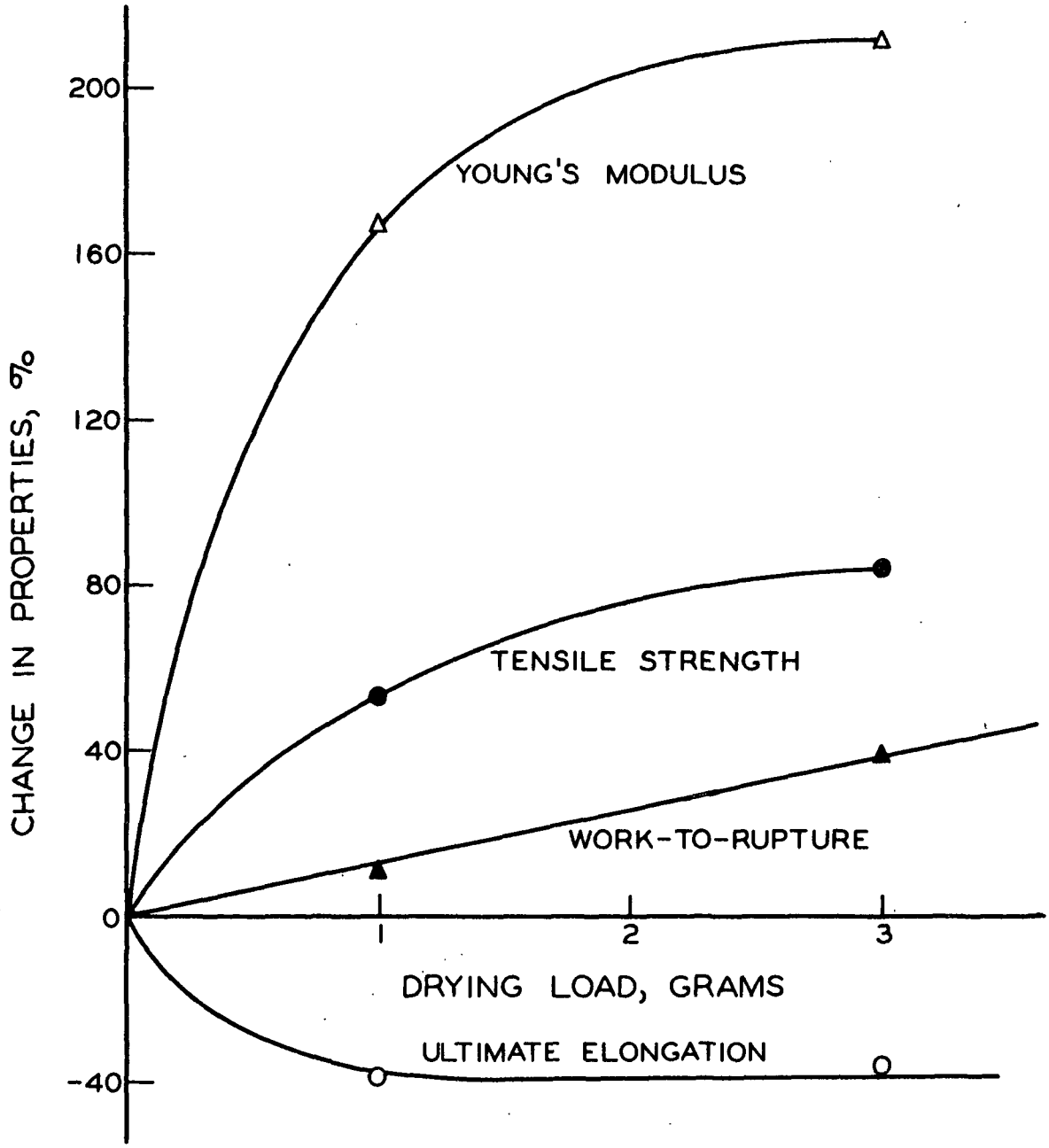

Figure 29. Changes in Mechanical Properties of Springwood Fibers Due to Drying Under a Load

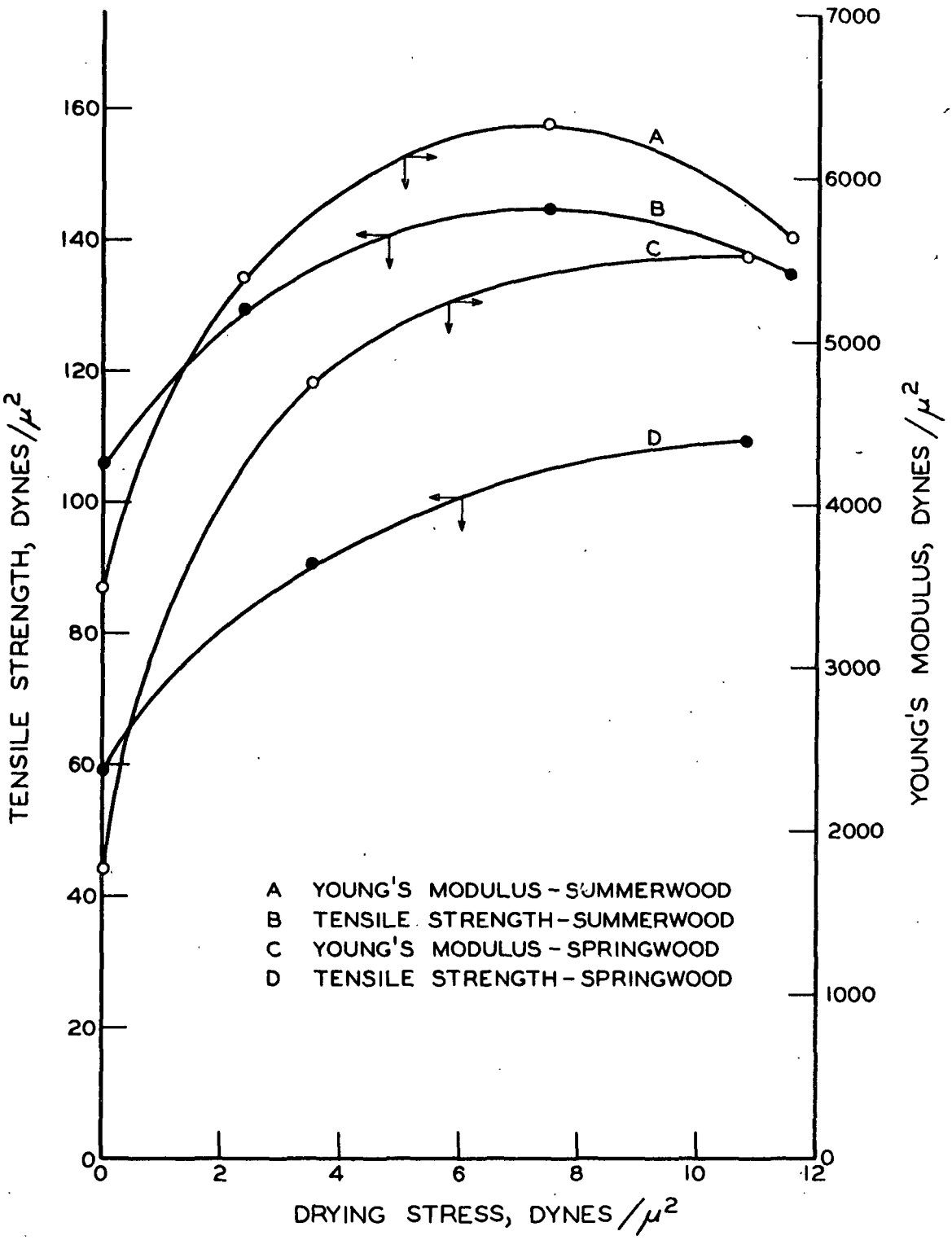

Figure 30. Young's Modulus and Tensile Strength as a Function of Drying Stress for Springwood and Summerwood

the summerwood as closely as the Young's moduli approach each other when the fibers are dried under stress.

The tabulated results show that the ultimate elongation of the springwood decreases more than that of the summerwood when the fibers are dried under stress. However, the absolute value of the ultimate elongation for both the springwood and summerwood fibers is the same after the fibers have been dried under a 1-gram load. Also, the stress/strain curves of the summerwood and springwood fibers correspond more closely when fibers are dried under load.

The results in Tables VII and IX show that the percentage standard deviation of the mechanical properties of the springwood fibers is greater than those of summerwood fibers, i.e., the springwood fiber sample is more heterogeneous than the summerwood sample. However, the percentage standard deviation of the springwood fibers is reduced more by corrections for mass per unit length than the standard deviation of the summerwood; this is particularly noticeable when the tensile strength is compared with the breaking load.

It also should be pointed out that the springwood fibers dried without a load gave an essentially linear load-elongation curve, and the springwood fibers dried under load gave a curved load-elongation relationship concave toward the elongation axis. These are similar to the curves shown for summerwood in Fig. 27.

CRYSTALLINITY AND CRYSTALLITE ORIENTATION

SUMMERWOOD

The results for the crystallinity and the crystallite orientation of the summerwood fibers are summarized in Table X. The crystallinity was measured both as the width at half height of the 002 diffraction arc and as the crystallinity

index. Both methods show that there is no significant difference between the crystallinity of the summerwood fibers dried under no load and the crystallinity of the fibers dried under a 5-gram load.

TABLE X

CRYSTALLINITY AND CRYSTALLITE ORIENTATION OF SUMMERWOOD FIBERS

	Drying Load, g.	Av.[a]	Standard Deviation	Fibers Tested
Width at half height of 002 diffraction arc	0	4.24°	0.47°	5
	5	3.95°	0.31°	5
Crystallinity index	0	61.6	6.3	5
	5	64.4	4.4	5
Orientation as standard deviation of circumferential arc	0	7.92°	1.71°	5
	5	6.33°	1.09°	5

[a]Data for individual fibers are tabulated in Appendix IV.

The crystallite orientation, as measured by the standard deviation of the normal curve fitted to the circumferential scan of the 002 diffraction arc, indicates a highly oriented structure for the summerwood fibers. The difference in the orientation of the fibers dried under no load and under a 5-gram load is significant within 88% confidence limits. The smallness of the change in the crystallite orientation due to drying under load is undoubtedly the result of the initial high degree of orientation.

SPRINGWOOD

The results for the crystallinity and the crystallite orientation of the springwood fibers are shown in Table XI. The crystallinity, as measured by the

width at half height of the 002 lattice diffraction and the crystallinity index, shows no significant change between fibers dried under no load and fibers dried under a 3-gram load. These results are consistent with those for the summerwood fibers.

TABLE XI

CRYSTALLINITY AND CRYSTALLITE ORIENTATION OF SPRINGWOOD FIBERS

	Drying Load, g.	Av.[a]	Standard Deviation	Fibers Tested
Width at half height of 002 diffraction arc	0	5.38°	1.65°	5
	3	4.52°	0.34°	5
Crystallinity index	0	50.5	12.4	5
	3	57.0	4.6	5
Orientation as standard deviation of circumferential arc	0	14.13°	4.55°	10
	1	7.30°	0.75°	10
	3	7.10°	0.50°	10

[a]Data for individual fibers are tabulated in Appendix IV.

The results show that the crystallite orientation changed significantly when the fibers were dried under no load and under a 1-gram load. However, when the fibers were dried under a 3-gram load, no further significant change in orientation was noted. The standard deviation of the orientation results was much greater for springwood fibers dried under no load than for springwood fibers dried under a 1-gram or 3-gram load. This indicates that the fiber population becomes more uniform with regard to orientation as the fibers are dried under load. It is interesting to note that the springwood is much less oriented than the summerwood when both types of fibers are dried under no load, but when the fibers are dried under a load the orientation of the springwood approaches that of the summerwood.

The changes in crystallinity shown in Table XI between springwood fibers dried with no load and with a 3-gram load should not be construed as representing a change in crystallinity if enough fibers were measured. Hermans and Weidinger (64, 66) have shown that the measured crystallinity is a function of orientation for oriented fiber samples. However, the samples do not show a difference in crystallinity if the oriented fibers are made into randomly oriented samples. Figure 31 shows the measured crystallinity index as a function of orientation for the springwood fibers which were dried under no load. The data, although scattered, show that a correlation does exist. If the orientation effect is to be eliminated, the more elaborate method of Hermans and Weidinger (66) should be used for evaluating the patterns. The large amount of time required for the more elaborate method was not justified in this work, due to the large amount of scatter noted in the crystallinity index.

The changes in orientation due to drying under load can be compared with the change in length of the fiber due to drying under load. Two different methods are available for deriving the relationship between permanent set and orientation. First, assume that the fibrils are in the form of a circular helix and that there are n revolutions of the helix for a fiber of length L. From the equations of the helix derived in Appendix II, it can be seen that $L = nz$. The total fibril length S, which is assumed to remain constant, equals $S = ns$. By a simple substitution it can be shown that $L = S \cos \theta$. Therefore, if the length of the fiber changes to L_1 due to drying under load, and the fibril length is assumed to remain constant,

$$L/L_1 = \cos \theta / \cos \theta_1.$$

Thus, it can be seen that the ratio of the lengths is related by the cosines of

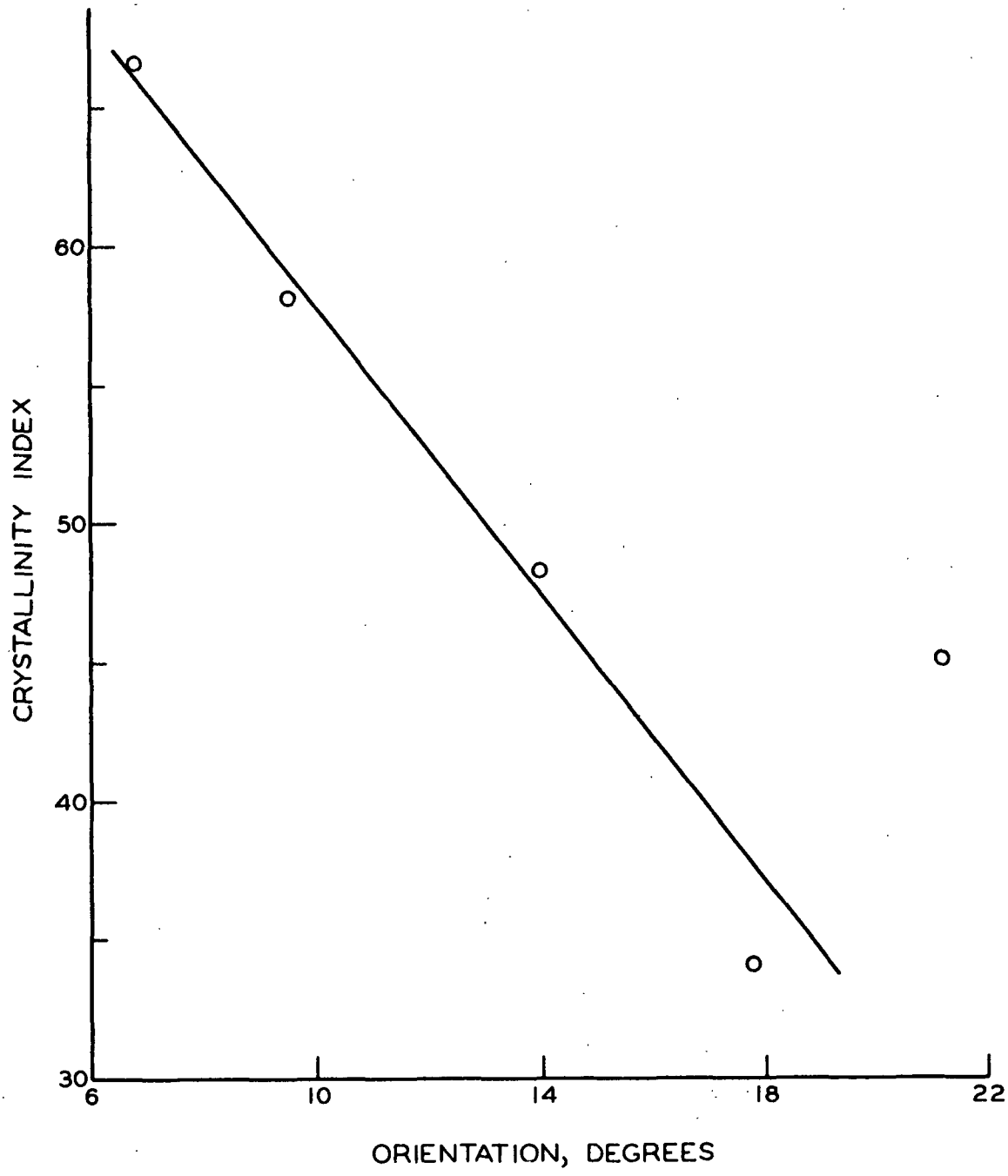

Figure 31. Crystallinity Index as a Function of Crystallite Orientation for Springwood Fibers Dried Under No Load

the orientation angles. This derivation is similar to the one of Balashov, Preston, Ripley, and Spark (45).

The second method of derivation, which is more general, assumes that the fiber is made up of m fibrils at an angle θ with the fiber axis, and each has an area A perpendicular to the fibril axis. The cross-sectional area of the fiber is $mA/\cos\theta$. When the fiber is dried under a load, the length changes from L to L_1. If the solid volume of the fiber is assumed to remain constant, then

$$LmA/\cos\theta = L_1 mA/\cos\theta_1.$$

The ratio of the length equals

$$L/L_1 = \cos\theta/\cos\theta_1.$$

Before the change in length of the fiber due to drying under load can be determined, it is necessary to evaluate the dry length of the fiber dried without a load. It should be pointed out again that all the permanent sets listed in Tables V and VI are with respect to wet fibers at a 1-gram load. The length of the fiber dried without load was calculated by plotting the permanent sets from Tables V and VI as a function of the drying load and extrapolating this curve to zero drying load as shown in Fig. 32. These extrapolations led to permanent sets at no load with respect to the wet fiber at 1-gram load of -0.2% for the springwood fibers and -0.2% for the summerwood fibers.

Considering the summerwood fibers first and assuming that the average fibril angle is equal to the standard deviation of the normal curve, the expected permanent set can be calculated from the orientation results in Table X. A permanent set of 0.35% is predicted for the summerwood fibers dried under a 5-gram load as compared to fibers dried under no load. The observed permanent set is

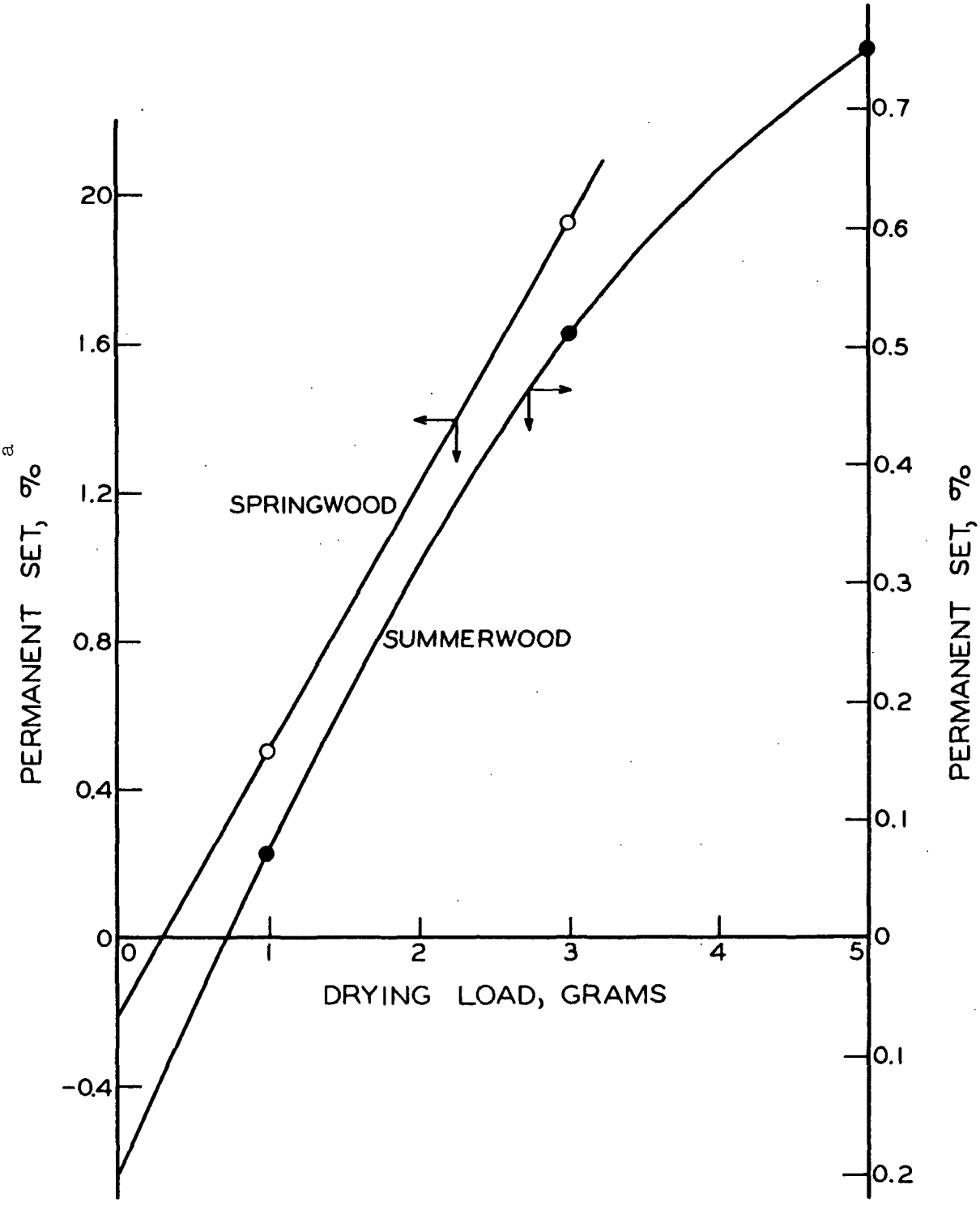

Figure 32. Relationship Between Permanent Set and Drying Load for Springwood and Summerwood Fibers

[a]Permanent set relative to the fiber length for a 1-gram load on the wet fiber.

0.95%. Similar calculations on the springwood fibers show a predicted permanent set of 2.2% for the fibers dried under a 1-gram load compared to the actual set of 0.70%. The springwood fibers dried under a 3-gram load would also have a predicted set of 2.2%, and their actual set is 2.10%.

There are several reasons for the difference between the predicted and the actual values of permanent set. First, the large variation from fiber to fiber leads to large confidence limits for the average values of orientation obtained. Second, all the mechanisms which lead to permanent set might not result in a change in the orientation of the crystallite; for example, there might be slippage of the fibrils relative to one another. Third, the permanent set and deformation probably are dependent only on the S_2 layer while the orientation as measured by x-ray diffraction is dependent on the mass percentages of the P, S_1, S_2, and S_3 layers as well as the pits. The measured orientation will be less than the actual orientation of the S_2 layer by some undetermined amount, due to the P, S_1, and S_3 layers, and this effect will become larger as the orientation increases. Furthermore, the orientation values of 6 to 7° may be approaching the limiting values measurable by x-ray diffraction, since all diffraction spots will have a certain finite size which is dependent on the size of the crystallites and imperfections in the crystal structure. Finally, the standard deviation of the normal curve fitted through the circumferential trace of the 002 arc may not be a good approximation for the actual fibril angle, although it is a good method for comparative purposes. Much better agreement between permanent set and orientation was obtained by Balashov, et al. (45); however, their fibers were much less oriented.

INTERPRETATION OF RESULTS IN TERMS OF CHANGES IN FIBER STRUCTURE

Drying fibers under an axial tensile load has been shown to have a large effect on both the mechanical properties of the fibers and the crystallite orientation. The changes in mechanical properties appear to be the result of two mechanisms. First, the fibers change in mechanical properties due to increases in crystallite and fibril orientation, and second, the fiber mechanical properties change due to a redistribution of stress within the fiber.

Direct experimental evidence has been obtained to show that the crystallite orientation increases due to drying under load. Many investigators have shown that the tensile strength and Young's modulus increase as the orientation increases for natural cellulosic fibers. The results show that the springwood fibers, which undergo the larger increase in orientation, also undergo the larger increase in mechanical properties. It is interesting to note that the percentage standard deviation of the mechanical properties decreases as the fibers are dried under load, and the percentage standard deviation of the orientation also decreases as the fibers are dried under load, indicating that some of the fiber-to-fiber variation in mechanical properties may be caused by differences in orientation.

When the fibers are dried under load the values of the springwood mechanical properties approach those of the summerwood mechanical properties, and concurrently the springwood crystallite orientation approaches the summerwood crystallite orientation. One might expect the mechanical properties to be dependent almost totally on the most highly oriented S_2 layer of the fiber. The summerwood fibers generally are agreed to have a larger mass percentage of the S_2 layer than springwood. From data given by Jayme and Hunger (21), and by assuming the thickness

of the P, S_1, and S_3 to be the same for both springwood and summerwood, the S_2 layer is calculated to represent 87.5% of the summerwood cross-sectional area and 78.5% of the springwood cross-sectional area. If the S_2 layer is assumed to have the same orientation in both springwood and summerwood after they have been dried under a 3-gram load, and if the S_2 layer only is responsible for the mechanical properties, then most of the 85% difference in Young's modulus between springwood and summerwood shown in Fig. 30 can be accounted for by the difference in the percentage of the S_2 layer in the two types of fibers.

The tensile strength of the springwood was only 73% of that of summerwood at a drying stress of 7.5 dynes/μ^2. This difference cannot be accounted for totally by the difference in the percentage of the S_2 layer. The tensile strength of a material is known to be governed by imperfections in the fiber structure, and therefore the conclusion can be made that springwood fibers have more and/or larger imperfections and discontinuities than summerwood fibers.

The percentage of the S_2 layer also may account for the difference in the orientation when springwood and summerwood fibers are dried under load. If the S_2 layer is assumed to have the same orientation in both types of fibers, then the one-degree difference in orientation may be accounted for by the orientation of the other layers. Although the P, S_1, and S_3 layers have only a small effect on orientation, the difference in their percentages, 12.5% in summerwood and 21.5% in springwood, could account for the difference noted in orientation.

The influence of orientation leads to interesting conclusions and speculations as to the mechanism of fiber deformation and fiber failure. The increase in Young's modulus with the increase in orientation indicates that the primary valence bonds play an increasingly more important part relative to that of the

secondary bonds. This is logical when it is realized that when the orientation increases, the component of the applied force along the fibril axis increases.

The increase of tensile strength with orientation indicates that small, local delaminations of the fibrils, together with the stress concentrations caused by the pits and other discontinuities, may initiate fiber failure. The delamination force is the component of the force perpendicular to the fibril axis, and this component decreases as the orientation increases. Therefore, for the delamination component of the applied force to remain constant as the orientation increases, the applied force must increase. The delamination is caused by breakage of secondary bonds, and the breakage of these bonds requires less energy than the breakage of primary valence bonds. There appears to be no doubt, however, that in the failure process there is breakage of cellulose molecules.

The experimental evidence indicating there is a redistribution of stress within the fiber due to drying under load is less direct than that showing a change in orientation; however, there is little doubt that it does occur. The most direct evidence appears to be from the loading and unloading cycles for the summerwood fibers dried under no load and under a 3-gram load. The fibers which were not dried under load undergo a stiffening when they are stressed, and this stiffening results in a 45% increase in Young's modulus. This large stiffening must be due to a redistribution of stress when the fiber is strained. The fibers that were dried under load did not show a stiffening during the dry straining; therefore, the redistribution of stress probably occurred when the fibers were dried under load. The final Young's modulus of the fibers dried without load did not equal that of the fibers dried under load, and it is apparent that it is easier for the stress to be more equally redistributed when the fiber is wet and there are many less secondary bonds.

Another piece of experimental evidence, which leads to the conclusion that there is a more equal redistribution of stress due to drying under load, is the magnitude of the change observed in Young's modulus when the fibers are dried under load. From the change in mechanical properties with orientation observed for cotton and other natural fibers, the large change in mechanical properties due to drying under load cannot be accounted for only on the basis of change in orientation. The only additional plausible explanation is a redistribution of stress.

There is some experimental evidence which allows speculation as to where the redistribution of stress occurs. In general, there are two places for redistribution of stress to occur—between the molecules within the fibrils, and between the fibrils themselves.

From the x-ray diffraction patterns, the cellulose fiber in the wet state is seen to be highly crystalline. Therefore, a large percentage of the cellulose molecules are in the highly ordered regions, and it is unlikely that molecules in these regions have enough freedom of movement to cause the large changes in mechanical properties attributable to redistribution of stress. Thus, the better explanation is that the redistribution takes place between the fibrils.

In the wet state, the percentage of secondary bonds between the fibrils is small compared to the dry state. Therefore, the fibrils are relatively free to move when a stress is applied, and a large redistribution of stress is possible. Further evidence for the redistribution of stress between the fibrils comes from the experiments in which the fibers were rewet and dried under no load after they were originally dried under a load. The fibers lost most of the change produced by drying under load because of the rewetting. When a fiber is wet, the water

penetrates more easily between the molecules in the less-ordered regions. The large loss in mechanical properties indicates that the redistribution of stress must have occurred in regions where the water could easily penetrate, i.e., in the less-ordered regions between the fibrils. Thus, an increase in orientation and a more even distribution of stress among the fibrils are the two principal mechanisms which account for the change in mechanical properties due to drying under load.

It is of interest to compare the theoretical Young's modulus for crystalline cellulose calculated by Meyer and Lotmar (49) with that obtained in this study. Meyer and Lotmar calculated a Young's modulus of 90 x 10^{10} dynes/sq. cm. for perfectly oriented cellulose. The highest value observed in this study was 63 x 10^{10} dynes/sq. cm. for summerwood fibers dried under a 3-gram load. If it is assumed that only the S_2 layer contributes significantly to Young's modulus, that the S_2 layer is perfectly oriented (the cosine of the small orientation values would not be significant), and that the S_2 layer composes 87.5% of the summerwood fiber, this leads to an effective modulus of 72 x 10^{10} dynes/sq. cm. Furthermore, it might be assumed that only the highly ordered cellulose contributes effectively to Young's modulus, and the chemical analysis of the summerwood in Table IV shows that only 70% of the pulp is glucose. The hemicellulose in the fiber is generally considered to be amorphous, so that the percentage of highly ordered material in the S_2 layer might be 70%. This then leads to an effective Young's modulus of 103 x 10^{10} dynes/sq. cm., which is in closer conformity with the value calculated by Meyer and Lotmar.

The highest value of Young's modulus for springwood fibers was 55 x 10^{10} dynes/sq. cm. for those dried under a 3-gram load. Correcting this value for the 78.5% of S_2 layer gives an effective modulus of 70 x 10^{10} dynes/sq. cm.

Finally, correcting this for the percentage of glucose gives 97 x 10^{10} dynes/sq. cm. The springwood and summerwood values of the maximum Young's modulus are equal within experimental error, when they are corrected for the percentage of S_2 layer.

The method of correcting for the percentage of the S_2 layer and the percentage of highly ordered cellulose is subject to many assumptions; however, it does give a crude comparison between the theoretical value of Young's modulus and that which may exist for the crystalline cellulose in the fiber. The calculated Young's modulus also gives information as to whether the fringed micelle theory or the fringed fibril theory is the more correct representation of the fiber structure. If the fringed micelle theory is correct, the less-ordered and highly-ordered regions are in series, and the total deformation is the sum of that from both regions. One would, therefore, predict a Young's modulus less than that for crystalline cellulose. If the fringed fibril theory is correct, then the less-ordered and highly-ordered regions are parallel, and the total deformation is determined by the stiffer highly-ordered regions. Young's modulus predicted from the fringed fibril theory would be essentially that of crystalline cellulose. From the determined values of Young's modulus, the conclusion can be drawn that the fringed fibril theory is a better representation of a holocellulose wood pulp fiber's structure than the fringed micelle theory.

CONSIDERATIONS ON SHEET STRUCTURE IN TERMS OF THE RESULTS OBTAINED WITH DRYING FIBERS UNDER LOAD

It is interesting to speculate on the effect of drying fibers under load on various commonly observed behaviors of sheets. The zero-span tensile strength has been proposed as a measure of fiber strength, and it appears to serve this purpose very well. However, this study has brought out several important factors

which can influence zero-span results. From the change in tensile strength due to drying under load, one would predict that the fibers in a sheet are stronger in the machine direction than in the cross direction because the sheet is dried under a tensile stress in the machine direction. Commercial papers are dried under a tensile stress; however, the fibers in these sheets are not randomly oriented, and by zero-span tests orientation effects cannot be separated from differences in fiber strength. Schulz (79) dried randomly oriented handsheets under a constant strain in one direction and found that the zero-span tensile strength differed by 27% in the two principal directions. The results of Schulz confirm the prediction that the zero-span tensile strength should change due to drying the sheets under load, and the sheets will be stronger in the machine direction than in the cross direction.

Van den Akker, et al. (53) have presented a theory relating the zero-span tensile test to the individual fiber strength. Care should be taken in applying this theory to be certain that the individual fibers measured are dried under as nearly as possible the same stress conditions as the fibers in the sheet. Perhaps the best way would be to dry both under no restraint. Care should also be taken in using TAPPI Suggested Method T 481 sm-60, which suggests using the zero-span tensile in different sheet directions as a measure of fiber orientation. If Schulz had applied this method, he would have predicted a 27% difference in orientation, while actually he just measured a difference in fiber strength.

Recently, Van den Akker (73) and several other workers in this field have presented theories which relate the sheet properties to the individual fiber properties. To apply these theories correctly, the individual fibers tested must be dried under the same stress scheme as the fibers in the sheet. If the sheet is restrained more in one direction during drying than in the other, the

fiber properties will be dependent on their angular orientation. The fiber property of main concern is Young's modulus, and this property was shown to undergo the largest change with drying under load.

Clark (80), Wink and Van Eperen (51), and Schulz (74) have found that zero-span tensile strength increases with beating and in some cases goes through a maximum. Kull (81) determined that the tensile strength of summerwood fibers decreased with beating while that of springwood fibers remained constant with beating. The work of Schulz (74) provides one of the clues to this apparently anomalous behavior. He found that the tension developed during drying when the sheet was held in a fixed position increased and then leveled off as a function of beating. Therefore, the increase in zero-span tensile strength with beating might be due partially to the sheets being dried under larger stresses. If the sheets were dried at constant stress rather than at constant strain, the zero-span tensile strength might be expected to remain essentially constant as a function of beating.

Beating generally increases both the tensile strength and Young's modulus of a sheet. In the customary method of making handsheets, the sheets are not allowed to shrink while they are dried, i.e., they are dried with zero degree of straining. Thus, when handsheets are dried in the customary manner the beating produces two effects. The first is the actual effect of beating on the pulp itself, and the second is the increase in drying stress. Brecht and Pothmann (75) found larger changes in the mechanical properties by drying under different stresses than Schulz (74) found by drying under different degrees of wet straining. In fact, the stress developed in Schulz's work was relatively independent of the degree of wet straining but was dependent on the amount of beating.

Therefore, some of the changes in the mechanical properties of handsheets attributable to beating may be caused by the changes in the mechanical properties of the fibers resulting from drying under greater stress.

SUMMARY OF RESULTS

The objectives of this thesis were to determine the effect of drying individual fibers under an axial tensile load on the mechanical properties of the individual fibers and on the structural changes which take place in the fibers. To fulfill these objectives a holocellulose pulp was prepared from longleaf pine, and the springwood and summerwood fibers of one growth ring were separated. The load-elongation properties of both the summerwood and springwood fibers were measured at several drying loads. To determine structural changes in the fibers, Laue x-ray diffraction patterns were run on individual fibers, and the crystallinity and crystallite orientation were measured. The results show that:

1. The summerwood and springwood fibers have nearly identical chemical composition.

2. The summerwood and springwood fibers underwent a sudden extension at the commencement of drying, which was almost independent of the drying load and was twice as large for springwood as for summerwood. After this sudden extension, the fibers underwent the normally reported axial shrinkage.

3. No significant difference in crystallinity was noted between the never-dried and the once-dried and rewet fibers.

4. The summerwood fibers showed a maximum increase of 37% in the tensile strength, 82% in Young's modulus, and 33% in the work-to-rupture, and a decrease of 10% in the ultimate elongation due to drying under load.

5. The springwood fibers showed a maximum increase of 85% in the tensile strength, 212% in Young's modulus, and 39% in the work-to-rupture, and a decrease of 40% in the ultimate elongation due to drying under load.

6. The never-dried and the once-dried and rewet summerwood fibers showed the same changes in mechanical properties due to drying under load.

7. Summerwood fibers which were dried under load and then were rewet and dried under no load had mechanical properties only slightly different from those fibers which were dried originally under no load.

8. The percentage standard deviation of the mechanical properties decreased due to drying under load and also decreased when the mechanical properties were corrected for fiber-to-fiber variation in the mass per unit length. Also, the percentage standard deviation of the orientation decreased as the fibers were dried under load.

9. Loading and unloading cycles run on the summerwood fibers showed that those dried under no load underwent an increase in Young's modulus from cycle to cycle, while those dried under a 3-gram load exhibited no change in Young's modulus.

10. No significant difference was noted in the crystallinity of fibers dried under no load and those dried under a load.

11. The crystallite orientation of both summerwood and springwood fibers increased due to drying under load. The springwood fibers underwent the larger increase in orientation; however, they were the less oriented when dried under no load.

GENERAL DISCUSSION AND CONCLUSIONS

The experimental observations made in this study have led to several conclusions. The sudden extension at the commencement of drying is caused partially by the shrinkage of the fiber diameter. The amount of extension is related to the initial fibril orientation and the amount of radial shrinkage. A fair agreement with the results can be obtained by using a model which assumes the fibrils to be in the form of a circular helix. The permanent set put into the fiber due to drying under load is caused by changes in crystallite orientation and molecular and fibril slippage.

The two principal mechanisms by which fibers undergo a change in mechanical properties due to drying under load are an increase in orientation and a more even distribution of stress among the fibrils of the fiber. In general, a poorly oriented fiber will undergo a larger change in mechanical properties than a highly oriented fiber. The fiber-to-fiber variation in mechanical properties is due to at least three major causes: differences in the distribution of the stress among the fibrils, differences in the crystallite orientation, and differences in the mass per unit length. The mass per unit length difference is overshadowed by differences in orientation and stress distribution when the fibers are not dried under a load.

The mechanical properties of pulp fibers appear to be governed by the S_2 layer. Most of the difference between the maximum obtainable values of the mechanical properties of springwood and summerwood can be accounted for by the difference in the percentage of S_2 layer in the cross-sectional area of the springwood and summerwood fibers. When it is assumed that only the S_2 layer contributes effectively to determining Young's modulus, the actual value of

Young's modulus approaches the value theoretically calculated for perfectly oriented crystalline cellulose. This suggests that the fringed fibril theory gives a better picture of the pulp fiber's structure than the fringed micelle theory.

Van den Akker's theory (73) predicts that when a sheet is dried under a tension in one direction, the fibers within the sheet will be dried under different tensile forces depending on their angular orientation. Therefore, from this theory and the results obtained in this study, the conclusion can be drawn that the fibers in a sheet which is dried under tension in one direction will have different mechanical properties depending on the angular orientation of the fiber. Thus, a significant portion of the differences in the mechanical properties of a sheet in the two principal directions can be attributed to the relationship between the fiber mechanical properties and the orientation of the fibers in the sheet.

ACKNOWLEDGMENTS

This thesis would not be possible without the aid and advice of many people. It would be difficult to list and even to remember all the people who have helped in some way toward the successful completion of this thesis. To all these people the author would like to express his appreciation.

There are several people who deserve special mention. The author would like to extend his sincere thanks to Dr. J. A. Van den Akker, the chairman of his thesis advisory committee, and to Dr. G. R. Sears and Dr. D. G. Williams, members of the thesis advisory committee, for their advice and criticism throughout the course of this work.

The aid of the following is also gratefully acknowledged:

Messrs. H. Marx and M. Filz of the Machine Shop of The Institute of Paper Chemistry for their help in the construction and design of the equipment used in this thesis.

Mrs. Judith Jentzen for doing all the typing in preparation of this dissertation and for her continual encouragement.

LITERATURE CITED

1. Ott, E., Spurlin, H. M., and Grafflin, M. W., Ed. Cellulose and cellulose derivatives. 2d ed. New York, Interscience Publishers, Inc., 1954. 1601 p.

2. Meredith, R., Ed. The mechanical properties of textile fibres. New York, Interscience Publishers, Inc., 1956. 333 p.

3. Morton, W. E., and Hearle, J. W. S. Physical properties of textile fibres. Manchester and London, Butterworth and Co., Ltd. and The Textile Institute, 1962. 609 p.

4. Heuser, E., and Jorgensen, L., Tappi 34, no. 2:57-67(1951).

5. Meyer, K. H., and Misch, L., Helv. Chim. Acta 20, no. 2:232-44(1937).

6. Mark, H. Interaction and arrangement of cellulose chains. In Ott's Cellulose and cellulose derivatives. 2d ed. Part I. p. 217-30. New York, Interscience Publishers, Inc., 1954.

7. Lindenmeyer, P. H., J. Polymer Sci. 10, no. 1:5-40(1963).

8. Howsmon, J. A., and Sisson, W. A. Submicroscopic structure of cellulose fibers. In Ott's Cellulose and cellulose derivatives. 2d ed. Part I. p. 231-346. New York, Interscience Publishers, Inc., 1954.

9. Hearle, J. W. S., J. Polymer Sci. 28, no. 117:432-5(1958).

10. Hearle, J. W. S., J. Textile Inst. Proc. 53, no. 8:P449-64(Aug., 1962).

11. Tønnesen, B. A., and Ellefsen, Ø., Norsk Skogind. 14, no. 7:266-9(1960).

12. Calkins, C. R., Tappi 33, no. 6:278-85(1950).

13. Verseput, H. W., Tappi 34, no. 12:572-6(1951).

14. Ticknor, L. B., J. Polymer Sci. 1A, no. 1:243-8(1963).

15. Frey-Wyssling, A. The general structure of fibres. In Bolam's Fundamentals of papermaking fibres. p. 1-6. Kenley, Surrey, England, Tech. Sect. of the Brit. Paper and Board Makers' Assoc., Inc., 1958.

16. Frey-Wyssling, A., Science 119, no. 3081:80-2(1954).

17. Wardrop, A. B., Svensk Papperstid. 66, no. 7:231-47(1963).

18. Emerton, H. W., The outer secondary wall. I. Its structure. In Bolam's Fundamentals of papermaking fibres. p. 35-54. Kenley, Surrey, England, Tech. Sect. of the Brit. Paper and Board Makers' Assoc., Inc., 1958.

19. Bucher, H. Discontinuities in the microscopic structure of wood fibres. In Bolam's Fundamentals of papermaking fibres. p. 7-26. Kenley, Surrey, England, Tech. Sect. of the Brit. Paper and Board Makers' Assoc., Inc., 1958.

20. Brown, H. P., Panshin, A. J., and Forsaith, C. C. Textbook of wood technology. Vol. I. New York, McGraw-Hill Book Company, Inc., 1949. 652 p.

21. Jayme, G., and Hunger, G. Electron microscope 2- and 3-dimensional classification of fibre bonding. In Bolam's The formation and structure of paper. Vol. I. p. 135-70. London, Tech. Sect. of the Brit. Paper and Board Makers' Assoc., Inc., 1962.

22. Meier, H., J. Polymer Sci. 51, no. 155:11-18(1961).

23. Leopold, B., Tappi 44, no. 3:232-5(1961).

24. Sachs, I. B., Clark, I. T., and Pew, J. C., J. Polymer Sci. 1C, no. 2:203-12 (1963).

25. Preston, R. D., Polymer 3:511-28(1962).

26. Rånby, B. G. The fine structure of cellulose fibrils. In Bolam's Fundamentals of papermaking fibres. p. 55-82. Kenley, Surrey, England, Tech. Sect. of the Brit. Paper and Board Makers' Assoc., Inc., 1958.

27. Leopold, B., and McIntosh, D. C., Tappi 44, no. 3:235-40(1961).

28. Leaderman, H. Elastic and creep properties of filamentous materials and other high polymers. Washington, D. C., The Textile Foundation, 1943. 278 p.

29. Hartler, N., Kull, G., and Stockman, L., Svensk Papperstid. 66, no. 8:301-8 (1963).

30. Peirce, F. T., J. Textile Inst. Trans. 17:T355-68(1926).

31. Hartler, N., Kull, G., and Stockman, L., Svensk Papperstid. 66, no. 8:309-11 (1963).

32. Wakeham, H. Mechanical properties of cellulose and its derivatives. In Ott's Cellulose and cellulose derivatives. 2d ed. Part III. p. 1247-1356. New York, Interscience Publishers, Inc., 1954.

33. Hessler, L. E., Simpson, M. E., and Berkley, E. E., Textile Res. J. 18, no. 11:679-83(1948).

34. Ziifle, H. M., Eggerton, F. V., and Segal, L., Textile Res. J. 29, no. 1:13-20(1959).

35. Orr, R. S., Burgis, A. W., Andrews, F. R., and Grant, J. N., Textile Res. J. 29, no. 4:349-55(1959).

36. Ward, K., Textile Res. J. 20, no. 6:363-72(1950).

37. Sisson, W. A., Textile Res. J. 7, no. 11:425-31(1937).

38. Orr, R. S., De Luca, L. B., Burgis, A. W., and Grant, J. N., Textile Res. J. 29, no. 2:144-50(1959).

39. Krassig, H., and Kitchen, W., J. Polymer Sci. 51, no. 155:123-72(1961).

40. Wardrop, A. B., Australian J. Sci. Res. (B4) 4, no. 4:391-414(1951).

41. Negishi, M., J. Soc. Textile Cellulose Ind., Japan 3:60-3(1947).

42. Negishi, M., J. Soc. Textile Cellulose Ind., Japan 2:34-8(1946).

43. Negishi, M., J. Soc. Textile Cellulose Ind., Japan 3:21-4(1947).

44. Berkley, E. E., and Kerr, T., Ind. Eng. Chem. 38, no. 3:304-9(1946).

45. Balashov, V., Preston, R. D., Ripley, G. W., and Spark, L. C., Proc. Royal Soc. (London) Series B 146:460-8(1957).

46. Rebenfeld, L., Textile Res. J. 32, no. 3:202-11(1962).

47. Jayne, B. A., Tappi 42, no. 6:461-7(1959).

48. Jayne, B. A., Forest Prod. J. 10, no. 6:316-22(1960).

49. Meyer, K. H., and Lotmar, W., Helv. Chim. Acta 19, no. 1:69-86(1936).

50. Thompson, N. S., and Kaustinen, O., Tappi, in press.

51. Wink, W. A., and Van Eperen, R. H., Tappi 45, no. 1:10-24(1962).

52. Hardacker, K. W., Tappi 45, no. 3:237-46(1962).

53. Van den Akker, J. A., Lathrop, A. L., Voelker, M. H., and Dearth, L. R., Tappi 41, no. 8:416-25(1958).

54. Helbert, J. R., and Brown, K. D., Anal. Chem. 31, no. 10:1700-2(1959).

55. Helbert, J. R., and Brown, K. D., Anal. Chem. 29, no. 10:1464-6(1957).

56. Bonting, S. L., Arch. Biochem. Biophys. 52, no. 1:272-9(1954).

57. Lowry, O. H., and Bessey, O. A., J. Biol. Chem. 163, no. 3:633-9(1946).

58. Taylor, A., J. Sci. Instr. 28, no. 7:200-5(1951).

59. Ronnebeck, H. R., J. Sci. Instr. 20, no. 10:154-9(1943).

60. Klug, H. P., and Alexander, L. E. X-ray diffraction procedures. p. 108 and 373. New York, John Wiley and Sons, Inc., 1954.

61. James, T. H., and Higgins, G. C. Fundamentals of photographic theory. New York, Morgan and Morgan, Inc., 1960. 345 p.

62. Segal, L., Creely, J. J., Martin, A. E., and Conrad, C. M., Textile Research J. 29, no. 10:786-94(1959). 28R

63. Gjonnes, J., Norman, N., and Viervol, H., Acta Chem. Scand. 12, no. 3:489-94, no. 10:2028-33(1958). 8R

64. Hermans, P. H., and Weidinger, A., J. Appl. Phys. 19, no. 5:491-506(1948).

65. Hermans, P. H., and Weidinger, A., J. Polymer Sci. 4, no. 2:135-44(1949).

66. Hermans, P. H., and Weidinger, A., Textile Res. J. 31, no. 6:558-71(1961). 28R

67. Klug, H. P., and Alexander, L. E. X-ray diffraction procedures. p. 132-3. New York, John Wiley and Sons, Inc., 1954.

68. Hermans, P. H. Physics and chemistry of cellulose fibers. New York, Elsevier Publishing Co., Inc., 1949. 534 p.

69. De Luca, L. B., and Orr, R. S., J. Polymer Sci. 54, no. 160:457-70(1961). 4R

70. Sisson, W. A., Ind. Eng. Chem. 27, no. 1:51-6(1935). 6R

71. Davies, O. L. Statistical methods in research and production. New York, Hafner Publishing Company, 1958. 396 p.

72. Ellis, K. D., and Warwicker, J. O., J. Polymer Sci. 1A, no. 4:1185-1200 (1963). 4R

73. Van den Akker, J. A. Some theoretical considerations on the mechanical properties of fibrous structures. In Bolam's The formation and structure of paper. Vol. I. p. 205-41. London, Tech. Assoc. of the Brit. Paper and Board Makers' Assoc., Inc., 1962.

74. Schulz, J. H. The effect of strain applied during drying on the mechanical behavior of paper. Doctor's Dissertation. Appleton, Wis., The Institute of Paper Chemistry, 1961. 161 p.

75. Brecht, W., and Pothmann, D., Papier 9, no. 13/14:304-11, no. 17/18:429-37 (1955).

76. Weidner, J. P. The influence of humidity on changes in diameter and length of sulphite fibers. Doctor's Dissertation. Appleton, Wis., The Institute of Paper Chemistry, 1938. 191 p.

77. Page, D. H., and Tydeman, P. A., Nature 199, no. 4802:471-2(Aug. 3, 1963).

78. Sumi, Y., Hale, R. D., and Rånby, B. G., Tappi 46, no. 2:126-30(1963).

79. Schulz, J. H., Unpublished work.

80. Clark, J. d'A., Tech. Assoc. Papers 26:285-90(1943).

81. Kull, L. G., Unpublished work.

APPENDIX I

CALCULATION OF THE AMOUNT OF THE TOTAL LOAD ON A SHEET WHICH AN INDIVIDUAL FIBER SUPPORTS

The following derivation is based on the theory of Van den Akker (73) for the mechanical properties of fibrous structures. The contribution of each fiber to the external load on the sheet is

$$S = \langle F \rangle_{Av} \cos\theta + T \sin\theta = (e/2h)(1+\nu_{xy})\sin\theta\cos^2\theta$$

$$+ eAE(\sin^3\theta - \nu_{xy}\sin\theta\cos^2\theta),$$

where $\langle F \rangle_{Av}$ is the average shear force, T is the tensile force, θ is the angle the fiber segment makes with the cross-machine direction (y-direction) of the sheet, e is the sheet strain in the x-direction, ν_{xy} is Poisson's ratio for the sheet with sheet stress in the x-direction, A is the cross-sectional area of the fiber wall, and E is Young's modulus of the fiber. The term h is defined by

$$h = (s^2/12EI) + (1/AG),$$

where s is the fiber segmental distance, I is the moment of inertia of fiber cross section, and G is the modulus of rigidity of the fiber for shear stress along cross section and parallel to F.

If the fiber is assumed to have a rectangular cross section, then $A = uw$ where u is the fiber width and w is the fiber thickness. Now let $u = Kw$ and $E = GK'$, where K and K' are constants. By making the appropriate substitutions,

$$h = [K' + (s^2/KA)]/AE.$$

The contribution of each fiber to the external load becomes

$$eAE\left[\frac{1+\nu_{xy}}{2(K'+Ks^2/A)}-\nu_{xy}\right]\sin\theta\cos^2\theta+eAE\sin^3\theta$$

The maximum tensile stress occurs on fibers which are oriented in the direction of the external stress, i.e., when $\theta = 90°$, and this maximum stress is $\underline{B}_{max} = \underline{eE}$.

From Van den Akker's theory, the total tensile force in the sheet is

$$\mathcal{T}_x = \frac{\mathcal{U}We_x}{\langle A\rangle_{av}\rho\langle s\rangle_{av}}\left[\frac{1}{2}(1+\nu_{xy})\int_0^{\pi}\int_0^{\infty}\int_0^{\infty}\int_0^{\infty}\frac{s}{h}\sin^2\theta\cos^2\theta\,P_\theta P_A P_I P_s\,ds\,dI\,dA\,d\theta\right.$$

$$-\nu_{xy}\int_0^{\pi}\int_0^{\infty}\int_0^{\infty}AEs\sin^2\theta\cos^2\theta\,P_\theta P_A P_s\,ds\,dA\,d\theta$$

$$\left.+\int_0^{\pi}\int_0^{\infty}\int_0^{\infty}AEs\sin^4\theta\,P_\theta P_A P_s\,ds\,dA\,d\theta\right],$$

where $\mathcal{U}$ is the width of the strip under tension, $\underline{W}$ is the mass of the fiber per unit area of the sheet, ρ is the density of the fiber wall, and $\underline{P}_\theta$, $\underline{P}_A$, $\underline{P}_I$, and $\underline{P}_s$ are the distribution functions for θ, $\underline{A}$, $\underline{I}$, and $\underline{s}$, respectively. If the assumptions are made that $\underline{A}$, $\underline{I}$, and $\underline{s}$ are constant and the fiber segments are randomly oriented, i.e., $\underline{P}_\theta = 1/\pi$, $\mathcal{T}_{\underline{x}}$ equals

$$\mathcal{T}_x = \frac{\mathcal{U}We_x}{\langle A\rangle_{Av}\rho\langle s\rangle_{Av}}\left[\frac{1}{2}(1+\nu_{xy})\frac{s}{h}\cdot\frac{1}{\pi}\int_0^{\pi}\sin^2\theta\cos^2\theta\,d\theta\right.$$

$$\left.-\nu_{xy}AEs\cdot\frac{1}{\pi}\int_0^{\pi}\sin^2\theta\cos^2\theta\,d\theta+AEs\cdot\frac{1}{\pi}\int_0^{\pi}\sin^4\theta\,d\theta\right].$$

Integration and simplification of this equation gives

$$\mathcal{T}_x = \frac{\mathcal{U} We_x}{\rho}\left[\frac{1}{2}(1+\nu_{xy})\,\frac{1}{8hA} - \frac{\nu_{xy}E}{8} + \frac{3E}{8}\right].$$

If the cross-sectional area of the sheet A_s and the cross-sectional areas of the fibers are calculated using the pycnometric density of cellulose, then

$$A_s = \mathcal{U} W/\rho.$$

Thus, the average stress on the sheet equals

$$B'_{Av} = \mathcal{T}_x/A_s = Ee_x\left\{\frac{1}{8}\left[\frac{(1+\nu_{xy})}{2hEA} - \nu_{xy}\right] + \frac{3}{8}\right\}$$

$$= Ee_x\left\{\frac{1}{8}\left[\frac{(1+\nu_{xy})}{2(K'+s^2/KA)} - \nu_{xy}\right] + \frac{3}{8}\right\}.$$

The ratio of the maximum stress on a fiber to the average stress on the sheet is

$$\frac{B_{max}}{B'_{Av}} = \frac{8}{\left[\dfrac{(1+\nu_{xy})}{2(K'+s^2/KA)} - \nu_{xy}\right] + 3}.$$

If the term in brackets is assumed to be zero, then the ratio of the maximum stress on any fiber to the average stress on the sheet is 8/3. Then, by selecting the appropriate value for the fiber cross-sectional area, the maximum drying load can be calculated. It should be emphasized that the purpose of this derivation was to obtain only a rough estimate of the maximum drying load a fiber in a sheet might have.

For a sheet dried under an equal strain in all directions it is interesting to calculate the load on the fibers at different orientations when an external strain is applied in the x-direction. From Van den Akker's theory, it can be shown that the tensile force on a fiber oriented at an angle θ equals

$$T = eAE(\sin^2 \theta - \nu_{xy} \cos^2 \theta).$$

For numerical purposes the following assumptions are made: $\underline{e} = 0.01$, $\nu_{xy} = 0.3$, $\underline{A} = 400\ \mu^2$, and $\underline{E} = 5400$ dynes/μ^2. The tensions can then be calculated as a function of the angle θ, and the results are presented in Table XII.

TABLE XII

TENSION IN FIBERS AT VARIOUS ORIENTATIONS

θ, degrees	Tension, dynes
0	-6,500
10	-5,600
20	-3,200
30	500
40	5,100
50	10,000
60	14,600
70	18,300
80	20,700
90	21,600

Thus, it can be observed that the fibers in the cross-machine direction will be under an appreciable compressive force and that those in the machine direction will be under a large tensile force.

APPENDIX II

EQUATIONS OF A CIRCULAR HELIX

The equations for a helix are most easily derived by using a polar coordinate system with the axis of the helix coinciding with the z axis. Any point on the helix is then defined in terms of the three variables, r, ω, and z. A differential length of the helix ds equals

$$ds = r d\omega / \sin \theta ,$$

where θ is the angle ds makes with the z axis. The length of the helix per revolution around its axis is

$$s = \int_0^{2\pi} \frac{r d\omega}{\sin\theta} = 2\pi r / \sin \theta .$$

The component of the ds along the z axis is

$$dz = ds \cos \theta .$$

The length of the helix along the z axis per revolution of the helix is

$$Z = \int_0^Z dz = \int_0^{2\pi} \frac{r d\omega}{\tan \theta} = \frac{2\pi r}{\tan \theta} .$$

APPENDIX III

DETERMINATION OF THE PROPER MEAN AREA TO BE USED FOR YOUNG'S MODULUS CALCULATIONS

When a material with a variable cross section is stressed, the extension of a differential length will be related to the cross-sectional area of the differential length. Consider a bar with a variable cross-sectional area being subjected to an axial force F. Now consider the bar to be made up of n segments, of equal length h. The i segment has a cross-sectional area A_i and has a strain e_i due to the force F. Considering the bar to have a Young's modulus E, the strain can be related to the axial force, and

$$e_i = F/EA_i.$$

The average strain in the bar will be e, and

$$e = \frac{\sum_{o}^{n} he_i}{\sum_{o}^{n} h} = \frac{h \sum_{o}^{n} e_i}{nh} = \frac{1}{n} \sum_{o}^{n} e_i = \frac{F}{E} \frac{1}{n} \sum_{o}^{n} \frac{1}{A_i}.$$

Young's modulus equals

$$E = \frac{F}{e} \frac{1}{n} \sum_{o}^{n} \frac{1}{A_i} = \frac{F}{e} \cdot \left(\frac{1}{A}\right)_{Av}.$$

Therefore, it can be seen that the correct average cross-sectional area to use in calculating Young's modulus is the harmonic mean.

APPENDIX IV

CRYSTALLINITY AND CRYSTALLITE ORIENTATION DATA

The results obtained for the crystallinity and crystallite orientation of summerwood and springwood fibers are given in Tables XIII and XIV. The following system is used for fiber identification. A typical fiber might have the designation SU-5-1. The SU represents summerwood (SP stands for springwood). The first number, 5, represents the drying load in grams, and the second number, 1, represents the first summerwood fiber dried under a 5-gram load. The results given are the average of four separate determinations on each fiber's x-ray diffraction pattern. The crystallinity is measured by both the crystallinity index and the width at half height of the 002 lattice diffraction, and the crystallite orientation is measured as the standard deviation of the normal curve fitted to the circumferential scan of the 002 lattice diffraction.

TABLE XIII

CRYSTALLINITY AND CRYSTALLITE ORIENTATION OF SUMMERWOOD FIBERS

Fiber Identification	Crystallinity Index	Width at Half Height, degrees	Crystallite Orientation, degrees
SU-0-1	58.7	4.47	9.68
SU-0-2	60.2	4.17	7.69
SU-0-3	63.3	4.20	6.35
SU-0-4	71.3	3.54	6.20
SU-0-5	54.5	4.81	9.67
Average	61.6	4.24	7.92
Standard deviation	6.3 2.8	0.47 .21	1.71 .77
SU-5-1	59.1	4.20	8.25
SU-5-2	60.9	4.32	5.76
SU-5-3	65.9	3.96	6.03
SU-5-4	70.1	3.62	5.58
SU-5-5	65.8	3.67	6.04
Average	64.4	3.95	6.33
Standard deviation	4.4 2.0	0.31 .14	1.09 .49

TABLE XIV

CRYSTALLINITY AND CRYSTALLITE ORIENTATION OF SPRINGWOOD FIBERS

Fiber Identification	Crystallinity Index	Width at Half Height, degrees	Crystallite Orientation, degrees
SP-0-1	66.6	3.67	6.82
SP-0-2	48.4	4.76	13.95
SP-0-3	45.2	6.02	21.17
SP-0-4	58.2	4.53	9.52
SP-0-5	34.1	7.93	17.77
SP-0-6	--	--	13.07
SP-0-7	--	--	12.00
SP-0-8	--	--	19.40
SP-0-9	--	--	16.49
SP-0-10	--	--	11.15
Average	50.5	5.38	14.13
Standard deviation	12.4	1.65	4.55
" Error	5.6	.74	1.49
SP-1-1	--	--	8.53
SP-1-2	--	--	8.28
SP-1-3	--	--	7.46
SP-1-4	--	--	6.34
SP-1-5	--	--	6.72
SP-1-6	--	--	7.10
SP-1-7	--	--	7.96
SP-1-8	--	--	6.58
SP-1-9	--	--	7.24

TABLE XIV (Continued)

CRYSTALLINITY AND CRYSTALLITE ORIENTATION OF SPRINGWOOD FIBERS

Fiber Identification	Crystallinity Index	Width at Half Height, degrees	Crystallite Orientation, degrees
SP-1-10	--	--	6.82
Average	--	--	7.30
Standard deviation	--	--	0.75
			S.E = .24
SP-3-1	55.7	4.66	6.88
SP-3-2	65.0	3.93	8.05
SP-3-3	55.7	4.52	7.30
SP-3-4	54.1	4.77	7.32
SP-3-5	54.2	4.73	7.32
SP-3-6	--	--	6.72
SP-3-7	--	--	6.28
SP-3-8	--	--	6.57
SP-3-9	--	--	7.33
SP-3-10	--	--	7.19
Average	57.0	4.52	7.10
Standard deviation	4.6	0.34	0.50
	S.E. = 2.1	.15	S.E. = .16